This is to certify that the
dissertation entitled

EFFECTS OF OZONE ON ACETAMINOPHEN-INDUCED
LIVER AND AIRWAY TOXICITY IN MICE

presented by

Daher Ibrahim Aibo

has been accepted towards fulfillment
of the requirements for the

Ph.D. degree in Pathology and Environmental Toxicology

Major Professor's Signature

12/14/09

Date

EFFECTS OF OZONE ON ACETAMINOPHEN-INDUCED LIVER AND AIRWAY TOXICITY IN MICE

By

Daher Ibrahim Aibo

A DISSERTATION

Submitted to
Michigan State University
in partial fulfillment of the requirements
for the degree of

DOCTOR OF PHILOSOPHY

Pathology and Environmental Toxicology

2009

ABSTRACT

EFFECTS OF OZONE ON ACETAMINOPHEN-INDUCED LIVER AND AIRWAY TOXICITY IN MICE

By

Daher Ibrahim Aibo

Acetaminophen (APAP) is the most frequently used over-the-counter analgesic and antipyretic in the United States (U.S.). APAP overdose is responsible for half of cases of acute liver failure in developed countries. At high doses, APAP also causes acute lung injury in people and laboratory animals. Ozone (O3) is the main oxidant air pollutant in photochemical smog. More than half of the U.S. population is daily exposed to levels of O3 exceeding the U.S. Environmental Protection Agency (EPA) national ambient air quality standards (NAAQS). Recently, O3 has been shown to modulate systemic levels of antioxidant as well as expression of several families of genes in the liver. The principal purpose of this work was to investigate the effects of combined APAP and O3 in the liver and pulmonary airways of mice compared to effects of individual substances. I also explored some of the mechanisms that could help explain the pathogenesis of APAP and O3 interaction in the liver and lung of these mice. Three specific aims have been generated. In aims 1 and 2, I studied the APAP and O3 effects in the liver and lung, respectively. To do so, I treated mice with saline or 300 mg/kg APAP intraperitoneally and 2 h later exposed them to filtered air, 0.25 or 0.5 ppm O3 for 6 h. Mice were euthanized 9 or 32 h after APAP administration. In the liver and pulmonary airways, APAP and O3 resulted in greater epithelial damage and acute inflammation compared to either substance alone. In addition, both locations exhibited APAP-induced increase in epithelial cell proliferation that was inhibited by O3 coexposure. IL-6, an

important mediator of initial phases of hepatocellular regeneration was upregulated at the gene and protein levels in the liver of APAP-treated animals but not in APAP/O3-coexposed mice. In aim 3, I hypothesized that the absence of IL-6 induction in the liver of APAP/O3-coexposed mice is responsible for the impaired hepatocellular regeneration that might have contributed to the heightened toxicity in this last group. I exposed IL-6 sufficient or deficient mice to the same experimental protocol and found that IL-6 deficient mice given APAP or APAP and O3 had deficient hepatocellular proliferation. At the same time, APAP/O3 deficient mice had greater toxicity than APAP-treated deficient animals suggesting that IL-6 is not involved in the impaired regeneration and enhanced toxicity detected in the APAP/O3 group. I also found that IL-6 deficient mice had impaired airway epithelial regeneration in either APAP or APAP/O3-coexposed groups suggesting that IL-6 had a role in airway epithelial regeneration. Finally, I detected several antioxidant or hypoxia-related genes or protein differentially expressed in the APAP/O3 or APAP alone suggesting a contributory role of oxidative stress or hypoxia in O3 exacerbation of APAP toxicity.

To Laurence, Marine-Ayan and Idil

ACKNOWLEDGMENTS

It is a pleasure and an honor to thank all the people who made this thesis possible.

First and foremost, I am heartily thankful to my mentor Dr. Jack Harkema, for his scientific guidance, encouragement, financial support and patience from the early stage of this research as well as giving me extraordinary opportunities to learn and grow as a scientist throughout this work and other projects. I am indebted to him more than he probably considers.

I am especially grateful to Drs. Robert Roth, Patricia Ganey and Jane Maddox who contributed to the financial and scientific realization of this work. I would also like to thank the rest of my thesis committee members Drs. Jim Wagner, Timothy Zacharewski and Colleen Hegg for their insightful comments and suggestions. I would like to thank Dr. John Lapres for letting me work in his Lab.

I owe my deepest gratitude to Lori Bramble and Ryan Lewandowski from our Lab for all their help and assistance. I would like to thank Ms. Amy Porter, Kathy Campbell and Rick Rosebury from the MSU Department of Physiology, Laboratory of Histopathology. Lori, Ryan, Amy, Kathy and Rick, this thesis would not have been possible without your support.

I would like to show my gratitude to Drs. Willie Reed, Jennifer Thomas and Laura McCutcheon, former and present Chairpersons of the Department of Pathobiology and Diagnostic Investigation at MSU, Dr. Susan Ewart, Associate Dean for Research and Graduate Studies in the College of Veterinary Medicine and Drs. Karen Klomparens and Tony Nunez, Dean and Associate Dean of the MSU Graduate School, for their support

made available in a number of ways to me and other students including through several awards.

I thank my former and present colleagues in our Lab; Drs Neil Birmingham, Steve Carey, Daven Jackson, Ms. Kara Corps, Ms. Xiao Pan and all the undergraduate students who helped me; Anthony Guzzardo, Ian Hotchkiss, Robert Buhsrobe and Jennifer Stokes. I also thank colleagues from others Programs with whom I shared expertise and friendship.

I wish to thank my entire extended family here and abroad, particularly my dad and mom for providing me a constant understanding. I am indebted to my wife Laurence and my two daughters Marine-Ayan and Idil for their love, burden-sharing, patience and understanding.

Lastly, I offer my regards to all of those who supported me in any respect during the completion of this thesis.

TABLE OF CONTENTS

LIST OF FIGURES

Images in this dissertation are presented in color

LIST OF ABBREVIATIONS

MSU: Michigan State University

APAP: n-acetyl-p-aminophenol

O3: ozone

h: hour

ALF: acute liver failure

FDA: Food and Drug Administration

NIH: National Institutes of Health

BrdU: 5-bromo-2-deoxyuridine

PH: partial hepatectomy

IL-6: interleukin-6

TNF-α: tumor necrosis factor-alpha

MIP-1α: macrophage inflammatory protein-1 alpha

MIP-2: macrophage inflammatory protein-2

IFN-γ: interferon-gamma

MCP-1: monocyte chemotactic protein-1

IL-12: interleukin-12

KC: keratinocyte-derived chemokine

IL-10: interleukin-10

IL-1(β): interleukin-1beta

NF-κB: nuclear factor-κB

STAT3: signal transducer and activator of transcription 3

GP130: glycoprotein 130

HGF: hepatocyte growth factor

TGF-α: transforming growth factor-alpha

EGF: epidermal growth factor

CCl4: carbon tetrachloride

P21: cyclin dependent kinase inhibitor

NOx: oxides of nitrogen

VOC: volatile organic compounds

EPA: Environmental Protection Agency

NAAQS: National Ambient Air Quality Standards

ELF: epithelium lining fluid

BALF: bronchoalveolar lavage

NO: nitric oxide

ALT: alanine aminotransferase

CGRP: calcitonin gene-related peptide

H&E: hematoxylin and eosin

HIF-1α: hypoxia inducible factor 1 alpha

GSH: reduced glutathione

GSSG: oxidized glutathione

TBARS: thiobarbituric acid-reactives substances

ND: not detected

CV: central vein

SE: standard error (of the mean)

PAI-1: plasminogen activator inhibitor-1

SOCS3: suppressor of cytokine signaling 3

HO-1: heme oxygenase-1

MT-1: metallothionein-1

GCLC: catalytic subunit of glutamate-cysteine ligase

G5: transverse lung section at the level of the fifth bifurcation from the axial airway

G11: transverse lung section at the level of the eleventh bifurcation from the axial airway

CCSP: Clara cell secretory protein

Vs: volume density

18S: small subunit of ribosomal RNA

GAPDH: glyceraldehyde 3-phophate dehydrogenase

COX-2: cyclooxygenase-2

Cpr: NADPH-cytochrome P450 reductase

CHAPTER 1

INTRODUCTION

I. ACETAMINOPHEN HEPATIC INJURY AND HEPATOCELLULAR REGENERATION

I – 1. Acetaminophen-induced hepatocellular injury and inflammation

Acetaminophen (N-acetyl-p-amino-phenol or APAP) is a derivative of acetanilide synthesized by Morse in the 19th century (Bertolini et al., 2006). It has been introduced into regular medical practice and marketed since the mid-twentieth century (Bertolini et al., 2006). By 1980, APAP use outweighed aspirin and phenacetin use (Bertolini et al., 2006) and became since then the most widely used over-the-counter analgesic and antipyretic drug in the United States (Larson et al., 2005). Analysis of non-prescription analgesic data from the third National Health and Nutritional Examination Survey (NHANES III, 1988–1994) showed that approximately 5% of U.S. adults reported frequent monthly use (>14 days/month) of APAP (Paulose-Ram et al., 2005; Paulose-Ram et al., 2003). In the United Kingdom, 3.2 to 3.5 billion tablets of APAP are used every year which translates to a mean of 55 tablets per person (Jones, 1998).

Prior to 1980, APAP overdose was not a major cause of acute liver failure (ALF) in the United States (Ritt et al., 1969). By the end of the 20th century however, APAP overdose was responsible for 20% of all the ALF cases (Schiodt et al., 1999). In a retrospective study between 1998 and 2003, Larson and collaborators (2005) showed that the incidence of ALF caused by APAP overdose rose from 28% in 1998 to 51% in 2003.

APAP is now the leading cause of acute liver failure (ALF) in developed countries and accounts for approximately 50% of ALF cases (Lee et al., 2008). Among these cases, 50% of APAP-related ALF were unintentional or non-suicidal which correlates with the widespread presence of this drug in analgesic over-the-counter multi-molecule preparations (Fontana, 2008). APAP is present in more than 100 over-the-counter preparations and numerous prescription drugs (Fontana, 2008). Recently, several studies suggested that APAP caused elevation of alanine aminotransferase (an indicator of liver injury) activity above normal limits in people receiving the maximal daily recommended dose of 4 g (Dart and Bailey, 2007; Watkins et al., 2006). Additionally, the Food and Drug Administration's (FDA) Adverse Event Reporting System and the Acute Liver Failure Study Group showed that APAP doses of 5 to 7.5 mg/day, close to the maximal recommended daily intake of 4 g can result in liver injury (http://www.fda.gov/AdvisoryCommittees/Calendar/ucm143083.htm). Because of this widespread presence of APAP in several composite analgesics and antipyretics and the narrow therapeutic range, a U.S. FDA working group recommended in 2009 better education of the general public about the name of this drug and its role as a liver toxin, clear indication of its name (acetaminophen and not APAP) when it's present in a multi-molecule drug and reduction of the maximal daily adult dose as well as the single adult dose (http://www.fda.gov/Drugs/DrugSafety/informationbyDrugClass/ucm165107.htm).

APAP is primarily detoxified in the liver by glucuronidation and sulfation (Bessems and Vermeulen, 2001). At therapeutic doses, only a small fraction is metabolized by cytochrome P450 isoforms (Bessems and Vermeulen, 2001). At high

doses however, more and more APAP molecules are processed by the cytochrome P450 enzymes leading to increased formation of the reactive metabolite, N-acetyl-p-benzoquinone (NAPQI) (Dahlin et al., 1984; Jollow et al., 1973; Mitchell et al., 1973a). NAPQI reacts and depletes glutathione (Mitchell et al., 1973b) and covalently binds to proteins leading to disruption of intracellular homeostasis and subsequent hepatocellular necrosis (Potter et al., 1973). APAP-induced hepatocellular necrosis has always been associated with protein covalent binding, however, there has been some evidence that protein covalent binding could occur without cell death (Tarloff et al., 1996). This led to the proposal of additional mechanisms to support or supplement the covalent modification of proteins. One of the most prominent hypotheses is the covalent modification of mitochondrial proteins and mitochondrial membrane permeability transition resulting in oxidative stress (Haouzi et al., 2002). In addition to oxidative stress, reactive nitrogen species such as peroxynitrite have also been detected in hepatocytes and endothelial cells after APAP overdose (Hinson et al., 1998; Hinson et al., 2004; Knight et al., 2001). Finally, mitochondrial and nuclear DNA damage have been associated with APAP overdose (Cover et al., 2005; Ray et al., 1990).

APAP overdose primarily targets the liver in mammals including laboratory mice and results in centrilobular hepatocellular necrosis (Bessems and Vermeulen, 2001; Black, 1984; Clark et al., 1973; Davis et al., 1974; Dixon et al., 1975; Dixon et al., 1971; Hinson et al., 1981; Placke et al., 1987a; Portmann et al., 1975). The preferential location of liver lesion around the central vein is thought to be associated with its greater regional content in cytochrome P450 isoforms, particularly CYP2E1 and its smaller oxygen supply (Hart et al., 1995). Placke and collaborators (1987a) showed that early in the

course of toxicity, ultrastructural changes in mitochondria and plasma membranes were among the most specific changes induced by APAP administration, in accordance with the covalent protein binding mechanisms. Neutrophil accumulation in necrotic regions after APAP overdose has been described since the early mechanistic studies of the APAP covalent binding hypothesis (Mitchell et al., 1973a). Infiltration of neutrophils in damaged areas followed the APAP centrilobular lesion in mice suggesting that neutrophils are recruited as scavengers of necrotic hepatocytes and did not initiate APAP damage (Bauer et al., 2000; Lawson et al., 2000). Others reported that depletion of neutrophils protected from APAP-induced liver injury in mice, suggesting that neutrophils are important at least in APAP lesions progression (Liu and Kaplowitz, 2005; Liu et al., 2004). At a dose of 300 mg/kg of body weight, the initial APAP-induced injury was first detected between 2 and 4 h after administration and continued to increase up to 24 h post-injection (Cover et al., 2006; Gujral et al., 2002). At the same dose of APAP, hepatocellular damage completely resolved by 72 h post-APAP in most strain of mice (Donahower et al., 2006; James et al., 2003).

I – 2. Hepatocellular repair after hepatectomy or chemical injury

The most frequently used model in liver regeneration is the rodent partial hepatectomy (PH) model (Martins et al., 2008). In this model, two-thirds of the liver are surgically removed and hepatocellular regeneration is studied and has been shown to proceed from remnant hepatocytes (Pahlavan et al., 2006). After partial hepatectomy in mice, bromodeoxyuridine (BrdU)-labeled hepatocytes (cells in S phase of the cell cycle)

begin to increase around 32 h post-hepatectomy and reach a maximum 48 h after hepatectomy (Satyanarayana et al., 2004; Wustefeld et al., 2000). At 72 h after hepatectomy, a very small proportion of hepatocytes were positive for BrdU immunostaining similar to non-hepatectomized mice.

Using this model, it has been established that the priming phase (first few hours after PH corresponding to the transition from the interphase or G0 to the first phase G1 of the cell cycle) of liver regeneration is under the control of cytokines (tumor necrosis factor-alpha or TNF-α and interleukin-6 or IL-6) (Fausto et al., 2006; Taub, 2004). TNF-α and IL-6 involvement in priming regeneration was supported by various findings including increase of these cytokines in the liver and serum after PH, the activation of several target transcriptions factors (Nuclear Factor-κB or NF-κB, Signal Transducer and Activator of Transcription-3 or STAT-3), the inhibition of liver regeneration after treatment with an anti-TNF-α antibody or in tumor necrosis factor receptor 1 or IL-6 KO mice and rescue of this inhibition by administration of IL-6 in the last case (Fausto et al., 2006). The role of TNF-α is to regulate IL-6 responsible for the priming phase (Michalopoulos and DeFrances, 1997). Subsequent to the initiation/priming phase, growth factors such hepatocyte growth factor (HGF), transforming growth factor-alpha (TGF-α) or epidermal growth factor (EGF) lead to the progression of primed hepatocytes through the remaining phases of the cell cycle (Pahlavan et al., 2006).

Most studies today agree that the role of IL-6 in liver regeneration is pro-proliferative. Mice deficient in IL-6 exhibited hepatocellular necrosis and degeneration as well as greater mortality after partial hepatectomy compared to IL-6 sufficient hepatectomized mice (Cressman et al., 1996). In the same study, IL-6 deficient

hepatectomized mice had 20 to 25% less BrdU-labeled hepatocytes compared to wild type hepatectomized mice. Administration of exogenous IL-6 in deficient mice rescued defective tissue regeneration and prevented necrosis. In another study, IL-6 deficient mice had impaired liver regeneration at 36, 48 and 60 h post-hepatectomy compared to IL-6 sufficient hepatectomized mice (Sakamoto et al., 1999). Similarly, mice deficient in IL-6 exhibited a high rate of mortality and IL-6 injection significantly decreased the rate of mortality in these mice (Blindenbacher et al., 2003). However, in this last case, only subcutaneous injection of recombinant IL-6 (sustained action of IL-6) rescued deficient mice while intravenous (short-acting) IL-6 injection did not show this effect. IL-6 has also been shown to be important in liver regeneration following chemical toxicity including APAP hepatotoxicity. Acute exposure to carbon tetrachloride (CCl4) resulted in greater hepatocellular injury, apoptosis and impaired regeneration in IL-6 deficient mice compared to similarly treated sufficient mice 36 or 48 h post-treatment (Kovalovich et al., 2000). In this study, IL-6 administration corrected liver regeneration in IL-6 deficient mice given CCl4. Finally, IL-6 deficient mice given 300 mg/kg of APAP exhibited greater hepatocellular damage but lower hepatic regenerative capacities relative to IL-6 wild type mice 48 h after APAP administration (James et al., 2003).

In addition to the expression of IL-6 in the liver, others studies showed that high systemic IL-6 levels could impair proliferation. Wustefeld and collaborators (2000) for instance used mice overexpressing the human IL-6 receptor in hepatocytes and stimulated those mice with human recombinant IL-6 3 h before hepatectomy. In these mice, STAT-3 was activated for more than 72 h whereas in unstimulated mice this elevation was limited to few early hours and liver regeneration was impaired as measured by BrdU

incorporation and Cyclin A and E expression (Wustefeld et al., 2000). Because STAT-3 controls the expression of cyclin-dependent kinase inhibitor P21, a known cell cycle inhibitor, expression at the transcriptional level, this team investigated the level of P21 and showed that IL-6 stimulation in transgenic mice overexpressing the IL-6 receptor resulted in increased P21 protein 6 h post-hepatectomy (Wustefeld et al., 2000).

I – 3. APAP-induced injury in the lung

APAP overdose also causes toxicity in other organ systems in laboratory animals and people including the upper and lower respiratory tract (Amatya et al., 2002; Baudouin et al., 1995; Dimova et al., 2005; Dimova et al., 2000; Genter et al., 1998; Jeffery and Haschek, 1988; Khanlou et al., 1999; Neff et al., 2003; Placke et al., 1987b). The morphologic hallmark of acute APAP overdose is epithelial degeneration and necrosis regardless of the tissue involved. In vitro, freshly isolated type II pneumocytes exposed to subtoxic doses of APAP exhibited dose-dependent increase in cytotoxicity and loss of intracellular glutathione (Dimova et al., 2000). In vivo, mice given APAP showed pulmonary bronchioles as well as nasal olfactory and respiratory epithelium and lateral nasal glands necrosis (Gu et al., 2005; Neff et al., 2003; Placke et al., 1987b).

Bartolone and collaborators (1989) showed that APAP-protein adducts were detected by western blotting only in organs where toxicity was observed (liver, lung and kidneys). In this study, the severity of tissue damage and the amount of protein adducts were reduced in those target tissues when mice were pre-treated with a mixed function oxidase inhibitor (Bartolone et al., 1989). In the lung, Clara cells have the highest level of

cytochrome P450s (Amatya et al., 2002; Devereux et al., 1989; Massaro et al., 1994) and are therefore potential sites for APAP bioactivation. In mice deficient in liver-specific NADPH-cytochrome P450 reductase (cpr), the electron donor of microsomal P450s, the severity of lung lesions was decreased while liver toxicity was abrogated suggesting that liver metabolism was only partially involved in APAP-induced airway epithelial damage (Gu et al., 2005). This result also suggests that local pulmonary APAP bioactivation is possible as lung toxicity was not completely eliminated in those cpr null mice. In the lung, expression of two isoforms responsible for hepatic APAP bioactivation, namely CYP2E1 and CYP1A2, or their activity have been identified (Dey et al., 1999; Forkert et al., 2001; Stoilov et al., 2006).

II. OZONE LOCAL AND SYSTEMIC EFFECTS AND AIRWAY REGENERATION

II – 1. Ozone-induced epithelial injury and inflammation in the lung

Ozone (O3) is the principal oxidant air pollutant in photochemical smog. It is formed at ground level by a chemical reaction of oxides of nitrogen (NOx) and volatile organic compounds (VOC) and oxygen in the presence of sunlight. Motor vehicle exhaust and industrial emissions, gasoline vapors, and chemical solvents as well as natural sources are the main sources of NOx and VOC (EPA, 2008). People are continuously exposed to O3 at levels detected in their geographical location. In 1997, the U.S. Environmental Protection Agency (U.S. EPA) set an air quality standard of 0.08 ppm for O3 for a 24-hour period. In 2006, this standard was revised based on a growing

number of geographical areas regularly exceeding the national standards and recent scientific knowledge of O3 effects on public health. This standard has since been lowered to 0.075 ppm for the same period of time

(EPA, http://www.epa.gov/air/O3pollution/naaqsrev2007.html). Elevated O3 levels exceeding the National Ambient Air Quality Standards (NAAQS) are commonly reported in heavily populated areas in Northeastern, Midwestern and Southwestern USA (Graham, 2004). The U.S. EPA reported that 474 counties have been designated as nonattainment zones (regions that do not meet the air quality standards) with an estimate of 159 million people living in those areas

(EPA, http://www.epa.gov/air/O3pollution/naaqsrev2007.html).

Pryor in 1992 demonstrated that O3 itself does not cross the airway epithelium lining fluid (ELF) where its thickness is greater than 0.1 μm. The thickness of this fluid varies from 20 to 0.1 μm across the airway tree and is patchy, lacking in some areas in the distal airway compartments (Pryor, 1992). In areas devoid of ELF, Pryor (1992) showed that O3 reacts with cell membranes and does not exit airway epithelial cells. In the ELF, O3 first reacts with antioxidants such as glutathione, uric acid, ascorbate and vitamin E (Mudway and Kelly, 2000). In a series of subsequent papers, Pryor showed that part of inhaled O3 not neutralized by small molecular weight antioxidants reacts with ELF or cell membrane lipids and generates secondary less reactive but longer-lasting derivatives (Pryor, 1994; Pryor et al., 2006; Pryor et al., 1995a, b). In this process, peroxidation of membrane lipids by O3 generates lipid ozonation products (aldehydes, hydroxyhydroperoxides and the criegee ozonide), probably the most important derivatives at the origin of O3-induced epithelial injury (Mudway and Kelly, 2000; Pryor

et al., 1995a). Indeed, these lipid ozonation products lead to the production of eicosanoids, platelet-activating factors, reactive oxygen species (hydrogen peroxides, hydroperoxides, etc) and cytokines responsible for O3-induced toxic effects (Pryor et al., 1995b).

In people, O3 inhalation in both environmental and experimental settings resulted in lung function decrement, inflammation and epithelial damage and compromised antioxidant concentrations in the ELF (Avissar et al., 2000; Calderon-Garciduenas et al., 2000; Holz et al., 1999; Jorres et al., 2000; Koren et al., 1989; Krishna et al., 1998; Lippmann and Schlesinger, 2000; Mudway et al., 1999; Seltzer et al., 1986). Exposure of healthy subjects to 0.3 ppm for 1 h during heavy exercise for instance resulted in neutrophil accumulation in the BALF that started at 1 h post-exposure and was maximal between 6 and 24 h post-exposure (Schelegle et al., 1991). Similarly, O3 exposure at high ambient concentrations (0.08 to 0.1 ppm) for 6.6 h was enough to initiate airway inflammatory responses in healthy subjects (Devlin et al., 1991). The effects of slightly greater levels of O3 on neutrophil infiltration in bronchial biopsies have subsequently been confirmed by morphometric evaluation (Aris et al., 1993). O3 is also a health hazard for people with pre-existing lung conditions (Bell et al., 2004; Cody et al., 1992; Fauroux et al., 2000; Friedman et al., 2001; Hiltermann et al., 1998; Thurston et al., 1992; Tolbert et al., 2000; White et al., 1994). Usually, asthmatic people have their symptoms exacerbated upon O3 inhalation (Blomberg, 2000). Exposure of subjects with mild allergic asthma to 0.25 ppm O3 for 3 h with intermittent exercise, exacerbated their bronchial allergen responsiveness 3 h after exposure. Although lower doses of O3 (0.2 ppm) for slightly shorter time (2 h of exposure and evaluation 6 h post-exposure) seemed

to contradict this effect (Jorres et al., 1996; Stenfors et al., 2002). Repeated exposure to O3 at similar levels also enhanced functional and inflammatory responses of people with pre-existing allergic asthma (Holz et al., 2002). Finally increased asthma symptoms and medication was reported by physician in children during peak O3 concentrations in Los Angeles, California (Avol et al., 1998).

In non-human primates, exposure to 0.8 ppm of O3 resulted in ciliated cells and type I cells loss in the centriacinar region (Castleman et al., 1980). Similarly, exposure to 0.96 ppm of O3 for 8 h resulted in tracheal and respiratory bronchiolar epithelial necrosis as early as 1 h and became maximal between 12 and 24 h post-exposure. Exposure to 1 ppm of O3 for 2 h resulted in increased neutrophils in the bronchoalveolar lavage (BALF) 2 h post-exposure (Plopper et al., 1998). Lung tissue and BALF neutrophil accumulation has been shown to be maximal at the time of epithelial necrosis around 12 h post-exposure and continued up to 24 h (Hyde et al., 1992). Plopper and co-workers (1998) found that O3 dose to tissue concentration was greatest in the terminal part of the airway tree where epithelial necrosis was maximal. In the same study, O3 dosimetry inversely correlated with the content in glutathione in the respiratory bronchioles. With longer duration of exposures (6 days at 0.15 ppm of O3), monkeys exhibited epithelial respiratory bronchioles hyperplasia along with an influx of macrophages and thickening of the underlying lamina propria due to an increase in cellular and acellular components (Harkema et al., 1993). In infant rhesus monkeys, cyclic exposure to O3 with or without house dust mite resulted in an array of airway changes that could predispose or aggravate airways to asthma later in life (Plopper et al., 2007) (reduced airway number, hyperplasia of bronchial epithelial cells, mucus cell hyperplasia, disorientation and change in

abundance of smooth muscle cells in distal pulmonary airways, interrupted basement membrane development, modifications of airway nerve fiber distribution and reorganization of the airway vascular and immune systems).

In rodents, acute or subacute exposure to O3 caused morphologic changes in the distal regions of the airway tree, particularly the distal airways and proximal alveolar ducts (centriacinar region or junction of the bronchioles with alveoli) (Boorman et al., 1980; Castleman et al., 1980; Dungworth et al., 1975; Mellick et al., 1975). This effect of O3 in distal pulmonary regions seems to be related to the O3 dose to tissues which has been found to be greater in terminal bronchioles and proximal alveolar regions as also described in non-human primate studies (Kimbell and Miller, 1999; Medinsky and Bond, 2001; Miller et al., 1978; Postlethwait et al., 2000). In an earlier study, rats exposed to 0.5 ppm of O3 developed loss of epithelial cells and type I pneumocytes in terminal bronchioles ciliated as early as after 2 h after exposure (Stephens et al., 1978). O3 effects in rats have been confirmed in subsequent studies where acute exposures to 0.5 to 1 ppm caused centriacinar epithelial cells degeneration, necrosis and sloughing off 4 h after the initiation of exposure (Pino et al., 1992; Sterner-Kock et al., 2000; Vesely et al., 1999). In those regions, ciliated cells in the terminal bronchioles and type I pneumocytes are the most susceptible cells to acute O3 exposure in rodents (Pino et al., 1992; Sterner-Kock et al., 2000). Dormans and colleagues reported that Clara cells were also affected with subacute O3 exposures (3 days of continuous exposure to 0.4 ppm of O3) (Dormans et al., 1999; Schwartz et al., 1976). An acute neutrophilic inflammatory infiltration followed in subacute cases by infiltration of macrophages is usually associated with O3 epithelial damage (Pino et al., 1992; Vesely et al., 1999). In mice, exposure to 2 ppm of O3 for 3 h

led to increased number of neutrophils in the BALF (Savov et al., 2004). In the C57BL/6 mice strain, this number of neutrophils first increased at 6 h and was maximal 24 h post-exposure. Exposure of mice to 0.3 ppm O3 for 48 continuous hours resulted in neutrophils infiltration in the BALF at the end of the exposure (Kleeberger et al., 1997). In these mice, neutrophil infiltration resolved by 48 h after the end of exposure.

In support of O3 role as an inflammagen, its exposure was also associated with an elevation of various proinflammatory cytokines. Alveolar macrophages were collected from rats exposed to 2 ppm O3 for 3 h and grown in vitro (Laskin et al., 1994; Pendino et al., 1994). Culture media from these alveolar macrophages showed greater amounts of TNF-α and interleukin-1 (IL-1) 48 h after the end of exposure when compared to filtered air controls. Alveolar macrophages isolated from guinea pigs exposed to 0.3 ppm O3 for 1 h had increased IL-6, TNF-α, interleukin (IL-8) and IL-1β (Arsalane et al., 1995). A lower concentration of O3 (0.1 ppm) caused these macrophages to release only TNF-α. Exposure of 129 mice to 1 ppm O3 for various times resulted in IL-6 mRNA increase in the lung starting at 2 h and maximal at 4 h (Mango et al., 1998). In C57BL/6J mice, exposure to 1 ppm O3 for 4 h or 2.5 ppm for 2 h increased the expression of IL-6 mRNA in the lung (Johnston et al., 1999). In the same study, macrophage inflammatory protein-1 alpha (MIP-1α) and macrophage inflammatory protein-2 (MIP-2) chemokines expression in the lung were also increased in mice exposed to O3. In a study by Vincent and collaborators (1996) using F344 rats and different O3 concentrations (0.4 or 0.8 ppm) and time points (2 versus 6 h), IL-6 protein level in the BALF fluid was elevated by O3 exposure. The elevation of IL-6 increased with the age of animals (from 2 months to 9 months to 24 months) and with the dose of O3 (Vincent et al., 1996).

II – 2. Ozone effects in the liver

O3-induced systemic changes are less well defined compared to their respiratory effects. Early studies showed that O3 exposure was associated with prolonged pentobarbital sleeping time in mice, rats and hamsters, this effect being more pronounced in females compared to males (Graham et al., 1981). Prolongation of sleeping time has been subsequently shown to be age-dependent and present in 18 months aged females but not in young mice (2.5 months of age) exposed to O3 (Canada et al., 1986). In a recent study by Last and collaborators (2005), exposure of C57BL/6 mice to 1 ppm O3, 8 h a day for 3 days resulted in a 14% decrease in body weight associated with a 42% decrease in total food consumption. In this study, O3 exposure also resulted in a significant downregulation of several cytochrome P450 mRNAs expression, including 1A2, 2A4, 2C9, 3A11, 8B1, 7B1, 2D11, 2D10 and 3A16 (Last et al., 2005). CYP4A14 was the only isoform whose expression was upregulated in this study. One of the conclusions drawn from this study was that the pentobarbital-increased sleeping time reported in previous studies was probably related to lower metabolic levels of cytochromes P450s enzymes in the liver. This team considered interferon-gamma (IFN-γ) as a candidate for the lung-liver interaction as several IFN-γ-dependent genes were downregulated in the liver of O3-exposed mice. One of the first reviews published on extrapulmonary effects of O3 was by Goldstein (1978) several decades ago. It was reported in this study that as O3 itself is too reactive to reach the bloodstream, the extrapulmonary effects are probably related to secondary products generated upon the interaction of O3 with ELF or cell membrane (Goldstein, 1978). Three groups of derivatives were discussed including reactive oxygen

species. According to Goldstein, reactive oxygen species are too reactive and short-lived (e.g. hydroxyl radical and singlet oxygen) or neutralized by enzymatic or non-enzymatic cell antioxidant cell defense mechanisms (e.g. superoxide and hydrogen peroxide). The second group of derivatives described was the products of interaction between O3 and polyunsaturated fatty acids (lipid hydroperoxides, endoperoxides and ozonides). Those were theoretically too bulky or hydrophobic to propagate O3 effects to some distance in the hydrophilic ELF or intracellular environment. Goldstein considered the third groups of derivatives whom he called end products (e.g. carbonyls such as malonaldehyde) to be the most promising due to their relative hydrophilicity and the absence of specific detoxification mechanisms in cells. We today know that this is not entirely the case as several mechanisms for the detoxification of carbonyls have been since described (Yin, 2000) and as the second group called lipid derivatives have been shown to play an important role in O3 toxicity at least in the respiratory system (Pryor et al., 1995a).

Others have suggested that signaling molecules generated from lung epithelial or alveolar macrophages and particularly cytokines such as TNF-α could be the mediators of O3 distant (and particularly liver) effects (Laskin et al., 1998). Laskin and colleagues (1998) exposed rat to O3 in the range of 0.5 to 2 ppm for 3 h followed by isolation and culture of hepatocytes 48 h post-exposure. This team showed greater nitric oxide (NO) production and protein synthesis by these cells when exposed to O3 alone or O3 followed by additional inflammatory stimuli (interferon-gamma or lipopolysaccharide) compared to hepatocytes isolated from air-exposed rats. They hypothesized that because some of the best known stimuli for NO or protein synthesis in hepatocytes are TNF-α and interleukin-1, those cytokines are the most likely mediators of O3 hepatic effects. In the

same study, NO and TNF-α were also produced in excess by alveolar macrophages in O3-exposed animals. Laskin and collaborators later suggested that at least in the lung, TNF-α has deleterious effects upon O3 exposure specially through activation of NF-κB and induction of NO and peroxinitrite (Roberts et al., 2009).

II – 3. Airway epithelium regeneration after injury

O3-induced airway epithelial injury in rodents is followed by epithelial regeneration as in any other organ. In the nose for instance, epithelial proliferation in rats exposed to 0.5 ppm for 8 h was first detected in the transitional epithelium at 12 h post-exposure and was maximal at 20 h (Hotchkiss et al., 1997). At 36 h, BrdU labeling indices were still above baseline levels in these rats. In the lung, rats exposed to 0.4 ppm O3 during 12 h had a significant elevation of the number of cycling epithelial cells in terminal bronchioles (van Bree et al., 2002). Similarly, rats exposed to 0.96 ppm O3 for 3 consecutive days exhibited an increase of radiolabeled thymidine indices in upper and lower parts of the tracheal epithelium at the end of exposure (Nikula et al., 1988). In C57BL/6 mice, acute (2 ppm for 3 h) or subacute (0.5 ppm for 24 h) O3 exposure caused significant elevation of BrdU-labeled cells in terminal bronchioles at the end of exposure (Longphre et al., 1999; Yu et al., 2002). At 10 days no more proliferation was observed in these airways. The renewal rate of the bronchiolar epithelium in mammals is very low and increased BrdU labeling usually reflects compensatory epithelial regeneration after induced cell demise (Evans, 1982; Kauffman, 1980; Stripp and Reynolds, 2008).

Murine axial airway are populated by ciliated, Clara and pulmonary neuroendocrine cells with a small number of basal cells whereas terminal bronchioles are mainly lined by Clara cells associated with a smaller proportion of ciliated cells (Liu et al., 2006; Plopper and Hyde, 2008). Most of what is known in cellular regeneration of the bronchiolar airway epithelium in mice has been done using a naphthalene toxicity model. This substance targets the Clara cells, particularly those containing the cytochrome P450 2F2 isoform (Plopper et al., 1992). Within 2 to 3 h after administration almost all Clara cells expressing the cytochrome P450 2F2 were killed and proliferation of variant Clara cells not expressing the above mentioned isoform began within 2 days and was complete by 2 weeks (Buckpitt et al., 1995; Stripp et al., 1995; Van Winkle et al., 1995). Basal cells and Clara cells in the axial airway and Clara cell in the more distal terminal bronchioles are probably the main regenerative cells within murine airways. Basal cells have been shown to repopulate naphthalene-injured airways in an inducible Cre-lox mice model under the control of cytokeratin 14 promoter (marker of basal cells) (Hong et al., 2004a, b). In the more distal airways, two airway microenvironments or niches populated by cells expressing Clara cell secretory protein and resistant to naphthalene injury (because lacking the cytochrome P450 2F2) have been identified and their cell population are called variant Clara cells. The first niche co-localized with neuroendocrine bodies (Hong et al., 2001; Reynolds et al., 2000a; Reynolds et al., 2000b) and the second one has been identified at the bronchoalveolar junction (Giangreco et al., 2002). These variant Clara cells are regarded as facultative progenitor cells capable of dividing on demand after an injury and regenerate both ciliated and fully differentiated Clara cells (Evans et al., 1978; Evans et al., 1976; Giangreco et al., 2009; Stripp and Reynolds, 2008; Zemke et

al., 2009). The main difference between these cells and an undifferentiated progenitor cell is the expression of differentiation markers detected in the former group (secretoglobin, family 1A, member 1 or SCGB1A1, calcitonin gene-related peptide or CGRP and pulmonary surfactant-associated protein C or SFTPC) (Rawlins and Hogan, 2006).

At the molecular level, mechanisms behind the induction of basal or Clara cell differentiation (and maybe "dedifferentiation" in the case of Clara cells) into their progeny are not well characterized. Numerous factors from different sources (respiratory epithelial cells, extracellular matrix and particularly the basement membrane and cellular and acellular components of the underlying subepithelial connective tissue) have been identified in the induction of epithelial cell regeneration and differentiation and thoroughly reviewed elsewhere (Coraux et al., 2005; Jetten, 1991). Several growth factors, their receptors or cytokines have been involved in respiratory epithelial migration (epidermal growth factor receptor, hepatocyte growth factor, keratinocyte growth factor, interleukin-1α and β) or proliferation and differentiation (epidermal growth factor, trefoil factor family 2, heregulin-α, monocyte chemoattractant protein-1 and platelet-derived growth factor) (Coraux et al., 2005). More recently, mice deficient in the signal transducer and activator of transduction 3 (STAT3, a transcription factor involved in IL-6 signaling) or glycoprotein 130 or GP130 (a co-receptor for the IL-6 family of cytokines) were unable to restore their bronchioles epithelial cell shape and number after naphthalene injury (Kida et al., 2008). The Wnt/β-catenin signaling pathway induction or inhibition is usually associated with stimulation or arrest of epithelial regeneration (Stripp and Reynolds, 2008). Recent studies showed that β-catenin is not involved in the

maintenance or repair of bronchiolar epithelium in mice exposed to naphthalene (Zemke et al., 2009). In this study, β-catenin deficient or sufficient mice exhibited similar regenerative epithelial units in specific niches of the bronchiolar epithelium, similar mitotic indices and similar restoration of this epithelium after damage. Finally, pretreatment of mice with an antagonist of CGRP receptor protected from O3-induced terminal bronchioles injury and at the same time reduced cell proliferation (Oslund et al., 2009). This team concluded that CGRP contributed to epithelial injury and repair after O3 exposure.

III. OVERALL HYPOTHESIS AND SPECIFIC AIMS

APAP targets the liver but also affects the lung and particularly Clara cells responsible for xenobiotic metabolism and protection from oxidative injury. In addition, these cells have a progenitor potential and are responsible for regeneration of themselves but also airway ciliated cells after injury. O3 also targets the airway epithelium but the ciliated cells are the prime targets. O3 inhalation also results in systemic effects and more and more data are becoming available to strengthen a novel role of O3 in liver pathobiology. We therefore sought to study the coexposure of APAP and O3 in the liver and in the lung.

The main hypothesis of my work was that O3 exposure exacerbates APAP-induced hepatocellular and pulmonary airway epithelial injury. The specific aims are:

Aim 1: to determine the effects of a single exposure of O3 on acute APAP-induced hepatic toxicity.

Aim 2: to determine the effects of a single exposure of O3 on acute APAP-induced pulmonary airway toxicity.

Aim 3: to determine the role of interleukin-6 in the acute APAP and O3 induced hepatic and pulmonary airway toxicity and repair.

To address aims 1 and 2, I used C57BL/6 mice as an animal model. Mice were fasted overnight and then injected saline or 300 mg/kg of APAP intraperitoneally. Two hours later, I exposed those mice to filtered air or to 0.25 or 0.5 ppm O3 for 6 h. Nine (1 h after O3) or 32 h (24 h after O3) after the APAP or saline administration, mice were euthanized. Before the latter sacrifice time, mice were injected intraperitoneally bromodeoxyuridine to label proliferating hepatocellular or airway epithelial cells. I utilized histopathological, histochemical (intracellular glycogen staining using the periodic acid Schiff) or immunohistochemical (neutrophils, bromodeoxyuridine for epithelial cell proliferation, Clara cell secretory protein and hypoxia inducible factor-1) and morphometric techniques to characterize and quantitate hepatocellular and pulmonary airway injury. In addition, molecular (real time PCR for gene expression analysis), biochemical (glutathione and thiobarbituric acid-reactive substances commercial kits used as indicators of oxidative stress induction) and immunological (cytokines evaluation by flow cytometry) methods have been used to explore plausible mechanisms behind O3 potentiation of APAP-induced epithelial injury.

In the liver, I found that O3 potentiated APAP-induced hepatocellular injury. I also observed that APAP and O3 when associated inhibited cell regeneration, a mechanism that might have contributed to O3 potentiation of APAP hepatic injury. I observed in aims 1 and 2 that IL-6 gene expression was elevated in the lung and plasma

in mice given APAP and O3 but not changed in the liver of these animals. At the same time, APAP alone caused increased expression of IL-6 in the liver. As stated previously, IL-6 is important in liver regeneration and in aim 3, I tested the hypothesis that IL-6 induced by APAP alone treatment but not by APAP and O3 coexposure might be the main contributor to the impaired regeneration in the latter group. To do so, I used an experimental design similar to the one described for aims 1 and 2 and compared the effects of APAP and O3 in IL-6 deficient and sufficient C57BL/6 mice. The results of these studies demonstrate for the first time that a high ambient O3 concentration could potentiate locally (respiratory tract) but also systemically (liver) the effects of APAP and may pose a risk to people with pre-existing liver or lung diseases.

IV. REFERENCES

Alexis, N., Urch, B., Tarlo, S., Corey, P., Pengelly, D., O'Byrne, P., Silverman, F., 2000. Cyclooxygenase metabolites play a different role in ozone-induced pulmonary function decline in asthmatics compared to normals. Inhal Toxicol 12, 1205-1224.

Amatya, B.M., Kimula, Y., Koike, M., 2002. The Clara cells activated by acetaminophen. J Med Dent Sci 49, 103-108.

Araujo, J.A., Barajas, B., Kleinman, M., Wang, X., Bennett, B.J., Gong, K.W., Navab, M., Harkema, J., Sioutas, C., Lusis, A.J., Nel, A.E., 2008. Ambient particulate pollutants in the ultrafine range promote early atherosclerosis and systemic oxidative stress. Circ Res 102, 589-596.

Aris, R.M., Christian, D., Hearne, P.Q., Kerr, K., Finkbeiner, W.E., Balmes, J.R., 1993. Ozone-induced airway inflammation in human subjects as determined by airway lavage and biopsy. Am Rev Respir Dis 148, 1363-1372.

Arsalane, K., Gosset, P., Vanhee, D., Voisin, C., Hamid, Q., Tonnel, A.B., Wallaert, B., 1995. Ozone stimulates synthesis of inflammatory cytokines by alveolar macrophages in vitro. Am J Respir Cell Mol Biol 13, 60-68.

Avissar, N.E., Reed, C.K., Cox, C., Frampton, M.W., Finkelstein, J.N., 2000. Ozone, but not nitrogen dioxide, exposure decreases glutathione peroxidases in epithelial lining fluid of human lung. Am J Respir Crit Care Med 162, 1342-1347.

Avol, E.L., Navidi, W.C., Rappaport, E.B., Peters, J.M., 1998. Acute effects of ambient ozone on asthmatic, wheezy, and healthy children. Res Rep Health Eff Inst, iii, 1-18; discussion 19-30.

Bartolone, J.B., Beierschmitt, W.P., Birge, R.B., Hart, S.G., Wyand, S., Cohen, S.D., Khairallah, E.A., 1989. Selective acetaminophen metabolite binding to hepatic and extrahepatic proteins: an in vivo and in vitro analysis. Toxicol Appl Pharmacol 99, 240-249.

Baudouin, S.V., Howdle, P., O'Grady, J.G., Webster, N.R., 1995. Acute lung injury in fulminant hepatic failure following paracetamol poisoning. Thorax 50, 399-402.

Bauer, I., Vollmar, B., Jaeschke, H., Rensing, H., Kraemer, T., Larsen, R., Bauer, M., 2000. Transcriptional activation of heme oxygenase-1 and its functional significance in acetaminophen-induced hepatitis and hepatocellular injury in the rat. J Hepatol 33, 395-406.

Bell, M.L., McDermott, A., Zeger, S.L., Samet, J.M., Dominici, F., 2004. Ozone and short-term mortality in 95 US urban communities, 1987-2000. JAMA 292, 2372-2378.

Bertolini, A., Ferrari, A., Ottani, A., Guerzoni, S., Tacchi, R., Leone, S., 2006. Paracetamol: new vistas of an old drug. CNS Drug Rev 12, 250-275.

Bessems, J.G., Vermeulen, N.P., 2001. Paracetamol (acetaminophen)-induced toxicity: molecular and biochemical mechanisms, analogues and protective approaches. Crit Rev Toxicol 31, 55-138.

Black, M., 1984. Acetaminophen hepatotoxicity. Annu Rev Med 35, 577-593.
Blindenbacher, A., Wang, X., Langer, I., Savino, R., Terracciano, L., Heim, M.H., 2003. Interleukin 6 is important for survival after partial hepatectomy in mice. Hepatology 38, 674-682.

Blomberg, A., 2000. Airway inflammatory and antioxidant responses to oxidative and particulate air pollutants - experimental exposure studies in humans. Clin Exp Allergy 30, 310-317.

Boorman, G.A., Schwartz, L.W., Dungworth, D.L., 1980. Pulmonary effects of prolonged ozone insult in rats. Morphometric evaluation of the central acinus. Lab Invest 43, 108-115.

Buckpitt, A., Chang, A.M., Weir, A., Van Winkle, L., Duan, X., Philpot, R., Plopper, C., 1995. Relationship of cytochrome P450 activity to Clara cell cytotoxicity. IV. Metabolism of naphthalene and naphthalene oxide in microdissected airways from mice, rats, and hamsters. Mol Pharmacol 47, 74-81.

Calderon-Garciduenas, L., Devlin, R.B., Miller, F.J., 2000. Respiratory tract pathology and cytokine imbalance in clinically healthy children chronically and sequentially exposed to air pollutants. Med Hypotheses 55, 373-378.

Canada, A.T., Calabrese, E.J., Leonard, D., 1986. Age-dependent inhibition of pentobarbital sleeping time by ozone in mice and rats. J Gerontol 41, 587-589.

Castleman, W.L., Dungworth, D.L., Schwartz, L.W., Tyler, W.S., 1980. Acute respiratory bronchiolitis: an ultrastructural and autoradiographic study of epithelial cell injury and renewal in rhesus monkeys exposed to ozone. Am J Pathol 98, 811-840.

Clark, R., Borirakchanyavat, V., Davidson, A.R., Thompson, R.P., Widdop, B., Goulding, R., Williams, R., 1973. Hepatic damage and death from overdose of paracetamol. Lancet 1, 66-70.

Cody, R.P., Weisel, C.P., Birnbaum, G., Lioy, P.J., 1992. The effect of ozone associated with summertime photochemical smog on the frequency of asthma visits to hospital emergency departments. Environ Res 58, 184-194.

Coraux, C., Hajj, R., Lesimple, P., Puchelle, E., 2005. [Repair and regeneration of the airway epithelium]. Med Sci (Paris) 21, 1063-1069.

Corradi, M., Alinovi, R., Goldoni, M., Vettori, M., Folesani, G., Mozzoni, P., Cavazzini, S., Bergamaschi, E., Rossi, L., Mutti, A., 2002. Biomarkers of oxidative stress after controlled human exposure to ozone. Toxicol Lett 134, 219-225.

Cover, C., Liu, J., Farhood, A., Malle, E., Waalkes, M.P., Bajt, M.L., Jaeschke, H., 2006. Pathophysiological role of the acute inflammatory response during acetaminophen hepatotoxicity. Toxicol Appl Pharmacol 216, 98-107.

Cover, C., Mansouri, A., Knight, T.R., Bajt, M.L., Lemasters, J.J., Pessayre, D., Jaeschke, H., 2005. Peroxynitrite-induced mitochondrial and endonuclease-mediated nuclear DNA damage in acetaminophen hepatotoxicity. J Pharmacol Exp Ther 315, 879-887.

Cressman, D.E., Greenbaum, L.E., DeAngelis, R.A., Ciliberto, G., Furth, E.E., Poli, V., Taub, R., 1996. Liver failure and defective hepatocyte regeneration in interleukin-6-deficient mice. Science 274, 1379-1383.

Dahlin, D.C., Miwa, G.T., Lu, A.Y., Nelson, S.D., 1984. N-acetyl-p-benzoquinone imine: a cytochrome P-450-mediated oxidation product of acetaminophen. Proc Natl Acad Sci U S A 81, 1327-1331.

Dart, R.C., Bailey, E., 2007. Does therapeutic use of acetaminophen cause acute liver failure? Pharmacotherapy 27, 1219-1230.

Davis, D.C., Potter, W.Z., Jollow, D.J., Mitchell, J.R., 1974. Species differences in hepatic glutathione depletion, covalent binding and hepatic necrosis after acetaminophen. Life Sci 14, 2099-2109.

Desqueyroux, H., Pujet, J.C., Prosper, M., Le Moullec, Y., Momas, I., 2002. Effects of air pollution on adults with chronic obstructive pulmonary disease. Arch Environ Health 57, 554-560.

Devereux, T.R., Domin, B.A., Philpot, R.M., 1989. Xenobiotic metabolism by isolated pulmonary cells. Pharmacol Ther 41, 243-256.

Devlin, R.B., McDonnell, W.F., Mann, R., Becker, S., House, D.E., Schreinemachers, D., Koren, H.S., 1991. Exposure of humans to ambient levels of ozone for 6.6 hours causes cellular and biochemical changes in the lung. Am J Respir Cell Mol Biol 4, 72-81.

Dey, A., Jones, J.E., Nebert, D.W., 1999. Tissue- and cell type-specific expression of cytochrome P450 1A1 and cytochrome P450 1A2 mRNA in the mouse localized in situ hybridization. Biochem Pharmacol 58, 525-537.

Dimova, S., Hoet, P.H., Dinsdale, D., Nemery, B., 2005. Acetaminophen decreases intracellular glutathione levels and modulates cytokine production in human alveolar macrophages and type II pneumocytes in vitro. Int J Biochem Cell Biol 37, 1727-1737.

Dimova, S., Hoet, P.H., Nemery, B., 2000. Paracetamol (acetaminophen) cytotoxicity in rat type II pneumocytes and alveolar macrophages in vitro. Biochem Pharmacol 59, 1467-1475.

Dixon, M.F., Dixon, B., Aparicio, S.R., Loney, D.P., 1975. Experimental paracetamol-induced hepatic necrosis: a light- and electron-microscope, and histochemical study. J Pathol 116, 17-29.

Dixon, M.F., Nimmo, J., Prescott, L.F., 1971. Experimental paracetamol-induced hepatic necrosis: a histopathological study. J Pathol 103, 225-229.

Donahower, B., McCullough, S.S., Kurten, R., Lamps, L.W., Simpson, P., Hinson, J.A., James, L.P., 2006. Vascular endothelial growth factor and hepatocyte regeneration in acetaminophen toxicity. Am J Physiol Gastrointest Liver Physiol 291, G102-109.

Dormans, J.A., van Bree, L., Boere, A.J., Marra, M., Rombout, P.J., 1999. Interspecies differences in time course of pulmonary toxicity following repeated exposure to ozone. Inhal Toxicol 11, 309-329.

Dungworth, D.L., Castleman, W.L., Chow, C.K., Mellick, P.W., Mustafa, M.G., Tarkington, B., Tyler, W.S., 1975. Effect of ambient levels of ozone on monkeys. Fed Proc 34, 1670-1674.

EPA, U.S., 2008. Air Quality Criteria for Ozone and Related Photochemical Oxidants (Final). EPA 600/R-05/004-aF-cF. In: EPA, U.S. (Ed.), vol. I, Research Triangle Park.

Evans, M., 1982. Cell death and cell renewal in small airways and alveoli. In: Witschi, H., Nettescheim, P. (Eds.) Mechanisms of Respiratory Toxicology, vol. 1. CRC Press, Boca Raton, FL, p. 189.

Evans, M.J., Cabral-Anderson, L.J., Freeman, G., 1978. Role of the Clara cell in renewal of the bronchiolar epithelium. Lab Invest 38, 648-653.

Evans, M.J., Johnson, L.V., Stephens, R.J., Freeman, G., 1976. Renewal of the terminal bronchiolar epithelium in the rat following exposure to NO2 or O3. Lab Invest 35, 246-257.

Fauroux, B., Sampil, M., Quenel, P., Lemoullec, Y., 2000. Ozone: a trigger for hospital pediatric asthma emergency room visits. Pediatr Pulmonol 30, 41-46.

Fausto, N., Campbell, J.S., Riehle, K.J., 2006. Liver regeneration. Hepatology 43, S45-53.
Fontana, R.J., 2008. Acute liver failure including acetaminophen overdose. Med Clin North Am 92, 761-794, viii.

Forkert, P.G., Boyd, S.M., Ulreich, J.B., 2001. Pulmonary bioactivation of 1,1-dichloroethylene is associated with CYP2E1 levels in A/J, CD-1, and C57BL/6 mice. J Pharmacol Exp Ther 297, 1193-1200.

Foster, W.M., Wills-Karp, M., Tankersley, C.G., Chen, X., Paquette, N.C., 1996. Bloodborne markers in humans during multiday exposure to ozone. J Appl Physiol 81, 794-800.

Friedman, M.S., Powell, K.E., Hutwagner, L., Graham, L.M., Teague, W.G., 2001. Impact of changes in transportation and commuting behaviors during the 1996 Summer Olympic Games in Atlanta on air quality and childhood asthma. JAMA 285, 897-905.

Genter, M.B., Liang, H.C., Gu, J., Ding, X., Negishi, M., McKinnon, R.A., Nebert, D.W., 1998. Role of CYP2A5 and 2G1 in acetaminophen metabolism and toxicity in the olfactory mucosa of the Cyp1a2(-/-) mouse. Biochem Pharmacol 55, 1819-1826.

Giangreco, A., Arwert, E.N., Rosewell, I.R., Snyder, J., Watt, F.M., Stripp, B.R., 2009. Stem cells are dispensable for lung homeostasis but restore airways after injury. Proc Natl Acad Sci U S A 106, 9286-9291.

Giangreco, A., Reynolds, S.D., Stripp, B.R., 2002. Terminal bronchioles harbor a unique airway stem cell population that localizes to the bronchoalveolar duct junction. Am J Pathol 161, 173-182.

Goldstein, B.D., 1978. The pulmonary and extrapulmonary effects of ozone. Ciba Found Symp, 295-319.

Gong, H., Jr., Wong, R., Sarma, R.J., Linn, W.S., Sullivan, E.D., Shamoo, D.A., Anderson, K.R., Prasad, S.B., 1998. Cardiovascular effects of ozone exposure in human volunteers. Am J Respir Crit Care Med 158, 538-546.

Graham, J.A., Menzel, D.B., Miller, F.J., Illing, J.W., Gardner, D.E., 1981. Influence of ozone on pentobarbital-induced sleeping time in mice, rats, and hamsters. Toxicol Appl Pharmacol 61, 64-73.

Graham, L.M., 2004. All I need is the air that I breath: outdoor air quality and asthma. Paediatr Respir Rev 5 Suppl A, S59-64.

Gu, J., Cui, H., Behr, M., Zhang, L., Zhang, Q.Y., Yang, W., Hinson, J.A., Ding, X., 2005. In vivo mechanisms of tissue-selective drug toxicity: effects of liver-specific

knockout of the NADPH-cytochrome P450 reductase gene on acetaminophen toxicity in kidney, lung, and nasal mucosa. Mol Pharmacol 67, 623-630.

Gujral, J.S., Knight, T.R., Farhood, A., Bajt, M.L., Jaeschke, H., 2002. Mode of cell death after acetaminophen overdose in mice: apoptosis or oncotic necrosis? Toxicol Sci 67, 322-328.

Haouzi, D., Cohen, I., Vieira, H.L., Poncet, D., Boya, P., Castedo, M., Vadrot, N., Belzacq, A.S., Fau, D., Brenner, C., Feldmann, G., Kroemer, G., 2002. Mitochondrial permeability transition as a novel principle of hepatorenal toxicity in vivo. Apoptosis 7, 395-405.

Harkema, J.R., Plopper, C.G., Hyde, D.M., St George, J.A., Wilson, D.W., Dungworth, D.L., 1993. Response of macaque bronchiolar epithelium to ambient concentrations of ozone. Am J Pathol 143, 857-866.

Hart, S.G., Cartun, R.W., Wyand, D.S., Khairallah, E.A., Cohen, S.D., 1995. Immunohistochemical localization of acetaminophen in target tissues of the CD-1 mouse: correspondence of covalent binding with toxicity. Fundam Appl Toxicol 24, 260-274.

Hiltermann, T.J., Peters, E.A., Alberts, B., Kwikkers, K., Borggreven, P.A., Hiemstra, P.S., Dijkman, J.H., van Bree, L.A., Stolk, J., 1998. Ozone-induced airway hyperresponsiveness in patients with asthma: role of neutrophil-derived serine proteinases. Free Radic Biol Med 24, 952-958.

Hinson, J.A., Pike, S.L., Pumford, N.R., Mayeux, P.R., 1998. Nitrotyrosine-protein adducts in hepatic centrilobular areas following toxic doses of acetaminophen in mice. Chem Res Toxicol 11, 604-607.

Hinson, J.A., Pohl, L.R., Monks, T.J., Gillette, J.R., 1981. Acetaminophen-induced hepatotoxicity. Life Sci 29, 107-116.

Hinson, J.A., Reid, A.B., McCullough, S.S., James, L.P., 2004. Acetaminophen-induced hepatotoxicity: role of metabolic activation, reactive oxygen/nitrogen species, and mitochondrial permeability transition. Drug Metab Rev 36, 805-822.

Holz, O., Jorres, R.A., Timm, P., Mucke, M., Richter, K., Koschyk, S., Magnussen, H., 1999. Ozone-induced airway inflammatory changes differ between individuals and are reproducible. Am J Respir Crit Care Med 159, 776-784.

Holz, O., Mucke, M., Paasch, K., Bohme, S., Timm, P., Richter, K., Magnussen, H., Jorres, R.A., 2002. Repeated ozone exposures enhance bronchial allergen responses in subjects with rhinitis or asthma. Clin Exp Allergy 32, 681-689.

Hong, K.U., Reynolds, S.D., Giangreco, A., Hurley, C.M., Stripp, B.R., 2001. Clara cell secretory protein-expressing cells of the airway neuroepithelial body microenvironment

include a label-retaining subset and are critical for epithelial renewal after progenitor cell depletion. Am J Respir Cell Mol Biol 24, 671-681.

Hong, K.U., Reynolds, S.D., Watkins, S., Fuchs, E., Stripp, B.R., 2004a. Basal cells are a multipotent progenitor capable of renewing the bronchial epithelium. Am J Pathol 164, 577-588.

Hong, K.U., Reynolds, S.D., Watkins, S., Fuchs, E., Stripp, B.R., 2004b. In vivo differentiation potential of tracheal basal cells: evidence for multipotent and unipotent subpopulations. Am J Physiol Lung Cell Mol Physiol 286, L643-649.

Hotchkiss, J.A., Harkema, J.R., Johnson, N.F., 1997. Kinetics of nasal epithelial cell loss and proliferation in F344 rats following a single exposure to 0.5 ppm ozone. Toxicol Appl Pharmacol 143, 75-82.

Hyde, D.M., Hubbard, W.C., Wong, V., Wu, R., Pinkerton, K., Plopper, C.G., 1992. Ozone-induced acute tracheobronchial epithelial injury: relationship to granulocyte emigration in the lung. Am J Respir Cell Mol Biol 6, 481-497.

James, L.P., Lamps, L.W., McCullough, S., Hinson, J.A., 2003. Interleukin 6 and hepatocyte regeneration in acetaminophen toxicity in the mouse. Biochem Biophys Res Commun 309, 857-863.

Jeffery, E.H., Haschek, W.M., 1988. Protection by dimethylsulfoxide against acetaminophen-induced hepatic, but not respiratory toxicity in the mouse. Toxicol Appl Pharmacol 93, 452-461.

Jetten, A.M., 1991. Growth and differentiation factors in tracheobronchial epithelium. Am J Physiol 260, L361-373.

Johnston, C.J., Stripp, B.R., Reynolds, S.D., Avissar, N.E., Reed, C.K., Finkelstein, J.N., 1999. Inflammatory and antioxidant gene expression in C57BL/6J mice after lethal and sublethal ozone exposures. Exp Lung Res 25, 81-97.

Jollow, D.J., Mitchell, J.R., Potter, W.Z., Davis, D.C., Gillette, J.R., Brodie, B.B., 1973. Acetaminophen-induced hepatic necrosis. II. Role of covalent binding in vivo. J Pharmacol Exp Ther 187, 195-202.

Jones, A.L., 1998. Mechanism of action and value of N-acetylcysteine in the treatment of early and late acetaminophen poisoning: a critical review. J Toxicol Clin Toxicol 36, 277-285.

Jorres, R., Nowak, D., Magnussen, H., 1996. The effect of ozone exposure on allergen responsiveness in subjects with asthma or rhinitis. Am J Respir Crit Care Med 153, 56-64.

Jorres, R.A., Holz, O., Zachgo, W., Timm, P., Koschyk, S., Muller, B., Grimminger, F., Seeger, W., Kelly, F.J., Dunster, C., Frischer, T., Lubec, G., Waschewski, M., Niendorf, A., Magnussen, H., 2000. The effect of repeated ozone exposures on inflammatory markers in bronchoalveolar lavage fluid and mucosal biopsies. Am J Respir Crit Care Med 161, 1855-1861.

Kauffman, S.L., 1980. Cell proliferation in the mammalian lung. Int Rev Exp Pathol 22, 131-191.

Kehrl, H.R., Hazucha, M.J., Solic, J.J., Bromberg, P.A., 1985. Responses of subjects with chronic obstructive pulmonary disease after exposures to 0.3 ppm ozone. Am Rev Respir Dis 131, 719-724.

Khanlou, H., Souto, H., Lippmann, M., Munoz, S., Rothstein, K., Ozden, Z., 1999. Resolution of adult respiratory distress syndrome after recovery from fulminant hepatic failure. Am J Med Sci 317, 134-136.

Kida, H., Mucenski, M.L., Thitoff, A.R., Le Cras, T.D., Park, K.S., Ikegami, M., Muller, W., Whitsett, J.A., 2008. GP130-STAT3 regulates epithelial cell migration and is required for repair of the bronchiolar epithelium. Am J Pathol 172, 1542-1554.

Kimbell, J., Miller, F., 1999. Regional respiratory-tract absorption on inhaled reactive gases: a modeling approach. In: Gardner, D., Crapo, J., McClellan, R. (Eds.) Toxicology of the Lung. Taylor and Francis, Philadelphia, pp. 557-598.

Kleeberger, S.R., Levitt, R.C., Zhang, L.Y., Longphre, M., Harkema, J., Jedlicka, A., Eleff, S.M., DiSilvestre, D., Holroyd, K.J., 1997. Linkage analysis of susceptibility to ozone-induced lung inflammation in inbred mice. Nat Genet 17, 475-478.

Knight, T.R., Kurtz, A., Bajt, M.L., Hinson, J.A., Jaeschke, H., 2001. Vascular and hepatocellular peroxynitrite formation during acetaminophen toxicity: role of mitochondrial oxidant stress. Toxicol Sci 62, 212-220.

Koren, H.S., Devlin, R.B., Graham, D.E., Mann, R., McGee, M.P., Horstman, D.H., Kozumbo, W.J., Becker, S., House, D.E., McDonnell, W.F., et al., 1989. Ozone-induced inflammation in the lower airways of human subjects. Am Rev Respir Dis 139, 407-415.

Kovalovich, K., DeAngelis, R.A., Li, W., Furth, E.E., Ciliberto, G., Taub, R., 2000. Increased toxin-induced liver injury and fibrosis in interleukin-6-deficient mice. Hepatology 31, 149-159.

Kreit, J.W., Gross, K.B., Moore, T.B., Lorenzen, T.J., D'Arcy, J., Eschenbacher, W.L., 1989. Ozone-induced changes in pulmonary function and bronchial responsiveness in asthmatics. J Appl Physiol 66, 217-222.

Krishna, M.T., Madden, J., Teran, L.M., Biscione, G.L., Lau, L.C., Withers, N.J., Sandstrom, T., Mudway, I., Kelly, F.J., Walls, A., Frew, A.J., Holgate, S.T., 1998.

Effects of 0.2 ppm ozone on biomarkers of inflammation in bronchoalveolar lavage fluid and bronchial mucosa of healthy subjects. Eur Respir J 11, 1294-1300.

Larson, A.M., Polson, J., Fontana, R.J., Davern, T.J., Lalani, E., Hynan, L.S., Reisch, J.S., Schiodt, F.V., Ostapowicz, G., Shakil, A.O., Lee, W.M., 2005. Acetaminophen-induced acute liver failure: results of a United States multicenter, prospective study. Hepatology 42, 1364-1372.

Laskin, D.L., Heck, D.E., Laskin, J.D., 1998. Role of inflammatory cytokines and nitric oxide in hepatic and pulmonary toxicity. Toxicol Lett 102-103, 289-293.

Laskin, D.L., Pendino, K.J., Punjabi, C.J., Rodriguez del Valle, M., Laskin, J.D., 1994. Pulmonary and hepatic effects of inhaled ozone in rats. Environ Health Perspect 102 Suppl 10, 61-64.

Last, J.A., Gohil, K., Mathrani, V.C., Kenyon, N.J., 2005. Systemic responses to inhaled ozone in mice: cachexia and down-regulation of liver xenobiotic metabolizing genes. Toxicol Appl Pharmacol 208, 117-126.

Lawson, J.A., Farhood, A., Hopper, R.D., Bajt, M.L., Jaeschke, H., 2000. The hepatic inflammatory response after acetaminophen overdose: role of neutrophils. Toxicol Sci 54, 509-516.

Lee, W.M., Squires, R.H., Jr., Nyberg, S.L., Doo, E., Hoofnagle, J.H., 2008. Acute liver failure: Summary of a workshop. Hepatology 47, 1401-1415.

Linn, W.S., Fischer, D.A., Medway, D.A., Anzar, U.T., Spier, C.E., Valencia, L.M., Venet, T.G., Hackney, J.D., 1982. Short-term respiratory effects of 0.12 ppm ozone exposure in volunteers with chronic obstructive pulmonary disease. Am Rev Respir Dis 125, 658-663.

Lippmann, M., Schlesinger, R.B., 2000. Toxicological bases for the setting of health-related air pollution standards. Annu Rev Public Health 21, 309-333.

Liu, L., Leech, J.A., Urch, R.B., Silverman, F.S., 1997. In vivo salicylate hydroxylation: a potential biomarker for assessing acute ozone exposure and effects in humans. Am J Respir Crit Care Med 156, 1405-1412.

Liu, X., Driskell, R.R., Engelhardt, J.F., 2006. Stem cells in the lung. Methods Enzymol 419, 285-321.

Liu, Z., Kaplowitz, N., 2005. Depletion of neutrophils protects mice against acetaminophen hepatotoxicity (abstract). Gastroenterology 128, A726.

Liu, Z.X., Govindarajan, S., Kaplowitz, N., 2004. Innate immune system plays a critical role in determining the progression and severity of acetaminophen hepatotoxicity. Gastroenterology 127, 1760-1774.

Longphre, M., Zhang, L., Harkema, J.R., Kleeberger, S.R., 1999. Ozone-induced pulmonary inflammation and epithelial proliferation are partially mediated by PAF. J Appl Physiol 86, 341-349.

Mango, G.W., Johnston, C.J., Reynolds, S.D., Finkelstein, J.N., Plopper, C.G., Stripp, B.R., 1998. Clara cell secretory protein deficiency increases oxidant stress response in conducting airways. Am J Physiol 275, L348-356.

Martins, P.N., Theruvath, T.P., Neuhaus, P., 2008. Rodent models of partial hepatectomies. Liver Int 28, 3-11.

Massaro, G.D., Singh, G., Mason, R., Plopper, C.G., Malkinson, A.M., Gail, D.B., 1994. Biology of the Clara cell. Am J Physiol 266, L101-106.

Medinsky, M.A., Bond, J.A., 2001. Sites and mechanisms for uptake of gases and vapors in the respiratory tract. Toxicology 160, 165-172.

Mellick, P.W., Schwartz, L.W., Dungworth, D.L., 1975. Ozone-induced pulmonary lesions in rats and rhesus monkeys. Vet Pathol 12, 61-62.

Meng, Y.Y., Rull, R.P., Wilhelm, M., Lombardi, C., Balmes, J., Ritz, B., 2009. Outdoor air pollution and uncontrolled asthma in the San Joaquin Valley, California. J Epidemiol Community Health.

Michalopoulos, G.K., DeFrances, M.C., 1997. Liver regeneration. Science 276, 60-66.

Miller, F.J., Menzel, D.B., Coffin, D.L., 1978. Similarity between man and laboratory animals in regional pulmonary deposition of ozone. Environ Res 17, 84-101.

Mitchell, J.R., Jollow, D.J., Potter, W.Z., Davis, D.C., Gillette, J.R., Brodie, B.B., 1973a. Acetaminophen-induced hepatic necrosis. I. Role of drug metabolism. J Pharmacol Exp Ther 187, 185-194.

Mitchell, J.R., Jollow, D.J., Potter, W.Z., Gillette, J.R., Brodie, B.B., 1973b. Acetaminophen-induced hepatic necrosis. IV. Protective role of glutathione. J Pharmacol Exp Ther 187, 211-217.

Mudway, I.S., Kelly, F.J., 2000. Ozone and the lung: a sensitive issue. Mol Aspects Med 21, 1-48.

Mudway, I.S., Krishna, M.T., Frew, A.J., MacLeod, D., Sandstrom, T., Holgate, S.T., Kelly, F.J., 1999. Compromised concentrations of ascorbate in fluid lining the respiratory tract in human subjects after exposure to ozone. Occup Environ Med 56, 473-481.

Neff, S.B., Neff, T.A., Kunkel, S.L., Hogaboam, C.M., 2003. Alterations in cytokine/chemokine expression during organ-to-organ communication established via acetaminophen-induced toxicity. Exp Mol Pathol 75, 187-193.

Nikula, K.J., Wilson, D.W., Giri, S.N., Plopper, C.G., Dungworth, D.L., 1988. The response of the rat tracheal epithelium to ozone exposure. Injury, adaptation, and repair. Am J Pathol 131, 373-384.

Oslund, K.L., Hyde, D.M., Putney, L.F., Alfaro, M.F., Walby, W.F., Tyler, N.K., Schelegle, E.S., 2009. Activation of calcitonin gene-related peptide receptor during ozone inhalation contributes to airway epithelial injury and repair. Toxicol Pathol 37, 805-813.

Pahlavan, P.S., Feldmann, R.E., Jr., Zavos, C., Kountouras, J., 2006. Prometheus' challenge: molecular, cellular and systemic aspects of liver regeneration. J Surg Res 134, 238-251.

Paulose-Ram, R., Hirsch, R., Dillon, C., Gu, Q., 2005. Frequent monthly use of selected non-prescription and prescription non-narcotic analgesics among U.S. adults. Pharmacoepidemiol Drug Saf 14, 257-266.

Paulose-Ram, R., Hirsch, R., Dillon, C., Losonczy, K., Cooper, M., Ostchega, Y., 2003. Prescription and non-prescription analgesic use among the US adult population: results from the third National Health and Nutrition Examination Survey (NHANES III). Pharmacoepidemiol Drug Saf 12, 315-326.

Paulu, C., Smith, A.E., 2008. Tracking associations between ambient ozone and asthma-related emergency department visits using case-crossover analysis. J Public Health Manag Pract 14, 581-591.

Pendino, K.J., Shuler, R.L., Laskin, J.D., Laskin, D.L., 1994. Enhanced production of interleukin-1, tumor necrosis factor-alpha, and fibronectin by rat lung phagocytes following inhalation of a pulmonary irritant. Am J Respir Cell Mol Biol 11, 279-286.

Pino, M.V., Levin, J.R., Stovall, M.Y., Hyde, D.M., 1992. Pulmonary inflammation and epithelial injury in response to acute ozone exposure in the rat. Toxicol Appl Pharmacol 112, 64-72.

Placke, M.E., Ginsberg, G.L., Wyand, D.S., Cohen, S.D., 1987a. Ultrastructural changes during acute acetaminophen-induced hepatotoxicity in the mouse: a time and dose study. Toxicol Pathol 15, 431-438.

Placke, M.E., Wyand, D.S., Cohen, S.D., 1987b. Extrahepatic lesions induced by acetaminophen in the mouse. Toxicol Pathol 15, 381-387.

Plopper, C.G., Hatch, G.E., Wong, V., Duan, X., Weir, A.J., Tarkington, B.K., Devlin, R.B., Becker, S., Buckpitt, A.R., 1998. Relationship of inhaled ozone concentration to acute tracheobronchial epithelial injury, site-specific ozone dose, and glutathione depletion in rhesus monkeys. Am J Respir Cell Mol Biol 19, 387-399.

Plopper, C.G., Hyde, D.M., 2008. The non-human primate as a model for studying COPD and asthma. Pulm Pharmacol Ther 21, 755-766.

Plopper, C.G., Smiley-Jewell, S.M., Miller, L.A., Fanucchi, M.V., Evans, M.J., Buckpitt, A.R., Avdalovic, M., Gershwin, L.J., Joad, J.P., Kajekar, R., Larson, S., Pinkerton, K.E., Van Winkle, L.S., Schelegle, E.S., Pieczarka, E.M., Wu, R., Hyde, D.M., 2007. Asthma/allergic airways disease: does postnatal exposure to environmental toxicants promote airway pathobiology? Toxicol Pathol 35, 97-110.

Plopper, C.G., Suverkropp, C., Morin, D., Nishio, S., Buckpitt, A., 1992. Relationship of cytochrome P-450 activity to Clara cell cytotoxicity. I. Histopathologic comparison of the respiratory tract of mice, rats and hamsters after parenteral administration of naphthalene. J Pharmacol Exp Ther 261, 353-363.

Portmann, B., Talbot, I.C., Day, D.W., Davidson, A.R., Murray-Lyon, I.M., Williams, R., 1975. Histopathological changes in the liver following a paracetamol overdose: correlation with clinical and biochemical parameters. J Pathol 117, 169-181.

Postlethwait, E.M., Joad, J.P., Hyde, D.M., Schelegle, E.S., Bric, J.M., Weir, A.J., Putney, L.F., Wong, V.J., Velsor, L.W., Plopper, C.G., 2000. Three-dimensional mapping of ozone-induced acute cytotoxicity in tracheobronchial airways of isolated perfused rat lung. Am J Respir Cell Mol Biol 22, 191-199.

Potter, W.Z., Davis, D.C., Mitchell, J.R., Jollow, D.J., Gillette, J.R., Brodie, B.B., 1973. Acetaminophen-induced hepatic necrosis. 3. Cytochrome P-450-mediated covalent binding in vitro. J Pharmacol Exp Ther 187, 203-210.

Pryor, W.A., 1992. How far does ozone penetrate into the pulmonary air/tissue boundary before it reacts? Free Radic Biol Med 12, 83-88.

Pryor, W.A., 1994. Mechanisms of radical formation from reactions of ozone with target molecules in the lung. Free Radic Biol Med 17, 451-465.

Pryor, W.A., Houk, K.N., Foote, C.S., Fukuto, J.M., Ignarro, L.J., Squadrito, G.L., Davies, K.J., 2006. Free radical biology and medicine: it's a gas, man! Am J Physiol Regul Integr Comp Physiol 291, R491-511.

Pryor, W.A., Squadrito, G.L., Friedman, M., 1995a. The cascade mechanism to explain ozone toxicity: the role of lipid ozonation products. Free Radic Biol Med 19, 935-941.

Pryor, W.A., Squadrito, G.L., Friedman, M., 1995b. A new mechanism for the toxicity of ozone. Toxicol Lett 82-83, 287-293.

Rage, E., Siroux, V., Kunzli, N., Pin, I., Kauffmann, F., 2009. Air pollution and asthma severity in adults. Occup Environ Med 66, 182-188.

Rawlins, E.L., Hogan, B.L., 2006. Epithelial stem cells of the lung: privileged few or opportunities for many? Development 133, 2455-2465.

Ray, S.D., Sorge, C.L., Raucy, J.L., Corcoran, G.B., 1990. Early loss of large genomic DNA in vivo with accumulation of Ca2+ in the nucleus during acetaminophen-induced liver injury. Toxicol Appl Pharmacol 106, 346-351.

Reynolds, S.D., Giangreco, A., Power, J.H., Stripp, B.R., 2000a. Neuroepithelial bodies of pulmonary airways serve as a reservoir of progenitor cells capable of epithelial regeneration. Am J Pathol 156, 269-278.

Reynolds, S.D., Hong, K.U., Giangreco, A., Mango, G.W., Guron, C., Morimoto, Y., Stripp, B.R., 2000b. Conditional clara cell ablation reveals a self-renewing progenitor function of pulmonary neuroendocrine cells. Am J Physiol Lung Cell Mol Physiol 278, L1256-1263.

Ritt, D.J., Whelan, G., Werner, D.J., Eigenbrodt, E.H., Schenker, S., Combes, B., 1969. Acute hepatic necrosis with stupor or coma. An analysis of thirty-one patients. Medicine (Baltimore) 48, 151-172.

Roberts, R.A., Laskin, D.L., Smith, C.V., Robertson, F.M., Allen, E.M., Doorn, J.A., Slikker, W., 2009. Nitrative and Oxidative Stress in Toxicology and Disease. Toxicol Sci.

Sakamoto, T., Liu, Z., Murase, N., Ezure, T., Yokomuro, S., Poli, V., Demetris, A.J., 1999. Mitosis and apoptosis in the liver of interleukin-6-deficient mice after partial hepatectomy. Hepatology 29, 403-411.

Satyanarayana, A., Geffers, R., Manns, M.P., Buer, J., Rudolph, K.L., 2004. Gene expression profile at the G1/S transition of liver regeneration after partial hepatectomy in mice. Cell Cycle 3, 1405-1417.

Savov, J.D., Whitehead, G.S., Wang, J., Liao, G., Usuka, J., Peltz, G., Foster, W.M., Schwartz, D.A., 2004. Ozone-induced acute pulmonary injury in inbred mouse strains. Am J Respir Cell Mol Biol 31, 69-77.

Scannell, C., Chen, L., Aris, R.M., Tager, I., Christian, D., Ferrando, R., Welch, B., Kelly, T., Balmes, J.R., 1996. Greater ozone-induced inflammatory responses in subjects with asthma. Am J Respir Crit Care Med 154, 24-29.

Schelegle, E.S., Siefkin, A.D., McDonald, R.J., 1991. Time course of ozone-induced neutrophilia in normal humans. Am Rev Respir Dis 143, 1353-1358.

Schiodt, F.V., Atillasoy, E., Shakil, A.O., Schiff, E.R., Caldwell, C., Kowdley, K.V., Stribling, R., Crippin, J.S., Flamm, S., Somberg, K.A., Rosen, H., McCashland, T.M., Hay, J.E., Lee, W.M., 1999. Etiology and outcome for 295 patients with acute liver failure in the United States. Liver Transpl Surg 5, 29-34.

Schwartz, L.W., Dungworth, D.L., Mustafa, M.G., Tarkington, B.K., Tyler, W.S., 1976. Pulmonary responses of rats to ambient levels of ozone: effects of 7-day intermittent or continuous exposure. Lab Invest 34, 565-578.

Seltzer, J., Bigby, B.G., Stulbarg, M., Holtzman, M.J., Nadel, J.A., Ueki, I.F., Leikauf, G.D., Goetzl, E.J., Boushey, H.A., 1986. O3-induced change in bronchial reactivity to methacholine and airway inflammation in humans. J Appl Physiol 60, 1321-1326.

Solic, J.J., Hazucha, M.J., Bromberg, P.A., 1982. The acute effects of 0.2 ppm ozone in patients with chronic obstructive pulmonary disease. Am Rev Respir Dis 125, 664-669.

Stenfors, N., Pourazar, J., Blomberg, A., Krishna, M.T., Mudway, I., Helleday, R., Kelly, F.J., Frew, A.J., Sandstrom, T., 2002. Effect of ozone on bronchial mucosal inflammation in asthmatic and healthy subjects. Respir Med 96, 352-358.

Stephens, R.J., Sloan, M.F., Groth, D.G., Negi, D.S., Lunan, K.D., 1978. Cytologic responses of postnatal rat lungs to O3 or NO2 exposure. Am J Pathol 93, 183-200.

Sterner-Kock, A., Kock, M., Braun, R., Hyde, D.M., 2000. Ozone-induced epithelial injury in the ferret is similar to nonhuman primates. Am J Respir Crit Care Med 162, 1152-1156.

Stieb, D.M., Beveridge, R.C., Brook, J.R., Smith-Doiron, M., Burnett, R.T., Dales, R.E., Beaulieu, S., Judek, S., Mamedov, A., 2000. Air pollution, aeroallergens and cardiorespiratory emergency department visits in Saint John, Canada. J Expo Anal Environ Epidemiol 10, 461-477.

Stieb, D.M., Burnett, R.T., Beveridge, R.C., Brook, J.R., 1996. Association between ozone and asthma emergency department visits in Saint John, New Brunswick, Canada. Environ Health Perspect 104, 1354-1360.

Stieb, D.M., Szyszkowicz, M., Rowe, B.H., Leech, J.A., 2009. Air pollution and emergency department visits for cardiac and respiratory conditions: a multi-city time-series analysis. Environ Health 8, 25.

Stoilov, I., Krueger, W., Mankowski, D., Guernsey, L., Kaur, A., Glynn, J., Thrall, R.S., 2006. The cytochromes P450 (CYP) response to allergic inflammation of the lung. Arch Biochem Biophys 456, 30-38.

Stripp, B.R., Maxson, K., Mera, R., Singh, G., 1995. Plasticity of airway cell proliferation and gene expression after acute naphthalene injury. Am J Physiol 269, L791-799.

Stripp, B.R., Reynolds, S.D., 2008. Maintenance and repair of the bronchiolar epithelium. Proc Am Thorac Soc 5, 328-333.

Tarloff, J.B., Khairallah, E.A., Cohen, S.D., Goldstein, R.S., 1996. Sex- and age-dependent acetaminophen hepato- and nephrotoxicity in Sprague-Dawley rats: role of tissue accumulation, nonprotein sulfhydryl depletion, and covalent binding. Fundam Appl Toxicol 30, 13-22.

Taub, R., 2004. Liver regeneration: from myth to mechanism. Nat Rev Mol Cell Biol 5, 836-847.

Thurston, G.D., Ito, K., Kinney, P.L., Lippmann, M., 1992. A multi-year study of air pollution and respiratory hospital admissions in three New York State metropolitan areas: results for 1988 and 1989 summers. J Expo Anal Environ Epidemiol 2, 429-450.

Tolbert, P.E., Mulholland, J.A., MacIntosh, D.L., Xu, F., Daniels, D., Devine, O.J., Carlin, B.P., Klein, M., Dorley, J., Butler, A.J., Nordenberg, D.F., Frumkin, H., Ryan, P.B., White, M.C., 2000. Air quality and pediatric emergency room visits for asthma in Atlanta, Georgia, USA. Am J Epidemiol 151, 798-810.

van Bree, L., Dormans, J.A., Koren, H.S., Devlin, R.B., Rombout, P.J., 2002. Attenuation and recovery of pulmonary injury in rats following short-term, repeated daily exposure to ozone. Inhal Toxicol 14, 883-900.

Van Winkle, L.S., Buckpitt, A.R., Nishio, S.J., Isaac, J.M., Plopper, C.G., 1995. Cellular response in naphthalene-induced Clara cell injury and bronchiolar epithelial repair in mice. Am J Physiol 269, L800-818.

Vesely, K.R., Schelegle, E.S., Stovall, M.Y., Harkema, J.R., Green, J.F., Hyde, D.M., 1999. Breathing pattern response and epithelial labeling in ozone-induced airway injury in neutrophil-depleted rats. Am J Respir Cell Mol Biol 20, 699-709.

Vincent, R., Vu, D., Hatch, G., Poon, R., Dreher, K., Guenette, J., Bjarnason, S., Potvin, M., Norwood, J., McMullen, E., 1996. Sensitivity of lungs of aging Fischer 344 rats to ozone: assessment by bronchoalveolar lavage. Am J Physiol 271, L555-565.

Watkins, P.B., Kaplowitz, N., Slattery, J.T., Colonese, C.R., Colucci, S.V., Stewart, P.W., Harris, S.C., 2006. Aminotransferase elevations in healthy adults receiving 4 grams of acetaminophen daily: a randomized controlled trial. JAMA 296, 87-93.

White, M.C., Etzel, R.A., Wilcox, W.D., Lloyd, C., 1994. Exacerbations of childhood asthma and ozone pollution in Atlanta. Environ Res 65, 56-68.

Wustefeld, T., Rakemann, T., Kubicka, S., Manns, M.P., Trautwein, C., 2000. Hyperstimulation with interleukin 6 inhibits cell cycle progression after hepatectomy in mice. Hepatology 32, 514-522.

Yin, D., 2000. Is carbonyl detoxification an important anti-aging process during sleep? Med Hypotheses 54, 519-522.

Yu, M., Zheng, X., Witschi, H., Pinkerton, K.E., 2002. The role of interleukin-6 in pulmonary inflammation and injury induced by exposure to environmental air pollutants. Toxicol Sci 68, 488-497.

Zemke, A.C., Teisanu, R.M., Giangreco, A., Drake, J.A., Brockway, B.L., Reynolds, S.D., Stripp, B.R., 2009. {beta}-Catenin is not Necessary for Maintenance or Repair of the Bronchiolar Epithelium. Am J Respir Cell Mol Biol.

CHAPTER 2

EFFECTS OF ACETAMINOPHEN AND ACUTE OZONE COEXPOSURE IN THE LIVER OF MICE

I. ABSTRACT

Ozone (O3), an oxidant air pollutant in photochemical smog, principally targets epithelial cells lining the respiratory tract. However, changes in gene expression have also been reported in livers of O3-exposed mice. Overdose with acetaminophen (APAP) is the most common cause of drug-induced liver injury in developed countries. In the present study, we examined the hepatic effects of acute O3 exposure in mice pretreated with a hepatotoxic dose of APAP. C57BL/6 male mice were fasted overnight and then given APAP (300 mg/kg ip) or saline vehicle (0 mg/kg APAP). Two hours (h) later, they were exposed to 0, 0.25 or 0.5 ppm O3 for 6 h, then were sacrificed 9 h or 32 h after APAP administration (1 h or 24 h after O3 exposure, respectively). Animals euthanized at 32 h were given 5-bromo-2-deoxyuridine (BrdU) 2 h before sacrifice to identify hepatocytes undergoing reparative DNA synthesis. Saline-treated mice exposed to either air or O3 had no liver injury. All APAP-treated mice developed marked centrilobular hepatocellular necrosis that increased in severity with time after APAP exposure. O3 exposure increased the severity of APAP-induced liver injury as indicated by an increase in necrotic hepatic tissue and plasma alanine aminotransferase (ALT) activity. O3 also caused an increase in neutrophil accumulation in livers of APAP-treated animals. APAP induced a 10-fold

increase in the number of bromodeoxyuridine-labeled hepatocytes that was markedly attenuated by O3. Gene expression analysis 9 h after APAP revealed differential expression of genes involved in inflammation, oxidative stress and genes related to regeneration in mice treated with APAP and O3 compared to APAP or O3 alone, possibly providing some indications of the mechanisms behind the APAP and O3 synergy. These results suggest that acute exposure to an oxidant air pollutant exacerbates APAP-induced liver injury and delays hepatic repair.

II. INTRODUCTION

O3 is the principal oxidant pollutant in photochemical smog. Approximately half of the U.S. population lives in areas that persistently exceed the U.S. environmental protection agency or EPA's National Ambient Air Quality Standard (NAAQS) for this highly reactive and irritant gas (EPA, 2008). Short- and long-term exposures to high ambient concentrations of O3 have been linked to adverse health outcomes that include increases in both morbidity and mortality from respiratory causes (Bell et al., 2004; Jerrett et al., 2009; Katsouyanni et al., 1995). Though numerous studies in laboratory animals and human subjects have documented the toxic effects of inhaled O3 on the lung, much less is known about its effects on extrapulmonary organs like the liver (EPA, 2008).

Recently, using global gene expression analyses, investigators found that livers of C57BL/6 mice acutely exposed to inhaled O3 had significant down-regulation of gene families related to lipid, fatty acid and carbohydrate metabolisms that were consistent

with systemic cachexic responses to exposure (Last et al., 2005). Transcription of several mRNAs encoding enzymes of xenobiotic metabolism was also decreased in livers of these O3-exposed mice. Since several interferon (IFN)-dependent hepatic genes were down-regulated with O3 exposure, the investigators suggested that IFN may act as the signaling molecule between the lung and liver. Interestingly, mice exposed to O3 have prolonged pentobarbital sleeping time (Graham et al., 1981) also suggesting impairment of hepatic drug metabolism.

To our knowledge, no studies investigating the potential hepatotoxic interactions of inhaled environmental pollutants and commonly used therapeutic drugs have been reported. In the present study we investigated the acute effects of inhaled high ambient concentrations of O3 on drug-induced liver injury in mice caused by a widely used antipyretic/analgesic agent, APAP. APAP is one of the most commonly used nonprescription drugs in the world, and although remarkably safe within therapeutic doses, it has a relatively narrow therapeutic window. Indeed, APAP overdose is a commonly reported cause of liver failure in the United States (Larson et al., 2005). Like in humans, mice receiving an overdose of APAP develop acute liver injury that is characterized pathologically by centrilobular hepatocellular degeneration and necrosis with elevated blood activity of liver enzymes such as alanine aminotransferase (ALT) (Jemnitz et al., 2008; Tee et al., 1987).

Commonly reported risk factors for APAP-induced liver injury include chronic alcohol use as well as the concurrent intake of some medicinal agents (e.g., isoniazid, phenytoin, zidovudine) (McClements et al., 1990; Shriner and Goetz, 1992). Environmental pollutants have also been recognized as risk factors in pulmonary,

cardiovascular and metabolic conditions such as type II diabetes (Gent et al., 2003; Morris et al., 1995; O'Neill et al., 2005). More recently, it has been reported that inhalation of ambient air particulates promotes systemic and liver oxidative stress in mice (Araujo et al., 2008). Though these risk factors are well documented, the potential interactive effects of inhaled air pollutants, like O3, with APAP have not been investigated. With the present study, we report for the first time that a single, near ambient exposure to O3 exacerbates APAP-induced hepatic injury in mice, resulting in more severe hepatocellular necrosis and attenuation of early hepatic repair mechanisms.

III. MATERIALS AND METHODS

III — 1. Laboratory Animals

Pathogen-free male, C57Bl/6 mice (8-10 weeks of age, the Jackson Laboratory, Bar Harbor, ME) were used in this study. Mice were housed in polycarbonate cages on heat-treated aspen hardwood bedding (Nepco-Northeastern Product Corp, Warrensburg, NY). Boxes were covered with filter bonnets, and animals were provided free access to food (Harlan Teklad Laboratory Rodents 22/5 diet, Madison, WI) and water. Mice were maintained in Michigan State University (MSU) animal housing facilities accredited by the Association for Assessment and Accreditation of Laboratory Animal Care and according to the National Institutes of Health guidelines as overseen by the MSU Institutional Animal Care and Use Committee. Rooms were maintained at temperatures

of 21-24°C and relative humidities of 45-70%, with a 12-hour light/dark cycle starting at 7:30 AM.

III – 2. Experimental protocol: APAP Treatment and O3 Exposures

Mice were randomly divided into twelve groups, each consisting of six animals. They were given intraperitoneally 0 (saline-vehicle) or 300 mg/kg APAP (Sigma Chemical Co., St. Louis, MO) in 20 ml/kg saline. Animals were fasted overnight before the administration of APAP. Two hours after APAP administration, mice were exposed to 0 (air), 0.25 or 0.5 ppm O3 for 6 h (Figure 1). Mice were killed 9 or 32 h after APAP (1 or 24 h after O3 exposure, respectively). As no significant differences were detected in preliminary studies, no morphological evaluation was conducted at 0.25 ppm for the 9 h time point and at 32 h, data analysis in animals given 0.25 ppm was limited to morphological evaluations (liver necrosis and BrdU immunostaining) and plasma ALT activity at the later time (32 h) (Figure 1).

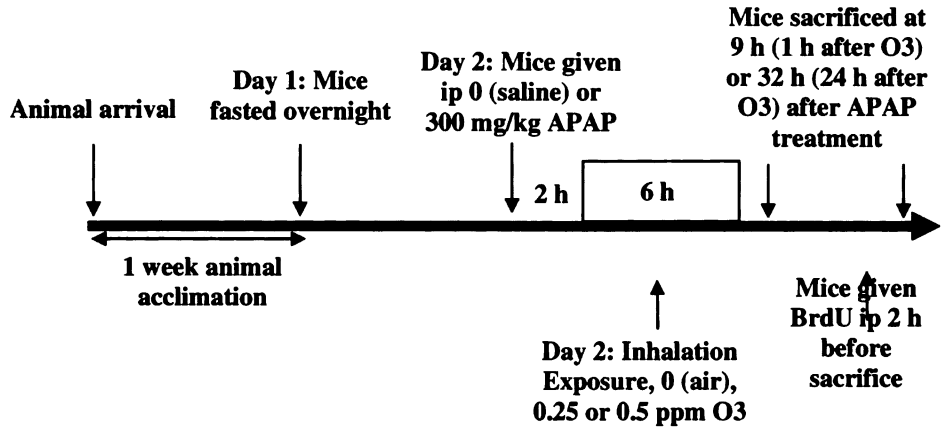

Figure 1. Experimental design of APAP and O3 studies in the liver. 8-10 weeks old C57BL/6 male mice were given 0 (saline) or 300 mg/kg APAP and then exposed to O3 (0 or air, 0.25 or 0.5 ppm) for 6 h. Mice were euthanized 9 or 32 h after APAP injection (1 or 24 h after O3 exposure, respectively).

Mice were housed individually and exposed to O3 in stainless steel wire cages, whole-body inhalation exposure chambers (HC-100, Lab Products, Maywood, NJ). O3 was generated with an OREC 03V1-O ozonizer (O3 Research and Equipment Corp., AZ) using compressed air as a source of oxygen. Total airflow through the exposure chambers was 250 L/min (15 chamber air changes/hour). The concentration of O3 within chambers was monitored during the exposure using Dasibi 1003 AH ambient air O3 monitors (Dasibi Environmental Corp., Glendale, CA). Two O3 sampling probes were placed in

the middle of the ozone chambers, 10-15 cm above cage racks. Airborne concentrations during the inhalation exposures were 0.26 +/- 0.02 ppm or 0.53 +/- 0.01 ppm (mean +/- standard error of the mean) for O3 chambers and 0.02 +/- 0.009 ppm for air chambers.

III – 3. Animal Necropsies and Microscopic and Biochemical Analyses

Two hours before sacrifice, mice euthanized at the 32 h time were given 5-bromo-2-deoxyuridine (BrdU; 50 mg/kg, Fisher Scientific, Fair Lawn, NJ) intraperitoneally. At the time of necropsy, mice were anesthetized with an intraperitoneal injection of sodium pentobarbital (50 mg/kg; Fatal Plus, Vortech Pharmaceuticals, Dearborn, MI), the abdominal cavity was opened, and blood was collected from the abdominal vena cava in heparinized tubes (BD Microtainer, Franklin Lakes, NJ). Animals were then killed by exsanguination.

The liver was removed from the abdominal cavity, and the left liver lobe was fixed in 10% neutral buffered formalin (Fisher Scientific, Fair Lawn, NJ) for light microscopic examination and morphometric analyses. The caudate liver lobe from each mouse was removed and placed in RNAlater (Qiagen, Valencia, CA) at 4°C for 24 h and then stored at -20°C for gene expression analyses using real time PCR. The remaining liver lobes were frozen and stored at -80°C for biochemical analysis of inflammatory cytokines, glutathione and thiobarbituric acid-reactive substances.

After collection of liver samples, hemidiaphragms were punctured to allow collapse of right and left lung lobes, and the thoracic cavity was opened for the removal of the trachea and heart-lung *en bloc*. After the trachea was cannulated, the heart-lung

block was excised and the lungs were gently lavaged twice with 0.9 ml of sterile saline. Approximately 75-90% of the intratracheally instilled saline was recovered as bronchoalveolar lavage fluid (BALF) from the lavaged lung lobes and immediately placed on ice until further analysis.

III – 4. Cellular and Biochemical Analyses of Bronchoalveolar Lavage Fluid

Total cell counts in the collected BALF from each mouse were determined using a hemocytometer. Cytological slides prepared by centrifugation at 600 rpm for 10 minutes using a Shandon cytospin 3 (Shandon Scientific, Sewickley, PA) were stained with Diff-Quick (Dade Behring, Newark, DE). Differential counts of neutrophils, eosinophils, macrophages and lymphocytes were assessed on a total of 200 cells. Remaining BALF was centrifuged at 1,500 rpm for 15 minutes to collect the supernatant fraction, which was stored at -80°C for later biochemical analysis.

III – 5. Flow Cytometric Analyses for Inflammatory Cytokines

BALF supernatants were assayed for inflammatory cytokines that included interleukin-1beta (IL-1β), tumor necrosis factor-alpha (TNF-α), interferon-gamma (IFN-γ), interleukin-6 (IL-6), monocyte chemoattractant protein-1 (MCP-1), interleukin-12 (IL-12), keratinocyte-derived chemokine (KC) and interleukin-10 (IL-10). Plasma cytokine concentrations for KC, TNF-α, MCP-1 and IL-6 were also determined. All cytokine kits were purchased as Flex Set reagents or as a preconfigured cytometric bead array kit (BD

Biosciences, San Diego, CA). Cytokines analysis was performed using a FACSCalibur flow cytometer (BD Franklin Lakes, NJ). Briefly, 50 µl of BALF or plasma was added to the antibody-coated bead complexes and incubation buffer. Phycoerythrin-conjugated secondary antibodies were added to form sandwich complexes. After acquisition of sample data using the flow cytometer, cytokine concentrations were calculated based on standard curve data using FCAP Array software (BD, Franklin Lakes, NJ).

Liver tissues designated for similar cytokine analyses were suspended in phosphate-buffered saline at 4°C and homogenized on ice. Homogenates were then centrifuged at 12,700 rpm for 10 minutes at 4°C. Fifty microliters of the resulting supernatant were collected and assayed for IL-6, MCP-1, KC, TNF-α and IL-10 by flow cytometry as described above.

III – 6. Plasma Alanine Aminotransferase (ALT) Assay

Blood collected at the time of necropsy was used to evaluate plasma ALT activity Spectrophotometrically using Infinity ALT reagents purchased from Thermo Electron Corp. (Louisville, CO).

III – 7. Liver Tissue Processing for Light Microscopy and Immunohistochemistry

Transverse sections from the middle of the left liver lobe were embedded in Paraffin, cut at a thickness of 5 µm and stained with hematoxylin and eosin (H&E) for routine histopathological examination and morphometric analyses. Other tissue sections

were histochemically stained with periodic acid Schiff staining and counterstained with hematoxylin (PASH) to identify intracellular glycogen.

Routine immunohistochemical techniques were used for hepatocellular detection of nuclear BrdU, hepatic infiltration of neutrophils, and hepatocellular expression of hypoxia inducible factor 1 alpha (HIF-1α). Briefly, liver sections were deparaffinized in xylene and rehydrated through descending grades of ethanol and immersed in 3% hydrogen peroxide to block endogenous peroxides. Sections were incubated with normal sera to inhibit nonspecific proteins (normal horse, rabbit or goat sera for BrdU, neutrophils or HIF-1α immunostaining, respectively, Vector Laboratories Inc., Burlingame, CA) followed by specific dilutions of primary antibodies (1:40, monoclonal mouse anti-BrdU antibody, BD, Franklin Lakes, NJ; 1:2500, monoclonal rat anti-neutrophil antibody, AbD Serotec, Raleigh, NC; 1:200, polyclonal rabbit anti-HIF-1α, Novus Biologicals, Littleton, CO). Tissue sections were subsequently covered with secondary biotinylated antibodies, and immunostaining was developed with the Vector RTU Elite ABC kit (BrdU and HIF-1α, Vector Laboratories Inc) or the RTU Phosphatase-labeled Streptavidin kit (neutrophils, Kirkegaard Perry Labs, Gaithersburg, MD) and visualized with Vector Red (neutrophils, Vector Laboratories Inc) or DAB (3,3'-diaminobenzidine) (BrdU or HIF-1α, Sigma Chemicals, St. Louis, MO) chromogens. Slides were counterstained with Gill 2 hematoxylin (Thermo Fisher, Pittsburgh, PA).

III – 8. Morphometric Analyses of Liver

BrdU-stained and unstained hepatocellular nuclei were counted in 10 medium power fields (X200) for each animal, starting with a randomly selected field and evaluating every third field. The hepatocellular labeling index (LI; % of hepatocytes undergoing DNA synthesis) was determined by counting the number of BrdU-labeled cells divided by the total number of hepatocytes and multiplying by 100.

Hepatic neutrophil accumulation was assessed by averaging the numbers of neutrophils in 10 medium power fields (X200) in each slide. Analyzed fields were selected in an unbiased manner with a random start and counting every third field. Neutrophils were identified by positive immunohistochemical staining with the neutrophil-specific antibody and their polymorphologic nuclear profiles.

Hepatocellular degeneration/necrosis in sections from the left liver lobe was quantified using standard morphometric methods that were similar to those previously described in detail (Yee et al., 2000). Briefly, H&E-stained liver sections from the left liver lobe were visualized with an Olympus BX-40 light microscope (Olympus Corp., Lake Success, NY) coupled with a 3.3-megapixel digital color camera (Qimaging, Surrey, BC, Canada). Images at a magnification of X200 were evaluated employing a 168-point lattice grid overlaying fields of hepatic parenchyma to determine (1) the total area of liver analyzed, (2) the area of degenerative/necrotic hepatic parenchyma and (3) the area of normal parenchyma. The area of each object of interest (e.g. lesion) was calculated using the following expression (Cruz-Orive, 1982):

$$Area_{Interest} = \Sigma\ Points_{Interest}\ X\ Area/Point$$

$$Area/Point = (Distance\ between\ Points)^2/Magnification^2$$

Distance between points was 13 μm. Accordingly, the area represented by each point was 511 μm^2. Section from the liver of each mouse was systematically scanned using adjacent, non-overlapping microscopic fields. The first image field analyzed in each section was chosen randomly. Thereafter, every third field was evaluated (approximately 10-14 fields evaluated/section). The measured fields represented approximately 65% of the total area of each liver section. Percent lesion area was estimated based on the following formula:

$$[Area_{Lesion\ of\ Interest}/(Area_{All\ Lesions} + Area_{Normal\ Parenchyma})]\ X\ 100.$$

III – 9. Quantitative Real Time RT-PCR for Hepatic Gene Expression

The caudate liver lobe was isolated and placed in RNAlater (Qiagen, Valencia, CA) and kept at 4°C for at least 24 h then transferred to -20°C until processed. Total RNA was extracted using RNeasy Mini Kit according to the manufacturer's instructions (Qiagen, Valencia, CA). Briefly, tissues were homogenized in RLT buffer containing β-mercaptoethanol with a 5 mm Rotor-Sator Homogenizer (PRO Scientific, Oxford, CT) and centrifuged at 10,700 rpm for 3 minutes. Samples were then treated with Rnase-Free Dnase, Rnase-free buffer and water on the column for 30 minutes (Qiagen). Eluted RNA was diluted 1:5 with Rnase free water and quantified using a GeneQuant Pro spectrophotometer (BioCrom, Cambridge, England).

Reverse transcription (RT) reaction was performed using reverse transcription high capacity cDNA reagents (Applied Biosystems, Foster City, CA) and a GeneAmp PCR System 9700 Thermocycler PE (Applied Biosystems). Each RT reaction was run in 5 μl of sample with 20 μl of cDNA Master Mix prepared according to the manufacturer's protocol (Applied Biosystems).

Expression analyses of isolated mRNA were performed by quantitative real-time PCR using individual animals' cDNA with the ABI PRISM 7900 HT Sequence Detection System using Taqman® Gene Expression Assay reagents (Applied Biosystems). The cycling parameters were 48°C for 2 minutes, 95°C for 10 minutes, and 40 cycles of 95°C for 15 seconds followed by 60°C for 1 minute. Individual data are reported as fold change of mRNA in experimental samples compared to the saline/air control group. Real-time PCR amplifications were quantified using the comparative Ct method normalized to the mean of two endogenous controls (18S and GAPDH). The cycle number at which each amplified product crosses the set threshold represented the Ct value. The amount of target gene normalized to the mean of the endogenous reference genes was calculated by substracting the endogenous reference Ct from the target gene Ct (ΔCt). Relative mRNA expression was calculated by substracting the mean ΔCt of the treated samples from the ΔCt of the control samples (saline-treated, air-exposed) (ΔΔCt). The absolute values of the comparative expression level (fold change) was then calculated by using the formula:

Fold change = $2^{-\Delta\Delta CT}$.

III – 10. Glutathione Assay

To determine hepatic concentrations of oxidized glutathione (GSSG) and total glutathione (reduced plus oxidized; GSH and GSSG, respectively), median lobes of the liver (preserved at -80°C) were homogenized in cold MES buffer (0.4 M 2-(N-morpholino)ethanesulfonic acid, 0.1 M phosphate, and 2 mM EDTA, pH = 6). Homogenates were centrifuged at 9,700 rpm for 15 minutes at 4°C, and the supernatants were collected and deproteinated. The total glutathione concentration was then assayed as recommended by the manufacturer (Cayman Chemical Co., Ann Arbor, MI). GSSG concentration was determined after derivatization of GSH with 2-vinylpyridine. Sample absorbance was determined at 405 nm, and the total or oxidized glutathione concentrations in liver homogenates was assessed by comparison of absorption to standard curves.

III – 11. Thiobarbituric Acid-Reactives Substances (TBARS) Assay

Lipid peroxidation in the liver was estimated using a commercially available kit according to the manufacturer's recommendations and malonaldehyde as a standard (TBARS kit, Cayman Chemical Co., Ann Arbor, MI). Liver tissue was homogenized on ice in RIPA Buffer and Proteases Inhibitor (Thermo Scientific, Rockford, IL). Homogenates were centrifuged at 3,900 rpm, and the supernatant was collected and used to detect malonaldehyde and TBARS adducts in acidic conditions and under high temperature (100°C). Absorbance was measured at 530 nm.

III – 12. Statistical Analyses

Data were reported as mean +/- SE. Differences among groups were analysed by a one- or two-way ANOVA followed by Student-Newman-Keuls post hoc test. When normality or variance equality failed, a Kruskal-Wallis ranked test was conducted. All analyses were performed using SigmaStat software (SigmaStat; Jandel Scientific, San Rafael, CA). Significance was assigned to p values smaller than or equal to 0.05.

IV. RESULTS

IV – 1. Inflammatory Responses Reflected in BALF

Saline treatment/O3 exposure (O3 alone or SAL/O3 group) did not cause changes in BALF total inflammatory cell number at any time compared to saline treatment/air exposure (controls or SAL/air group) (Figure 2A, B). As compared to control mice, animals that were administered APAP and were exposed to either air (APAP/air or APAP alone) or O3 (APAP/0.5 ppm O3 or APAP and O3-coexposed mice) had a time-dependent, statistical increase in the number of total inflammatory cells in the BALF at 9 and 32 h after APAP administration (Figure 2A, B). Though not statistically significant, there was a trend for greater total inflammatory cells in the lungs of the APAP and 0.5 ppm O3-coexposed mice compared to APAP alone (Figure 2A, B). No difference in total inflammatory cell number was detected between APAP alone and APAP/0.25 ppm O3 groups at 32 h (Figure 2B).

Pulmonary inflammatory cell responses, as reflected in the BALF, were due to increases in alveolar macrophages and/or neutrophils (Figure 2C, D, E, F). O3 alone did not cause changes in neutrophil or macrophage number in BALF at any time (Figure 2C, D, E, F). At 9 and 32 h after APAP treatment, mice exposed to APAP alone or with O3 had significant increases of alveolar macrophages (Figure 2E, F). This response was somewhat greater at 32 compared to 9 h. On the other hand, the number of neutrophils in BALF was not affected by APAP at 9 h (Figure 2C, D). At 32 h, only APAP/O3-coexposed mice had marked increases in neutrophil numbers in BALF (Figure 2D), indicating a synergistic effect.

Figure 2. Inflammatory cell accumulation in the BALF of APAP and O3 exposed mice. Graphs represent total inflammatory cells (A and B), neutrophils (C and D) and macrophages (E and F) per ml of BALF. Animals were given 0 (saline) or 300 mg/kg APAP ip and 2 h later exposed to 0 (air), 0.25 (32 h only) or 0.5 ppm O3 for 6 h. 9 or 32 h after APAP administration, animals were euthanized and BALF harvested and analyzed as described in Materials and Methods. Data are expressed as mean ± SE (n = 6). a, significantly different from saline/air group; b, significantly different from saline/0.5 ppm O3 group; c, significantly different from saline/0.25 ppm O3; ($p \leq 0.05$). ND, not detected.

Figure 2

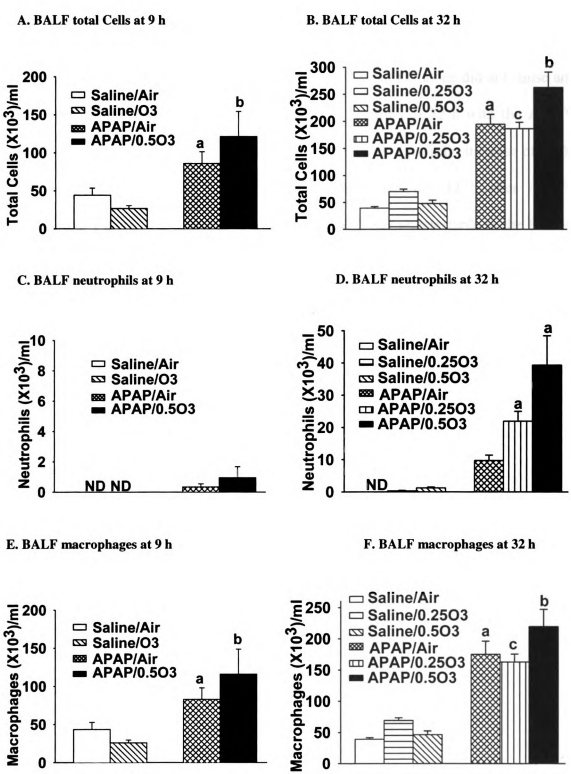
A. BALF total Cells at 9 h
Total Cells (X10³)/ml
Saline/Air
Saline/O3
APAP/Air
APAP/0.5O3
a
b
B. BALF total Cells at 32 h
Total Cells (X10³)/ml
Saline/Air
Saline/0.25O3
Saline/0.5O3
APAP/Air
APAP/0.25O3
APAP/0.5O3
a
c
b
C. BALF neutrophils at 9 h
Neutrophils (X10³)/ml
Saline/Air
Saline/O3
APAP/Air
APAP/0.5O3
ND ND
D. BALF neutrophils at 32 h
Neutrophils (X10³)/ml
Saline/Air
Saline/0.25O3
Saline/0.5O3
APAP/Air
APAP/0.25O3
APAP/0.5O3
ND
a
E. BALF macrophages at 9 h
Macrophages (X10³)/ml
Saline/Air
Saline/O3
APAP/Air
APAP/0.5O3
a
b
F. BALF macrophages at 32 h
Macrophages (X10³)/ml
Saline/Air
Saline/0.25O3
Saline/0.5O3
APAP/Air
APAP/0.25O3
APAP/0.5O3
a
c
b

BALF was analyzed by flow cytometry for exposure-induced changes in several inflammatory cytokines (IL-1, TNF-α, IL-10, IFN-γ, IL-6, MCP-1, IL-12 and KC, IL-10). Most of these cytokines were not significantly changed at either examined time (data not shown), with the exception of IL-6 and MCP-1. APAP or O3 alone did not cause an increase in IL-6 at 9 h and only a minimal increase occurred at 32 h with the APAP treatment (Figure 3A, B). APAP/O3 coexposure resulted in a significant increase of IL-6 in BALF compared to either substance alone at 9 h, but not 32 h after APAP administration (Figure 3A, B). At the early time, MCP-1 was undetectable in the BALF of mice from any of the groups (Figure 3C). O3 exposure caused a slight, but significant, elevation of MCP-1 at 32 h after APAP treatment (Figure 3D). MCP-1 in BALF was similarly and significantly elevated in APAP alone- or APAP/O3-coexposed mice 32 h after APAP (Figure 3D).

Figure 3. IL-6 (A and B) and MCP-1 (C and D) protein concentrations in the BALF of APAP and O3 exposed mice. Animals were given 0 (saline) or 300 mg/kg APAP ip and 2 h later exposed to 0 (air) or 0.5 ppm O3 for 6 h. 9 or 32 h after APAP administration, animals were euthanized and BALF harvested and cytokine concentrations evaluated as described in Materials and Methods. Data are expressed as mean ± SE (n = 6). a, significantly different from saline/0.5 ppm O3 group; b, significantly different from APAP/air group; c, significantly different from saline/air group; ($p \leq 0.05$). ND, not detected.

Figure 3

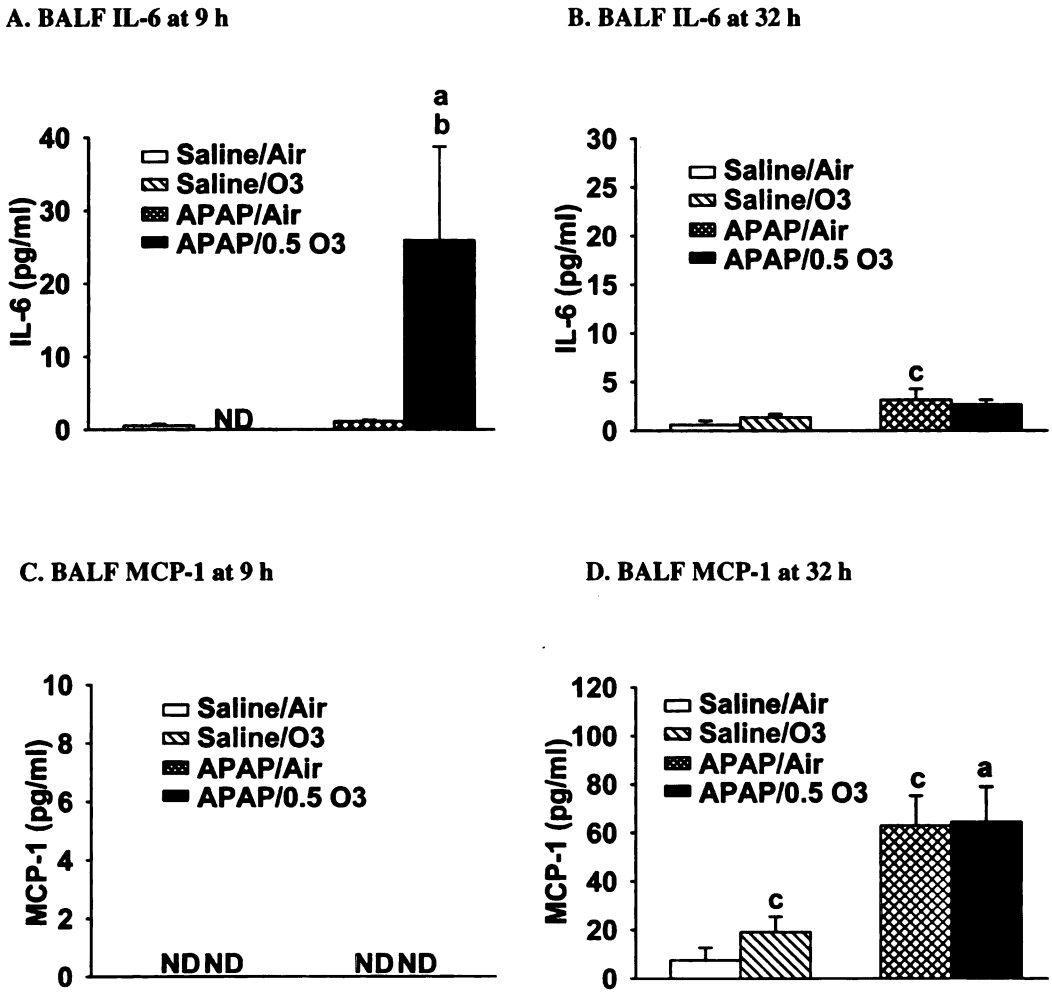
A. BALF IL-6 at 9 h
IL-6 (pg/ml)
40
30
20
10
0
Saline/Air
Saline/O3
APAP/Air
APAP/0.5 O3
a
b
ND
B. BALF IL-6 at 32 h
IL-6 (pg/ml)
30
25
20
15
10
5
0
Saline/Air
Saline/O3
APAP/Air
APAP/0.5 O3
c
C. BALF MCP-1 at 9 h
MCP-1 (pg/ml)
10
8
6
4
2
0
Saline/Air
Saline/O3
APAP/Air
APAP/0.5 O3
ND ND
ND ND
D. BALF MCP-1 at 32 h
MCP-1 (pg/ml)
120
100
80
60
40
20
0
Saline/Air
Saline/O3
APAP/Air
APAP/0.5 O3
c
c
a

IV – 2. Inflammatory Cytokine Concentrations in Plasma

Exposure-related changes in plasma cytokines were restricted to IL-6, MCP-1 and KC. Changes in plasma IL-6 reflected those in BALF with only APAP/O3 coexposure inducing significant elevation in IL-6 concentration and only at 9 h after treatment (Figure 4A, B). O3 alone-exposed mice had no plasma MCP-1 change at any time compared to controls. APAP alone caused significant elevation of plasma MCP-1 concentration 9 h after treatment that was not observed in the APAP/O3 coexposure group (Figure 4C). At 32 h, APAP alone and APAP/O3-coexposed mice had similar increases in plasma MCP-1 compared to controls (Figure 4D).

O3 exposure did not change the plasma concentrations of KC, a neutrophil chemokine (Figure 4E, F). KC was significantly elevated only in APAP/O3-coexposed mice at 9 h after APAP treatment (Figure 4E). At the later time, plasma KC was slightly above saline/O3 levels in APAP/O3-coexposed mice and there was a significant elevation in KC concentration in the plasma of mice given APAP alone (Figure 4F).

Figure 4. IL-6 (A and B), MCP-1 (C and D) and KC (E and F) protein concentrations in the plasma of APAP and O3 exposed mice. Animals were given 0 (saline) or 300 mg/kg APAP ip and 2 h later exposed to 0 (air) or 0.5 ppm O3 for 6 h. 9 or 32 h after APAP administration, animals were euthanized and blood collected and analyzed as described in Materials and Methods. Data are expressed as mean ± SE (n = 6). a, significantly different from saline/0.5 ppm O3 group; b, significantly different from APAP/air group; c, significantly different from saline/air group; ($p \leq 0.05$).

Figure 4

A. Plasma IL-6 at 9 h

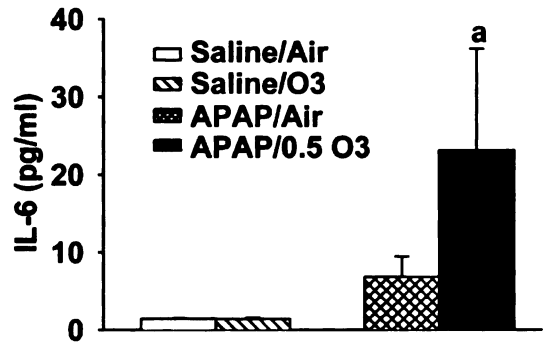

B. Plasma IL-6 at 32 h

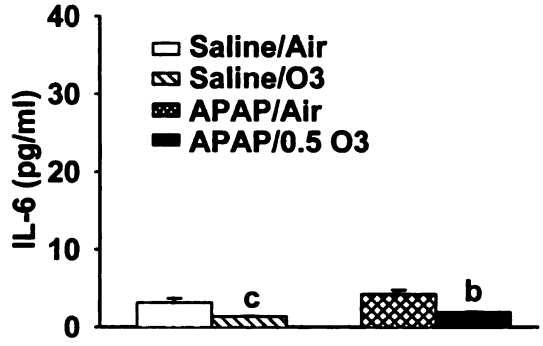

C. Plasma MCP-1 at 9 h

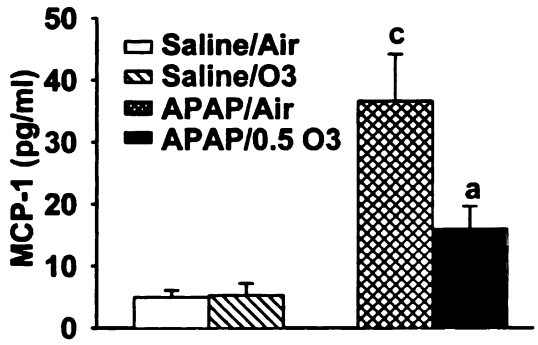

D. Plasma MCP-1 at 32 h

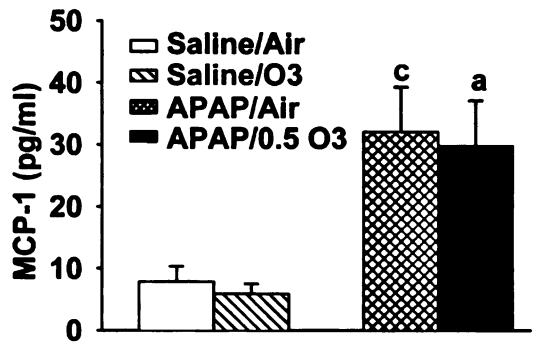

E. Plasma KC at 9 h

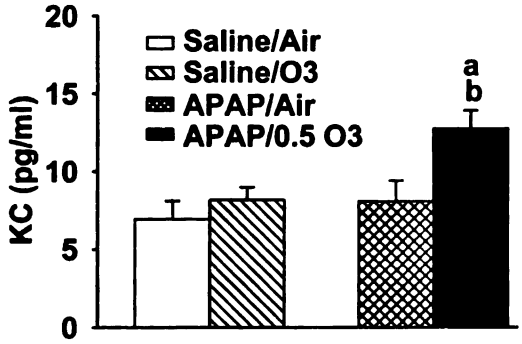

F. Plasma KC at 32 h

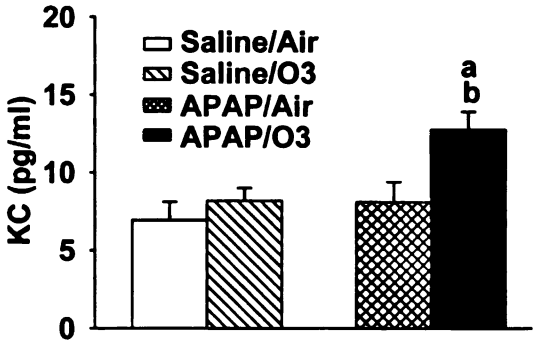

IV – 3. Histopathology and Morphometric Assessment of Liver Injury

Saline-treated mice exposed to either air or O3 had no hepatic histopathology at either time postexposure (Figure 5A, B). All APAP-treated mice developed hepatic centrilobular necrosis at 9 (data not shown) and 32 h (Figure 5C, D). This drug-induced liver lesion increased in severity with time after APAP administration. Inhalation exposures to either 0.25 or 0.5 ppm O3 markedly increased the APAP-induced centrilobular necrosis at 32 h (Figure 5F), but not 9 h after APAP administration (24 h and 1 h after O3 exposure, respectively). At the later time, APAP and O3-coexposed mice had expanded areas of centrilobular necrosis compared to APAP alone-treated mice. These expanded areas were rimmed by a distinctive layer of enlarged hepatocytes with highly vacuolated cytoplasm and pyknotic nuclei. This 1-2 cell layer of hepatocytes undergoing ballooning degeneration separated the conspicuous centrilobular areas of coagulative necrosis from the normal midzonal and periportal hepatocytes. Morphometrically, APAP-treated mice exposed to 0.25 or 0.5 ppm O3 had 1.46 or 1.62 time increases, respectively, in hepatocellular necrosis compared to APAP alone-treated mice (Figure 5F).

No changes in plasma ALT activity, a marker of hepatocellular injury in circulating blood, were detected in O3 alone-exposed mice as compared to control mice (Figure 5E). As expected, plasma ALT activity was significantly elevated in APAP-treated mice at 9 (data not shown) or 32 h after administration (Figure 5E). At the early time, no significant differences in ALT activity were observed between APAP alone- and APAP/O3-coexposed mice (data not shown). At 32 h after APAP injection, however,

ALT activity was significantly greater in APAP/O3-coexposed mice as compared to APAP/air-exposed mice (Figure 5E). This finding was reflected in differences in the extent of the centrilobular lesions between these groups.

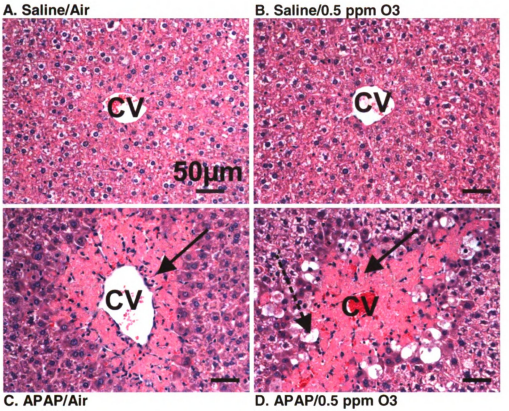

Figure 5. Liver damage induced by APAP and O3 exposure 32 h after APAP. Effects of APAP and O3 on alanine aminotransferase (ALT) activity (E) in plasma. Morphometric evaluation of hepatocellular damage (F). Animals were given 0 (saline) or 300 mg/kg APAP ip and 2 h later exposed to 0 (air), 0.25 or 0.5 ppm O3 for 6 h. Thirty-two hours after APAP administration, animals were euthanized, blood and liver tissue were collected and ALT and liver tissue evaluated as described in Materials and Methods. Data are expressed as mean ± SE (n = 6). a, significantly different from saline/air group; b, significantly different from saline/0.25 ppm O3 group; c, significantly different from saline/0.5 ppm O3; d, significantly different from APAP/air group; ($p \leq 0.05$). Solid arrow, centrilobular necrosis; stippled arrow, vacuolar degeneration; CV, central vein. ND, not detected.

Figure 5 (cont'd)

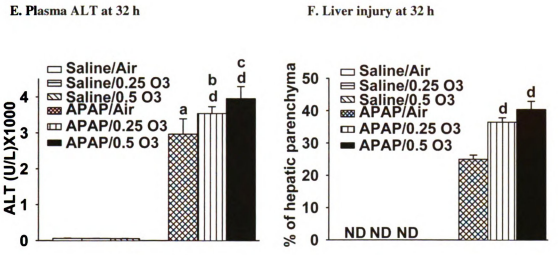

No neutrophilic accumulation was observed in livers of O3 alone-exposed mice at either time postexposure compared to controls (Figure 6A, B, E). In APAP-treated mice, neutrophilic accumulation was observed predominantly within the areas of hepatocellular degeneration and necrosis (Figure 6C, D). APAP/air and APAP/O3 groups had similar numbers of neutrophils in the liver as determined by morphometric analyses 9 h post-treatment (data not shown). At 32 h, the number of neutrophils in the livers of APAP/O3 mice was slightly but not significantly greater compared to APAP/air mice (Figure 6E).

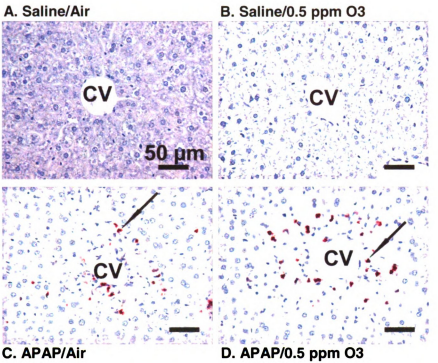

Figure 6. Liver neutrophil infiltration in APAP and O3 exposed mice 32 h after APAP. Morphometric evaluation of neutrophil infiltration in hepatic parenchyma (E). Animals were given 0 (saline) or 300 mg/kg APAP ip and 2 h later exposed to 0 (air) or 0.5 ppm O3 for 6 h. Animals were euthanized and livers collected and evaluated as described in Materials and Methods. Data are expressed as mean ± SE (n = 6). a, significantly different from saline/air group; b, significantly different from saline/O3 group; ($p \leq 0.05$). Black arrows indicate neutrophils; CV, central vein.

Figure 6 (cont'd)

E. Liver neutrophils at 32 h

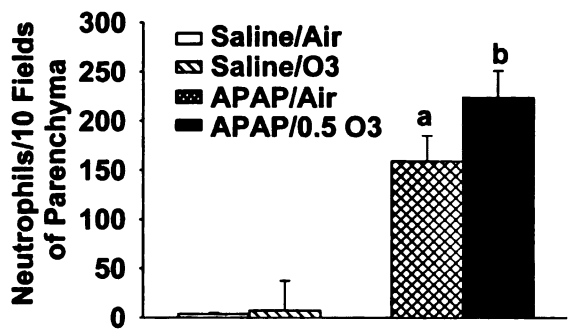

IV – 4. Hepatocellular Regeneration and Hypoxia

BrdU was administered to mice euthanized 32 h after APAP to identify hepatocytes undergoing DNA synthesis (S phase of the cell cycle). O3 exposure alone had no effect on hepatocellular BrdU incorporation compared to controls (Figure 7A, B, E). APAP treatment caused a marked increase of BrdU immunopositive nuclei which was dose-dependently reduced by coexposure with O3 (Figure 7C, D, E). 0.5 ppm O3 completely blocked the APAP-induced increase in BrdU incorporation in the liver (Figure 7E).

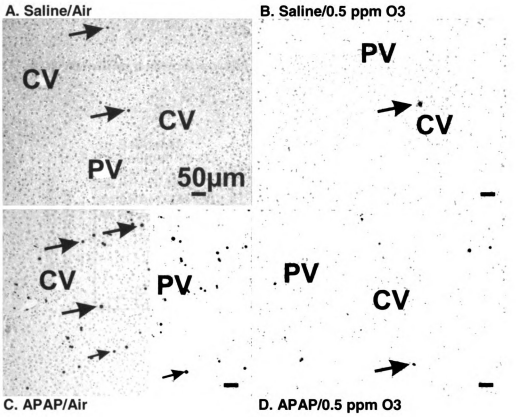

Figure 7. Hepatocellular proliferation in APAP and O3 exposed mice 32 h after APAP. Morphometric evaluation of cycling hepatocytes in S phase (E). Animals were given 0 (saline) or 300 mg/kg APAP ip and 2 h later exposed to 0 (air), 0.25 or 0.5 ppm O3 for 6 h. Two hours before euthanasia, mice received BrdU administration. Animals were euthanized and livers collected and evaluated as described in Materials and Methods. Data are expressed as mean ± SE (n = 6). a, significantly different from saline/air group; b, significantly different from APAP/air group; ($p \leq 0.05$). Black arrows indicate BrdU-labeled hepatocellular nuclei; PV, portal vein; CV, central vein.

Figure 7 (con't)

E. Hepatocellular proliferation at 32 h

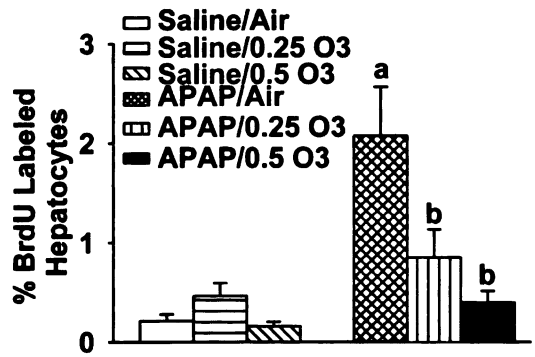

At 32 h, no change in glycogen or HIF-1α staining was seen in mice exposed to O3 alone compared to controls (Figure 8A1-2, 8B1-2). At the same time, necrotic areas in the liver of APAP-treated mice were surrounded by a one to two cell-thick layer of glycogen-depleted hepatocytes (Figure 8A3). Interestingly, in APAP/O3-coexposed mice, the ballooning degeneration of hepatocytes were located in this layer of glycogen depletion and appeared to be the targeted tissue for the O3-induced expansion of APAP-induced liver injury (Figure 8A4). APAP hepatotoxicity was accompanied by an increase in hepatocellular HIF-1α, a key transcription factor that mediates cellular response to hypoxia (Pouyssegur et al., 2006; Semenza, 2003). HIF-1α accumulation in APAP-treated mice was consistently found in the cytoplasm and less frequently in the nucleus of

hepatocytes located in glycogen-depleted areas (junction of centrilobular necrotic zone and healthy parenchyma) (Figure 8B3). In the APAP/O3 group, few hepatocellular nuclei, located primarily at the periphery of the necrotic zone, had HIF-1α accumulation (Figure 8B4).

Figure 8. Intracellular glycogen (A) and HIF-1α (B) staining 32 h after APAP. Light photomicrographs of liver sections from mice given saline/air (A1, B1), saline/0.5 ppm O3 (A2, B2), APAP/air (A3, B3) and APAP/0.5 ppm O3 (A4, B4). Animals were given 0 (saline) or 300 mg/kg APAP ip and 2 h later exposed to 0 (air) or 0.5 ppm O3 for 6 h. Animals were euthanized and livers collected and evaluated as described in Material and Methods. nH, normal hepatocytes, HH, hypoxic hepatocytes; *, hepatocellular necrosis; black arrows in A or black arriowheads in B indicate hepatocellular degeneration; black arrows in B indicate HIF-1α hepatocellular cytoplasmic staining, open arrowhead in B indicate endothelial cell HIF-1α staining; stippled arrow in B, HIF-1α nuclear staining; CV, central vein.

Figure 8

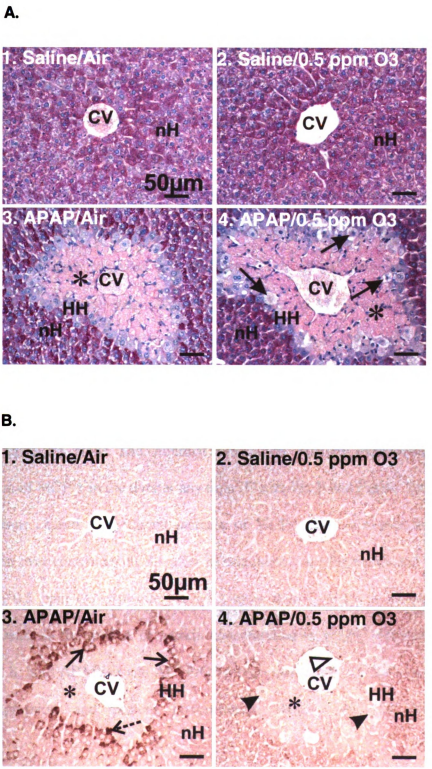
A.
1. Saline/Air
CV
nH
50µm
2. Saline/0.5 ppm O3
CV
nH
3. APAP/Air
CV
HH
nH
4. APAP/0.5 ppm O3
CV
HH
nH
B.
1. Saline/Air
CV
nH
50µm
2. Saline/0.5 ppm O3
CV
nH
3. APAP/Air
CV
HH
nH
4. APAP/0.5 ppm O3
CV
HH
nH

IV – 5. Relative Gene Expression and Protein Concentration of Inflammatory Cytokines in the Liver

O3 exposure alone did not cause relative gene expression changes in neutrophil chemokines KC or MIP-2 in the livers at any time postexposure (Figure 9A-D). This correlated with the lack of neutrophil liver accumulation in these mice. APAP treatment or APAP/O3 coexposure caused significant increases in relative expression of KC and MIP-2 genes 9 h after APAP (Figure 9A, C). KC protein concentration was also elevated in APAP/air and APAP/O3 groups at both 9 and 32 h after APAP (Figure 10A, B). At 9 h, no differences were observed in expression levels of KC between APAP/air and APAP/O3 groups (Figure 9A). At the same time, APAP/O3-coexposed mice had approximately three times the MIP-2 mRNA expression level of the APAP-alone group (Figure 9C). Relative gene expression of these chemokines declined to levels similar to those of controls at 32 h after APAP (Figure 9B, D).

O3 exposure alone had minimal effects on relative expression or protein concentration of MCP-1 in the liver at any time (Figure 9E, F and Figure 10C, D). APAP treatment alone caused a significant increase of MCP-1 relative expression or protein concentration over control levels 9 h after its administration (Figure 9E and Fig 10C). In comparison, 0.5 ppm O3 exposure caused a more than five-fold reduction in APAP-induced increase in the mRNA or protein concentration of MCP-1 (Figure 9E and Fig 10C). At 32 h, both APAP/air and APAP/O3 groups had significant increases in MCP-1 mRNA expression and protein concentration (Figure 9F and Figure 10D).

Figure 9. KC (A and B), MIP-2 (C and D) and MCP-1 (E and F) genes expression in livers of APAP and O3 exposed mice. Animals were given 0 (saline) or 300 mg/kg APAP ip and 2 h later exposed to 0 (air) or 0.5 ppm O3 for 6 h. 9 or 32 h after APAP administration, animals were euthanized and liver samples collected in RNALater and evaluated as described in Materials and Methods. Data are expressed as mean ± SE (n = 6). a, significantly different from saline/air group; b, significantly different from saline/0.5 ppm O3 group; c, significantly different from APAP/air group; ($p \leq 0.05$). FC, fold change.

Figure 9

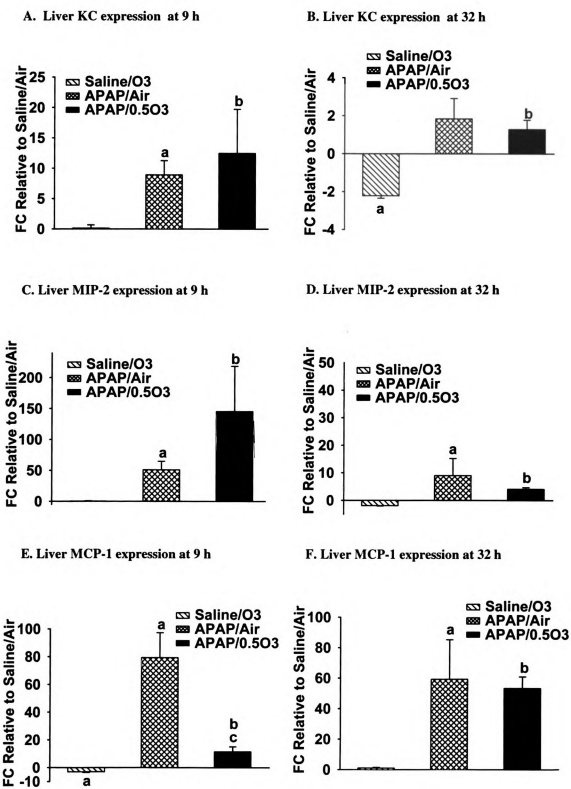
A. Liver KC expression at 9 h
B. Liver KC expression at 32 h
C. Liver MIP-2 expression at 9 h
D. Liver MIP-2 expression at 32 h
E. Liver MCP-1 expression at 9 h
F. Liver MCP-1 expression at 32 h
FC Relative to Saline/Air
Saline/O3
APAP/Air
APAP/0.5O3
a
b
c

Figure 10. KC (A and B), MCP-1 (C and D) and IL-6 (E and F) protein concentrations in livers of APAP and O3 exposed mice. Animals were given 0 (saline) or 300 mg/kg APAP ip and 2 h later exposed to 0 (air) or 0.5 ppm O3 for 6 h. 9 or 32 h after APAP administration, animals were euthanized and liver samples collected and evaluated as described in Materials and Methods. Data are expressed as mean ± SE (n = 6). a, significantly different from saline/air group; b, significantly different from saline/0.5 ppm O3 group; c, significantly different from APAP/O3 group; ($p \leq 0.05$).

Figure 10

A. Liver KC at 9 h

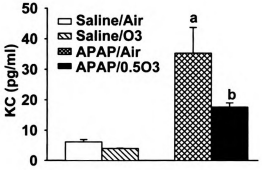

B. Liver KC at 32 h

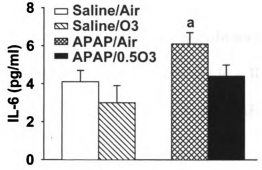

C. Liver MCP-1 at 9 h

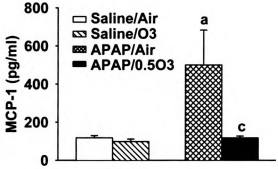

D. Liver MCP-1 at 32 h

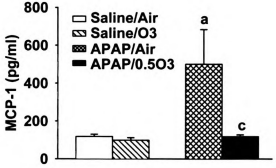

E. Liver IL-6 at 9 h

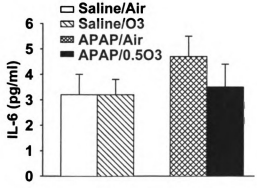

F. Liver IL-6 at 32 h

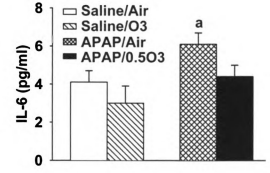

O3 exposure had no effect on IL-6 or plasminogen activator inhibitor 1 (PAI-1) relative expression at any time (Figure 11A-D). APAP treatment on the other hand resulted in significantly elevated hepatic IL-6 and PAI-1 mRNA 9 or 32 h after its administration (Figure 11A, B). O3 coexposure tended to reduce the increases of IL-6 and PAI-1 mRNA caused by APAP, but this reduction reached statistical significance at the early time only (Figure 11A, B). In agreement with these gene expression data, IL-6 protein was increased in the liver by APAP, but not APAP/O3, at 9 h only after APAP treatment (Figure 10E, F).

Figure 11. IL-6 (A and B) and PAI-1 (C and D) genes expression in livers of APAP and O3 exposed mice. Animals were given 0 (saline) or 300 mg/kg APAP ip and 2 h later exposed to 0 (air) or 0.5 ppm O3 for 6 h. 9 or 32 h after APAP administration, animals were euthanized and liver samples collected in RNALater and evaluated as described in Materials and Methods. Data are expressed as mean ± SE (n = 6). a, significantly different from saline/air group; b, significantly different from APAP/air group; c, significantly different from saline/O3 group; ($p \leq 0.05$). FC, fold change.

Figure 11

A. Liver IL-6 expression at 9 h

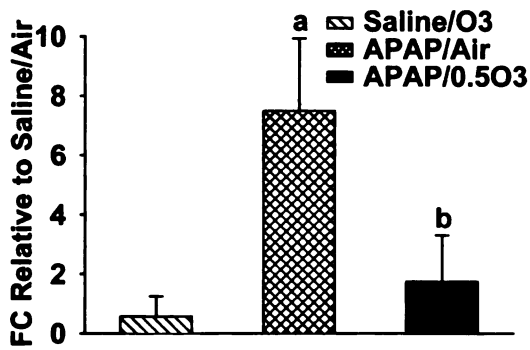

B. Liver IL-6 expression at 32 h

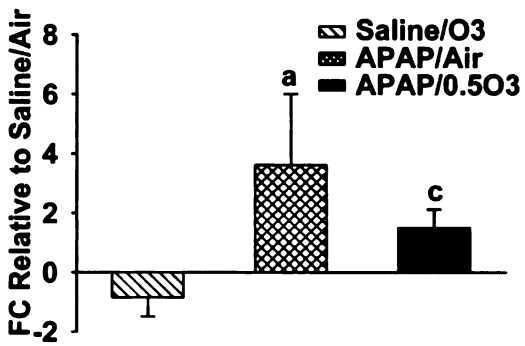

C. Liver PAI-1 expression at 9 h

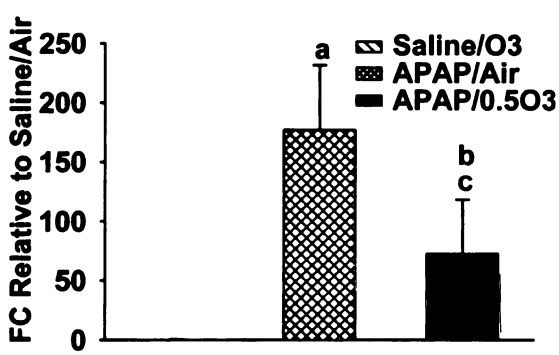

D. Liver PAI-1 expression at 32 h

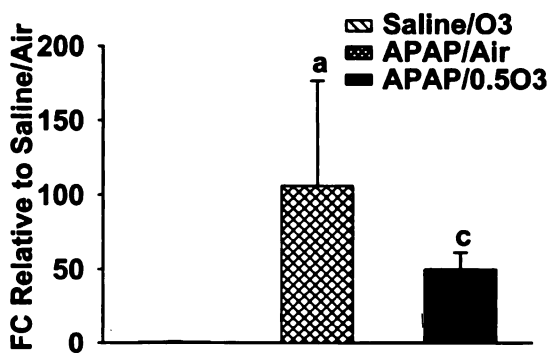

IV – 6. Regeneration-Related Gene Expression in Liver Tissue

O3 or APAP alone caused an increase in liver mRNA expression of the cyclin dependent kinase inhibitor P21, at the early time postexposure (Figure 12A). At the same time, APAP/O3 coexposure resulted in significantly greater expression of P21 mRNA expression compared to either APAP or O3 (Figure 12A). At 9 h, suppressor of cytokine signaling 3 (SOCS3) expression was decreased by O3 exposure but increased by APAP treatment (Figure 12C). APAP/O3 group had no statistically significant increase in expression of SOCS3 as compared to APAP-alone group (Figure 12C). At 32 h, APAP-alone and APAP/O3 mice had similar increases in the expression of P21 and SOCS3 as compared to control mice (Figure 12B, D).

Figure 12. P21 (A and B) and SOCS3 (C and D) genes expression in APAP and O3 exposed mice. Animals were given 0 (saline) or 300 mg/kg APAP ip and 2 h later exposed to 0 (air) or 0.5 ppm O3 for 6 h. 9 or 32 h after APAP administration, animals were euthanized and liver samples collected and evaluated as described in Materials and Methods. Data are expressed as mean ± SE (n = 6), a, significantly different from saline/air group; b, significantly different from saline/0.5 ppm O3 group; c, significantly different from APAP/air group; ($p \leq 0.05$). FC, fold change.

Figure 12

A. Liver P21 expression at 9 h

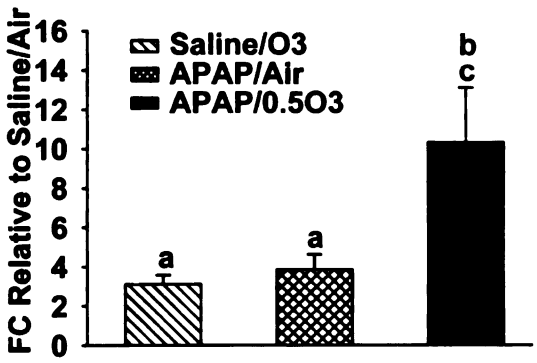

B. Liver P21 expression at 32 h

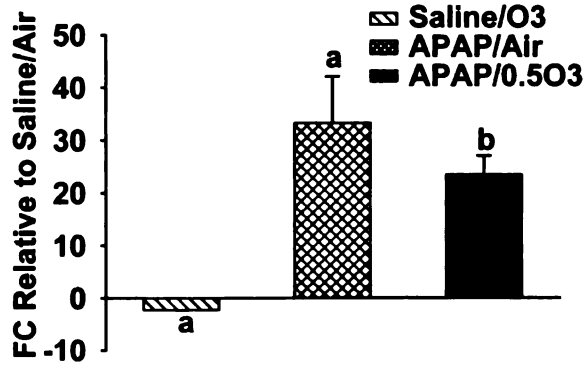

C. Liver SOCS3 expression at 9 h

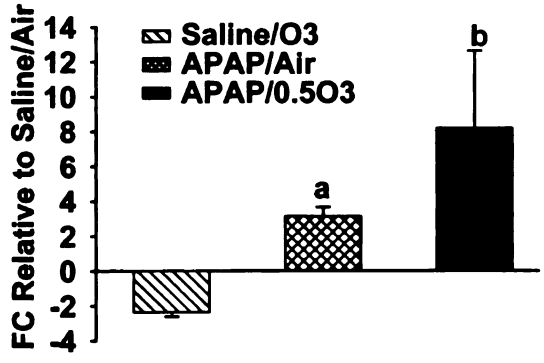

D. Liver SOCS3 expression at 32 h

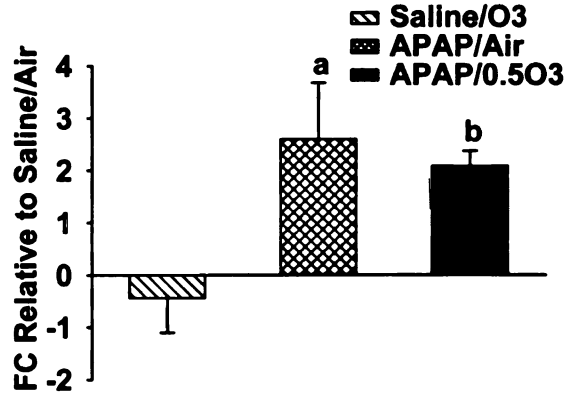

IV – 7. Liver Oxidative Damage (Antioxidant Genes, Glutathione and TBARS Assays)

Heme oxygenase-1 (HO-1), metallothionein-1 (MT-1) and the catalytic subunit of glutamate-cysteine ligase (GCLC) were evaluated as markers of oxidative stress. For all three of these antioxidant genes, mRNA expression was significantly elevated with APAP treatment whereas only MT-1 was increased with O3 exposure 9 h after APAP (Figure 13A, C, E). At 9 h, APAP/O3 coexposure resulted in significant increase of MT-1 expression above APAP or O3 levels (Figure 13A). At the later time (32 h), expression of these genes declined in APAP/air or APAP/O3 groups as compared to the early time, and APAP/O3-coexposed mice had less or comparable mRNA expression compared to APAP/air-treated mice (Figure 13B, D, F).

Figure 13. MT-1 (A and B), HO-1 (C and D) and GCLC (E and F) genes expression in livers of APAP and O3 exposed mice. Animals were given 0 (saline) or 300 mg/kg APAP ip and 2 h later exposed to 0 (air) or 0.5 ppm O3 for 6 h. 9 or 32 h after APAP administration, animals were euthanized and liver samples collected in RNALater and evaluated as described in Materials and Methods. Data are expressed as mean ± SE (n = 6). a, significantly different from saline/air group; b, significantly different from saline/0.5 ppm O3 group; c, significantly different from APAP/air group; ($p \leq 0.05$). FC, fold change.

Figure 13

A. Liver MT-1 expression at 9 h

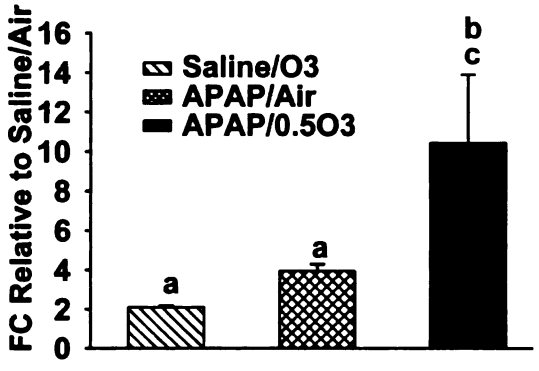

B. Liver MT-1 expression at 32 h

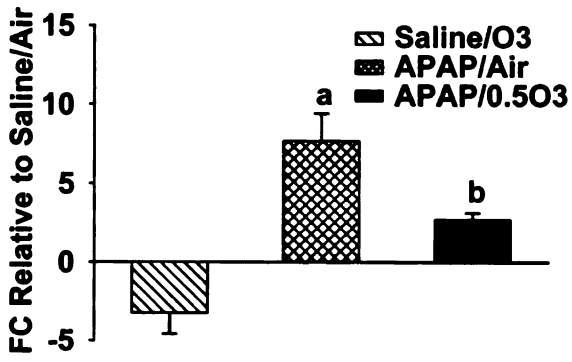

C. Liver HO-1 expression at 9 h

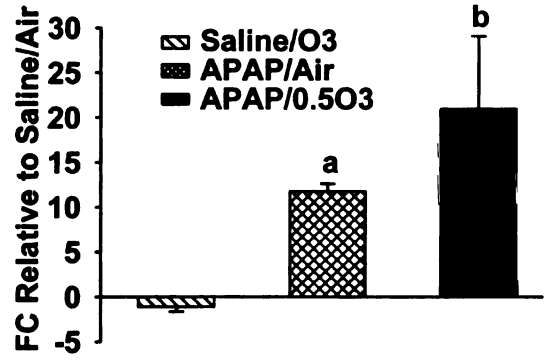

D. Liver HO-1 expression at 32 h

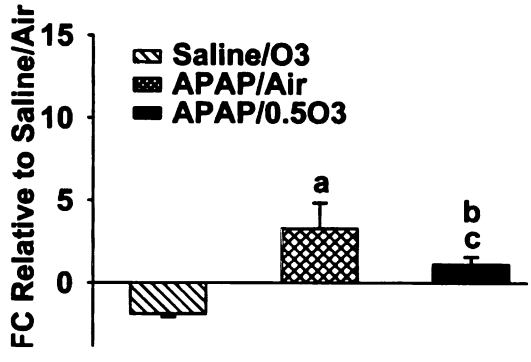

E. Liver GCLC expression at 9 h

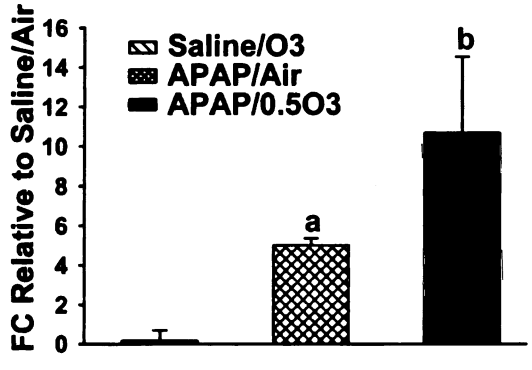

F. Liver GCLC expression at 32 h

To explore further O3 exacerbation of APAP-induced liver toxicity and the role of oxidative stress, we evaluated concentrations of GSH and GSSG. At 9 h, total glutathione concentration was greater in APAP alone and APAP/O3 coexposure groups than in control animals (Figure 14A). At the same time, O3-exposed mice had less total glutathione concentration in the liver compared to control mice (Figure 14A). Interestingly, O3 alone and APAP/O3 groups had more GSSG than control and APAP alone groups, respectively (Figure 14B).

We also evaluated lipid peroxidation levels in livers using TBARS assay. Mice coexposed to APAP and O3 had greater concentrations of TBARS at the early time postexposure relative to APAP alone-treated mice. (Figure 14C). O3 alone-exposed mice had no significant increase in the concentration of TBARS compared to controls (Figure 14C). By 32 h, TBARS concentrations in APAP alone and APAP/O3 groups were less than that of their respective control groups (Figure 14D).

Figure 14. Total (A) or oxidized (B) glutathione and TBARS (C and D) concentrations in livers of APAP and O3 exposed mice. Animals were given 0 (saline) or 300 mg/kg APAP ip and 2 h later exposed to 0 (air) or 0.5 ppm O3 for 6 h. 9 or 32 h after APAP administration, animals were euthanized and liver samples collected and evaluated as described in Materials and Methods. Data are expressed as mean ± SE (n = 6). a, significantly different from saline/air group; b, significantly different from saline/0.5 ppm O3 group; c, significantly different from APAP/air group; ($p \leq 0.05$).

Figure 14

A. Liver total glutathione at 9 h

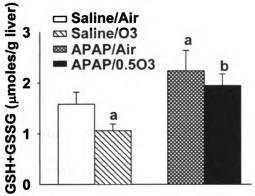

B. Liver oxidized glutathione at 9 h

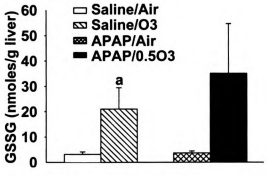

C. Liver TBARS at 9 h

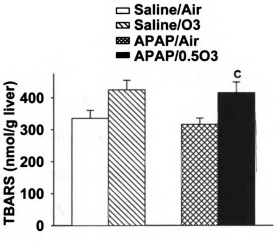

D. Liver TBARS at 32 h

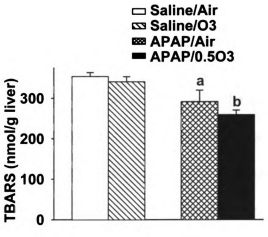

V. DISCUSSION

To our knowledge, this is the first study to examine the pulmonary and systemic effects of APAP/O3 coexposure in laboratory animals. Acute exposure to 0.25 or 0.5 ppm O3 alone did not cause pulmonary inflammation in the mice of our study, as evidenced by BALF analysis. In contrast, APAP treatment alone did cause acute inflammation of the lung, and this drug-induced pulmonary response was exacerbated by O3 coexposure. The most remarkable finding, however, was that a single 6 h inhalation exposure to O3 resulted in exacerbation of APAP-induced liver injury. After a hepatotoxic dose of APAP, exposure of mice to 0.5 ppm O3 resulted in a 60% increase in hepatocellular necrosis and an 80% decrease in hepatocellular regeneration as compared to mice treated with APAP alone. How a single acute exposure of O3 caused such marked enhancement of this drug-induced liver injury in mice is unknown.

It is not likely that O3 caused direct injury to the liver, since it is one of the most reactive chemicals known and others have demonstrated that when inhaled it reacts quickly with airway surface lining fluid and is converted to secondary lipid ozonation products (Miller, 1995; Pryor, 1992; Pryor et al., 1995). These secondary products (e.g., aldehydes, hydroxyhydroperoxides etc) are thought to be the principal toxicants responsible for O3's toxicity to epithelial cells lining the airway surfaces. Therefore O3 could not have entered the systemic circulation to be transported from the lung to the liver resulting in direct hepatotoxicity.

Though the present study was not designed to definitively determine how acute inhalation exposure to O3 caused exacerbation of APAP-induced liver injury, the results

of our biochemical and molecular analyses suggest some plausible hypotheses that will have to be addressed in future studies.

One possibe hypothesis is that the O3-induced enhancement of APAP hepatotoxicity is due in part to increased oxidative stress in the liver (i.e., more injurious oxidant free radicals than protective antioxidants). Goldstein et al. (1978) suggested that extrapulmonary effects of O3 are related to lipid oxidation products, particularly malonaldehyde released after the interaction of O3 with airway epithelial cell membrane fatty acids. Interestingly, oxidative stress has also been suggested to be play a key role in the progression of APAP-induced liver injury, specifically through induction of mitochondrial permeability transition pore formation (Jaeschke et al., 2003). It is plausible that the systemic increase in oxidative stress induced by inhaled O3 may have been partially responsible for the exacerbation of both APAP-induced liver injury observed in of our study.

In the present study, APAP/O3 coexposure resulted in significant expression of the oxidative stress-responsive genes, MT-1, HO-1, and GCLC in the liver. We also found that O3 exposure in either APAP- or saline-treated mice caused significant increases of hepatic GSSG, another indicator of oxidative stress (i.e., oxidation of GSH). In addition, lipid peroxidation, an indicator of oxidant-induced cellular injury, was biochemically evident in the livers of O3-exposed mice.

The greatest measured response in antioxidant gene expression in the liver of APAP/O3-coexposed mice was MT-1. Metallothioneins, including MT-1, are cysteine-rich proteins with various protective roles including antioxidant properties (Kang, 2006). Both APAP and O3 have been shown to induce increases of these proteins in the liver

and lung of mice, respectively (Johnston et al., 1999; Wormser and Calp, 1988). In addition, mice lacking MT-1 and MT-2 are more sensitive to APAP or O3 toxicity compared to their wild-type counterparts (Inoue et al., 2008; Liu et al., 1999). Last et al. (2005) also reported that mice exposed to O3 exhibited greater hepatic expression of MT-1 compared to air-exposed animals.

The antioxidant effects of MTs have been ascribed to their abundant cysteine moieties and direct scavenging properties of phenoxyl or hydroxyl radicals and superoxide anions as demonstrated by in vitro studies (Schwarz et al., 1994). Alternatively, the effect of MTs could be due to antioxidant properties of zinc released from MTs by reactive oxygen species (Powell, 2000; Schwarz et al., 1994). Owing to these roles, it is probable that the greater induction of MT-1 in the combined APAP and O3 coexposure was in response to enhanced oxidative stress.

With immunohistochemical analysis, we found that mice given APAP had conspicuous accumulation of HIF-1α in hepatocytes immediately surrounding the centrilobular areas of necrosis. These same hepatocytes had concurrent loss of cytoplasmic glycogen as demonstrated by PAS histochemistry. It was these HIF-1α-overexpressing, glycogen-depleted hepatocytes at the edge of the drug-induced necrotic regions that appeared microscopically to be further altered (e.g., ballooning degeneration and necrosis) by acute coexposure to O3. It is known that APAP directly targets mitochondria inhibiting oxidative phosphorylation and compromising ATP synthesis with subsequent induction of glycolysis (Kon et al., 2004). APAP also induces HIF-1α accumulation in a hypoxia-unrelated, oxidative stress-dependent fashion (James et al., 2006). In addition, HIF-1α induction results in decreased oxidative phosphorylation

and stimulation of glycolysis in the liver of mice (Denko, 2008). Thus, glycogen depletion in the peri-necrotic hepatocytes in APAP-treated mice might have been mediated by HIF-1α in our study.

O3 inhalation is also known to compromise cardiopulmonary function by increasing breathing frequency and pulmonary resistance, and decreasing tidal volume, forced vital capacity, heart rate, and mean arterial pressure (EPA, 2008). These alterations in function could decrease the delivery of adequately oxygenated blood to distant extrapulmonary organs and enhance damage in poorly oxygenated areas like the centrilobular hepatic zone. Interestingly, other studies in mice have recently demonstrated that chronic intermittent hypoxia can cause lipid peroxidation in the liver and exacerbate APAP-induced hepatic injury (Savransky et al., 2007). It is therefore reasonable to believe that the APAP-induced loss of glycogen and increased HIF-1α in these hepatocytes might have made these cells more susceptible to O3 toxicity.

In the present study, PAI-1 expression was increased in the livers of APAP-treated mice similar to that reported by others (Bajt et al., 2008; Ganey et al., 2007; Reilly et al., 2001). In contrast, APAP/O3-coexposed mice in our study had markedly less PAI-1 liver expression as compared to mice given APAP alone. PAI-1inhibits plasminogen activators involved in the formation of plasmin and as such inhibits fibrinolysis in mice (Bajt et al., 2008). In mice deficient in PAI-1, APAP caused greater plasma ALT activity, hepatocellular necrosis and reduced hepatocellular regeneration (Bajt et al., 2008). Like these PAI-1 deficient animals, the APAP/O3-coexposed mice in our study had greater hepatocellular injury and impaired hepatocellular repair (i.e., reduction in BrdU labeling index). One explanation for the role of PAI-1 in APAP/O3 co-

toxicity could be that reduced PAI-1 led to early fibrinolysis in these animals which then resulted in an ischemia/reperfusion-like mechanism.

It has been reported that P21 mRNA was increased in APAP-treated, PAI-1 deficient mice (Bajt et al., 2008). In our study, APAP/O3-coexposed mice had reduced expression of PAI-1 compared to APAP alone and an increase in the expression of P21 mRNA. P21 halts the cell cycle in the G1 phase by inhibiting the activity of cyclinE/cdk2 complexes (Weinberg and Denning, 2002). Therefore it is possible that the enhanced liver pathology in APAP/O3 -coexposed mice might be due in part to an O3-induced reduction in PAI-1 which in turn caused an increase in P21 that led to impairment of hepatocellular regeneration.

As mentioned above, the results of our study clearly demonstrated that O3 exposure significantly impaired reparative hepatocellular regeneration in APAP-treated mice. This suggested to us that the O3 enhancement of APAP-induced liver injury may be due in part to reduced repair mechanisms. Mehendale and collaborators have proposed that the severity of acute chemical-induced liver toxicity is strongly dependent upon tissue repair processes (Soni et al., 1999). They have shown that cotreatment with small doses of hepatotoxicants (e.g., chlordecone and carbon tetrachloride, CCl4) can cause synergistic toxicity by inhibition of tissue repair (Soni and Mehendale, 1998). The differential expression of several genes in the livers of APAP/O3-coexposed mice in our study suggests some possible mechanisms by which O3 exposure might have compromised the hepatocellular regeneration after APAP-induced injury. For example, IL-6 gene and protein expression in the liver of APAP/O3-coexposed mice was significantly reduced compared to that in mice treated with APAP alone. This correlated

with the marked reduction in hepatocellular BrdU-labeling (reduced DNA synthesis). IL-6 is known to be an essential protein for the initial phases of hepatocellular regeneration, transitioning cells from the G0 to the G1 phase of the cell cycle (Fausto et al., 2006; Taub, 2004).

Cressman and co-workers (1996) have shown that after partial hepatectomy, mice deficient in IL-6 had greater hepatocellular injury and reduced reparative regeneration as compared to IL-6 sufficient hepatectomized mice. IL-6 deficient mice treated with CCl4 had greater hepatocellular damage and decreased number of hepatocytes in the S phase of the cell cycle as compared to IL-6 sufficient mice (Kovalovich et al., 2000). Pretreatment of IL-6 deficient mice with IL-6 significantly reduced CCl-4-induced liver injury and restored the reparative induction of DNA synthesis. We found that O3 inhalation caused impairment of hepatocellular repair following APAP-induced injury. Though the downregulation of hepatic IL-6 expression may be responsible for impaired liver regeneration 32 h after APAP, there may be other mechanisms involved.

Other potential candidates responsible for the impaired regeneration in APAP/O3-coexposed mice are P21 and MCP-1. In APAP/O3-coexposed mice, expression of P21 was increased relative to mice given APAP or O3 alone. Activation of P21 after DNA damage is known to delay or arrest the cell cycle (Garner and Raj, 2008). APAP treatment or O3 exposure cause DNA damage in the liver or lung, respectively (Bornholdt et al., 2002; Hongslo et al., 1994; Ito et al., 2005; Ray et al., 1990). In the present study, mice treated with APAP or exposed to O3 alone had greater hepatic P21 expression than saline-treated and air-exposed control mice. APAP/O3-coexposed mice had even greater P21 expression compared to mice receiving only one of these chemical

agents. Though the level of DNA damage in the liver was not measured in this study, the marked increase in P21 expression in the liver of coexposed mice might have been due to increased DNA damage which is known to lead to hepatic cell death (Corcoran and Ray, 1992).

Another interesting finding in this study was the effect of APAP and O3 on the expression of the inflammatory chemokine MCP-1 in the liver. APAP treatment caused a significant increase in the expression of this chemokine, but O3 exposure caused a marked reduction in MCP-1 expression. This reduction was associated with enhanced liver toxicity and defective hepatocellular regeneration responses. MCP-1 has been shown to be involved in cell regeneration and tissue repair in various tissues after different types of induced cell injury (Kim et al., 2003; Low et al., 2001; Shireman et al., 2007). Mice lacking MCP-1 or the receptor for MCP-1 have been reported to be more (Hogaboam et al., 2000) or similarly (Dambach et al., 2002) sensitive to APAP-induced hepatotoxicity compared to their wild-type counterparts. Interestingly, mice lacking the receptor for MCP-1 also had decreased reparative DNA synthesis in a murine model of arterial injury (Kim et al., 2003). It is not known how a reduction of MCP-1 could lead to impaired cell regeneration, but the role of MCP-1 in the O3 enhancement of APAP-induced hepatotoxicity should be explored in future studies.

In conclusion, we found that a single 6 h inhalation exposure of mice to high ambient concentrations of O3 caused marked enhancement of APAP-induced hepatotoxicity in mice. The present study was not designed to determine the underlying mechanism(s) responsible for this observed sytemic effect caused by this common oxidant air pollutant. Several biochemical and molecular markers of oxidative stress were

elevated in the livers of APAP/O3-coexposed mice compared to mice that received only APAP or O3 alone. In addition, we found that concurrent with the enhancement of hepatotoxicity, O3 also caused a marked attenuation of normal increases in DNA synthesis necessary for hepatocellular regeneration and repair in response to chemical-induced liver injury. This specific finding suggests a possible role of impaired cellular regeneration and enhanced toxicity in the liver of coexposed mice. Though it is unclear how inhalation of this highly reactive gas could enhance chemical-induced liver injury, several endogenous hepatic proteins such as IL-6, HIF-1α, PAI-1, P21, and MCP-1 have been identified as potentially playing important roles.

These results in mice also suggest that exposures to high ambient concentrations of O3 and other air pollutants (e.g., particulate matter) may pose a risk to people with pre-existing chemical-induced and other liver diseases. Further studies are needed not only to understand the biological mechanisms underlying this sytemic effect of inhaled O3, but also to determine the smallest doses of O3 and APAP at which these synergistic responses in the liver occur. In addition, epidemiological studies investigating the potential interactive effects of pharmaceutical agents and air pollutants on both hepatic and pulmonary disease appear to be warranted, especially in the light of recent reports that headaches are commonly reported in association with increased concentrations of air pollutants (Larrieu et al., 2009) and that APAP and other nonsteroidal, over-the-counter pain medications, are commonly taken by the general public.

VI. REFERENCES

Araujo, J.A., Barajas, B., Kleinman, M., Wang, X., Bennett, B.J., Gong, K.W., Navab, M., Harkema, J., Sioutas, C., Lusis, A.J., Nel, A.E., 2008. Ambient particulate pollutants in the ultrafine range promote early atherosclerosis and systemic oxidative stress. Circ Res 102, 589-596.

Bajt, M.L., Yan, H.M., Farhood, A., Jaeschke, H., 2008. Plasminogen activator inhibitor-1 limits liver injury and facilitates regeneration after acetaminophen overdose. Toxicol Sci 104, 419-427.

Bell, M.L., McDermott, A., Zeger, S.L., Samet, J.M., Dominici, F., 2004. Ozone and short-term mortality in 95 US urban communities, 1987-2000. JAMA 292, 2372-2378.

Bornholdt, J., Dybdahl, M., Vogel, U., Hansen, M., Loft, S., Wallin, H., 2002. Inhalation of ozone induces DNA strand breaks and inflammation in mice. Mutat Res 520, 63-71.

Corcoran, G.B., Ray, S.D., 1992. The role of the nucleus and other compartments in toxic cell death produced by alkylating hepatotoxicants. Toxicol Appl Pharmacol 113, 167-183.

Dambach, D.M., Watson, L.M., Gray, K.R., Durham, S.K., Laskin, D.L., 2002. Role of CCR2 in macrophage migration into the liver during acetaminophen-induced hepatotoxicity in the mouse. Hepatology 35, 1093-1103.

Denko, N.C., 2008. Hypoxia, HIF1 and glucose metabolism in the solid tumour. Nat Rev Cancer 8, 705-713.

EPA, U.S., 2008. Air Quality Criteria for O3 and Related Photochemical Oxidants (Final). EPA 600/R-05/004-aF-cF
Research Triangle Park.

Fausto, N., Campbell, J.S., Riehle, K.J., 2006. Liver regeneration. Hepatology 43, S45-53.

Ganey, P.E., Luyendyk, J.P., Newport, S.W., Eagle, T.M., Maddox, J.F., Mackman, N., Roth, R.A., 2007. Role of the coagulation system in acetaminophen-induced hepatotoxicity in mice. Hepatology 46, 1177-1186.

Garner, E., Raj, K., 2008. Protective mechanisms of p53-p21-pRb proteins against DNA damage-induced cell death. Cell Cycle 7, 277-282.

Gent, J.F., Triche, E.W., Holford, T.R., Belanger, K., Bracken, M.B., Beckett, W.S., Leaderer, B.P., 2003. Association of low-level ozone and fine particles with respiratory symptoms in children with asthma. JAMA 290, 1859-1867.

Graham, J.A., Menzel, D.B., Miller, F.J., Illing, J.W., Gardner, D.E., 1981. Influence of ozone on pentobarbital-induced sleeping time in mice, rats, and hamsters. Toxicol Appl Pharmacol 61, 64-73.

Hogaboam, C.M., Bone-Larson, C.L., Steinhauser, M.L., Matsukawa, A., Gosling, J., Boring, L., Charo, I.F., Simpson, K.J., Lukacs, N.W., Kunkel, S.L., 2000. Exaggerated hepatic injury due to acetaminophen challenge in mice lacking C-C chemokine receptor 2. Am J Pathol 156, 1245-1252.

Hongslo, J.K., Smith, C.V., Brunborg, G., Soderlund, E.J., Holme, J.A., 1994. Genotoxicity of paracetamol in mice and rats. Mutagenesis 9, 93-100.

Inoue, K., Takano, H., Kaewamatawong, T., Shimada, A., Suzuki, J., Yanagisawa, R., Tasaka, S., Ishizaka, A., Satoh, M., 2008. Role of metallothionein in lung inflammation induced by ozone exposure in mice. Free Radic Biol Med 45, 1714-1722.

Ito, K., Inoue, S., Hiraku, Y., Kawanishi, S., 2005. Mechanism of site-specific DNA damage induced by ozone. Mutat Res 585, 60-70.

Jaeschke, H., Knight, T.R., Bajt, M.L., 2003. The role of oxidant stress and reactive nitrogen species in acetaminophen hepatotoxicity. Toxicol Lett 144, 279-288.

James, L.P., Donahower, B., Burke, A.S., McCullough, S., Hinson, J.A., 2006. Induction of the nuclear factor HIF-1alpha in acetaminophen toxicity: evidence for oxidative stress. Biochem Biophys Res Commun 343, 171-176.

Jemnitz, K., Veres, Z., Monostory, K., Kobori, L., Vereczkey, L., 2008. Interspecies differences in acetaminophen sensitivity of human, rat, and mouse primary hepatocytes. Toxicol In Vitro 22, 961-967.

Jerrett, M., Burnett, R.T., Pope, C.A., 3rd, Ito, K., Thurston, G., Krewski, D., Shi, Y., Calle, E., Thun, M., 2009. Long-term ozone exposure and mortality. N Engl J Med 360, 1085-1095.

Johnston, C.J., Stripp, B.R., Reynolds, S.D., Avissar, N.E., Reed, C.K., Finkelstein, J.N., 1999. Inflammatory and antioxidant gene expression in C57BL/6J mice after lethal and sublethal ozone exposures. Exp Lung Res 25, 81-97.

Kang, Y.J., 2006. Metallothionein redox cycle and function. Exp Biol Med (Maywood) 231, 1459-1467.

Katsouyanni, K., Zmirou, D., Spix, C., Sunyer, J., Schouten, J.P., Ponka, A., Anderson, H.R., Le Moullec, Y., Wojtyniak, B., Vigotti, M.A., et al., 1995. Short-term effects of air pollution on health: a European approach using epidemiological time-series data. The APHEA project: background, objectives, design. Eur Respir J 8, 1030-1038.

Kim, W.J., Chereshnev, I., Gazdoiu, M., Fallon, J.T., Rollins, B.J., Taubman, M.B., 2003. MCP-1 deficiency is associated with reduced intimal hyperplasia after arterial injury. Biochem Biophys Res Commun 310, 936-942.

Kon, K., Kim, J.S., Jaeschke, H., Lemasters, J.J., 2004. Mitochondrial permeability transition in acetaminophen-induced necrosis and apoptosis of cultured mouse hepatocytes. Hepatology 40, 1170-1179.

Kovalovich, K., DeAngelis, R.A., Li, W., Furth, E.E., Ciliberto, G., Taub, R., 2000. Increased toxin-induced liver injury and fibrosis in interleukin-6-deficient mice. Hepatology 31, 149-159.

Larrieu, S., Lefranc, A., Gault, G., Chatignoux, E., Couvy, F., Jouves, B., Filleul, L., 2009. Are the short-term effects of air pollution restricted to cardiorespiratory diseases? Am J Epidemiol 169, 1201-1208.

Larson, A.M., Polson, J., Fontana, R.J., Davern, T.J., Lalani, E., Hynan, L.S., Reisch, J.S., Schiodt, F.V., Ostapowicz, G., Shakil, A.O., Lee, W.M., 2005. Acetaminophen-induced acute liver failure: results of a United States multicenter, prospective study. Hepatology 42, 1364-1372.

Last, J.A., Gohil, K., Mathrani, V.C., Kenyon, N.J., 2005. Systemic responses to inhaled ozone in mice: cachexia and down-regulation of liver xenobiotic metabolizing genes. Toxicol Appl Pharmacol 208, 117-126.

Liu, J., Liu, Y., Hartley, D., Klaassen, C.D., Shehin-Johnson, S.E., Lucas, A., Cohen, S.D., 1999. Metallothionein-I/II knockout mice are sensitive to acetaminophen-induced hepatotoxicity. J Pharmacol Exp Ther 289, 580-586.

Low, Q.E., Drugea, I.A., Duffner, L.A., Quinn, D.G., Cook, D.N., Rollins, B.J., Kovacs, E.J., DiPietro, L.A., 2001. Wound healing in MIP-1alpha(-/-) and MCP-1(-/-) mice. Am J Pathol 159, 457-463.

McClements, B.M., Hyland, M., Callender, M.E., Blair, T.L., 1990. Management of paracetamol poisoning complicated by enzyme induction due to alcohol or drugs. Lancet 335, 1526.

Miller, F.J., 1995. Uptake and fate of ozone in the respiratory tract. Toxicol Lett 82-83, 277-285.

Morris, R.D., Naumova, E.N., Munasinghe, R.L., 1995. Ambient air pollution and hospitalization for congestive heart failure among elderly people in seven large US cities. Am J Public Health 85, 1361-1365.

O'Neill, M.S., Veves, A., Zanobetti, A., Sarnat, J.A., Gold, D.R., Economides, P.A., Horton, E.S., Schwartz, J., 2005. Diabetes enhances vulnerability to particulate air pollution-associated impairment in vascular reactivity and endothelial function. Circulation 111, 2913-2920.

Pouyssegur, J., Dayan, F., Mazure, N.M., 2006. Hypoxia signalling in cancer and approaches to enforce tumour regression. Nature 441, 437-443.

Powell, S.R., 2000. The antioxidant properties of zinc. J Nutr 130, 1447S-1454S.

Pryor, W.A., 1992. How far does ozone penetrate into the pulmonary air/tissue boundary before it reacts? Free Radic Biol Med 12, 83-88.

Pryor, W.A., Squadrito, G.L., Friedman, M., 1995. The cascade mechanism to explain ozone toxicity: the role of lipid ozonation products. Free Radic Biol Med 19, 935-941.

Ray, S.D., Sorge, C.L., Raucy, J.L., Corcoran, G.B., 1990. Early loss of large genomic DNA in vivo with accumulation of Ca2+ in the nucleus during acetaminophen-induced liver injury. Toxicol Appl Pharmacol 106, 346-351.

Reilly, T.P., Bourdi, M., Brady, J.N., Pise-Masison, C.A., Radonovich, M.F., George, J.W., Pohl, L.R., 2001. Expression profiling of acetaminophen liver toxicity in mice using microarray technology. Biochem Biophys Res Commun 282, 321-328.

Savransky, V., Nanayakkara, A., Vivero, A., Li, J., Bevans, S., Smith, P.L., Torbenson, M.S., Polotsky, V.Y., 2007. Chronic intermittent hypoxia predisposes to liver injury. Hepatology 45, 1007-1013.

Schwarz, M.A., Lazo, J.S., Yalowich, J.C., Reynolds, I., Kagan, V.E., Tyurin, V., Kim, Y.M., Watkins, S.C., Pitt, B.R., 1994. Cytoplasmic metallothionein overexpression protects NIH 3T3 cells from tert-butyl hydroperoxide toxicity. J Biol Chem 269, 15238-15243.

Semenza, G.L., 2003. Targeting HIF-1 for cancer therapy. Nat Rev Cancer 3, 721-732.

Shireman, P.K., Contreras-Shannon, V., Ochoa, O., Karia, B.P., Michalek, J.E., McManus, L.M., 2007. MCP-1 deficiency causes altered inflammation with impaired skeletal muscle regeneration. J Leukoc Biol 81, 775-785.

Shriner, K., Goetz, M.B., 1992. Severe hepatotoxicity in a patient receiving both acetaminophen and zidovudine. Am J Med 93, 94-96.

Soni, M.G., Mehendale, H.M., 1998. Role of tissue repair in toxicologic interactions among hepatotoxic organics. Environ Health Perspect 106 Suppl 6, 1307-1317.

Soni, M.G., Ramaiah, S.K., Mumtaz, M.M., Clewell, H., Mehendale, H.M., 1999. Toxicant-inflicted injury and stimulated tissue repair are opposing toxicodynamic forces in predictive toxicology. Regul Toxicol Pharmacol 29, 165-174.

Taub, R., 2004. Liver regeneration: from myth to mechanism. Nat Rev Mol Cell Biol 5, 836-847.

Tee, L.B., Davies, D.S., Seddon, C.E., Boobis, A.R., 1987. Species differences in the hepatotoxicity of paracetamol are due to differences in the rate of conversion to its cytotoxic metabolite. Biochem Pharmacol 36, 1041-1052.

Weinberg, W.C., Denning, M.F., 2002. P21Waf1 control of epithelial cell cycle and cell fate. Crit Rev Oral Biol Med 13, 453-464.

Wormser, U., Calp, D., 1988. Increased levels of hepatic metallothionein in rat and mouse after injection of acetaminophen. Toxicology 53, 323-329.

Yee, S.B., Kinser, S., Hill, D.A., Barton, C.C., Hotchkiss, J.A., Harkema, J.R., Ganey, P.E., Roth, R.A., 2000. Synergistic hepatotoxicity from coexposure to bacterial endotoxin and the pyrrolizidine alkaloid monocrotaline. Toxicol Appl Pharmacol 166, 173-185.

CHAPTER 3

EFFECTS OF ACETAMINOPHEN AND ACUTE OZONE COEXPOSURE IN THE LUNG OF MICE

I. ABSTRACT

Acetaminophen (APAP) is a safe drug when used within its therapeutic limits. Overdoses of APAP cause hepatic and pulmonary toxicity in laboratory animals and people. Ozone (O3), the principal oxidant pollutant in photochemical smog is also a pulmonary toxicant. The purpose of our study was to investigate adverse effects of APAP and O3 coexposure in the murine lung. C57BL/6 male mice were treated with APAP (0 or 300 mg/kg ip). Two hours later, mice were exposed to 0, 0.25 or 0.5 ppm O3 for 6 h. They were sacrificed 9 and 32 h after APAP treatment. Bronchoalveolar lavage fluid (BALF) was collected and lungs were processed for morphometric and biochemical analyses. At 300 mg/kg, APAP alone induced a bronchiolitis with necrosis and loss of epithelial cell in both axial airways and terminal bronchioles. O3 alone did not cause epithelial or inflammatory changes in either location. APAP and O3 coexposure induced loss of epithelial cell greater than the one elicited by APAP alone in the axial airway and terminal bronchioles. Neutrophil numbers were increased in the BALF and airways after APAP treatment, but were greatest with coexposure. In addition, APAP and O3 coexposure compromised the regenerative capacity of bronchiolar epithelium. Several oxidant stress responsive genes (MT-1, GCLC) as well as the cyclin dependent kinase inhibitor P21 were elevated in the combined treatment. Coexposure of these 2 pulmonary

toxicants pose a greater risk when combined compared to either of these substances. This might constitutes a health risk in certain populations such as people with preexisting respiratory conditions or under chronic use of acetaminophen in heavily polluted urban areas.

II. INTRODUCTION

Ozone (O3) is the most pervasive oxidant air pollutant. It is generated upon the interaction of atmospheric oxygen, ultraviolet solar radiation and anthropogenic and biogenic pollutants (nitrogen oxides, volatile organic compounds, carbon monoxide, etc) (EPA, 2008). As of June 2009, more than 100 million people in the United States were located in areas that do not meet the national ambient air quality standards (NAAQS) for O3 established by the U.S. Environmental Protection Agency (U.S. EPA) (http://www.epa.gov/oar/oaqps/greenbk/gnsum.html). Experimental studies have shown that O3 inhalation cause pulmonary epithelial injury and inflammation and airway hyperresponsiveness (Bhalla and Gupta, 2000; Carey et al., 2007; Depuydt et al., 1999; Dormans et al., 1999; Dye et al., 1999; Harkema et al., 1993; Hotchkiss et al., 1997; Hotchkiss et al., 1989; Pino et al., 1992b). More recently, several studies reported potential interactions and harmful toxic synergies between O3 and other pollutants or biological substances on the respiratory tract (Cassee et al., 2002; Churg, 2003; Goldsmith et al., 2002; Han et al., 2008; Harkema and Wagner, 2005; Jakab and Hemenway, 1994; Kobzik et al., 2001; Last and Pinkerton, 1997; Osebold et al., 1988; Vincent et al., 1997; Wagner et al., 2003; Yu et al., 2002). Several of these studies

showed that the harmful potential of these pollutants is greater in people with pre-existing lung conditions (i.e., asthmatics, etc) and animal models of human lung diseases compared to healthy subjects (Balmes et al., 1997; Depuydt et al., 2002; Goldsmith et al., 2002; Last et al., 2004a; Last et al., 2004b; Miller et al., 2009; Wagner et al., 2007). Very few studies however have investigated the interaction of commonly used drugs and environmental pollutants. In a model of pulmonary fibrosis for instance, instillation of bleomycin followed by O3 exposure resulted in enhanced inflammation and fibrosis (Oyarzun et al., 2005). In addition, coexposure of rat lung fibroblasts to O3 and several antineoplastic agents showed that the combination of O3 with vitamin K3 resulted in greater injury as measured by chromium 51 radioisotope release (Wenzel and Morgan, 1983).

APAP is one of the most commonly used over-the-counter analgesic and antipyretic and is a remarkably safe drug when used within prescribed therapeutic limits, although this therapeutic window is narrow (Larson et al., 2005). In cases of overdosage, APAP targets several organs including the respiratory system (Baudouin et al., 1995; Placke et al., 1987b). In addition, frequent therapeutic use of APAP has recently been associated with asthma and allergic rhinitis in adults and children (Newson et al., 2000; Shaheen et al., 2000). Several studies showed that frequent use of APAP by women in mid-to-late pregnancy resulted for the offspring in greater risk of having higher levels of immunoglobulin E, asthma and wheezing later in life (Persky et al., 2008; Shaheen et al., 2005).

Interestingly one of the most prevalent hypothesis through which APAP might contribute to asthma is oxidative stress and depletion of glutathione (GSH) (Eneli et al.,

2005; Fogarty and Davey, 2005; Shaheen et al., 2000). Moreover, both APAP and O3 have been shown to affect airway glutathione concentrations in vivo and in vitro (Dimova et al., 2005; Micheli et al., 1994; Plopper et al., 1998). APAP or O3 also targets Clara cells known to produce Clara cell secretory protein (CCSP). CCSP has been shown to be protective against oxidative lung injury such as hyperoxia or O3 inhalation (Amatya et al., 2002; Stripp et al., 2000). These effects of APAP or O3 on the airway antioxidant levels (e.g. GSH, CCSP) or Clara cells themselves might potentially constitute the basis for a toxic synergy between these substances.

In the present study we investigated the acute effects of near ambient concentrations of O3 on APAP-induced airway epithelial injury and inflammation in male mice. Our hypothesis was that O3 inhalation would potentiate APAP induced pulmonary toxic changes. The findings of this study demonstrate for the first time that O3 inhalation exacerbates APAP-induced airway epithelial injury and acute inflammation and impairs epithelial regeneration. We found that APAP and O3 sequential exposure resulted in more Clara cell damage than either one of these substances alone and results in greater induction of oxidative stress responsive genes.

III. MATERIAL AND METHODS

III – 1. Laboratory Animals

Pathogen-free male, C57Bl/6 mice (8-10 weeks of age, the Jackson Laboratory Bar Harbor, ME) were used in this study. Mice were housed in polycarbonate cages on heat-treated aspen hardwood bedding (Nepco-Northeastern Product Corp, Warrensburg, NY). Boxes were covered with filter bonnets, and animals were provided free access to food (Harlan Tekad laboratory rodents 22/5 diet, Madison, WI) and water. Mice were maintained in Michigan State University (MSU) animal housing facilities accredited by the Association for Assessment and Acreditation of Laboratory Animal Care and according to National Institutes of Health guidelines as overseen by the MSU Institutional Animal Care and Use Committee. Rooms were maintained at temperatures of 21-24°C and relative humidities of 45-70%, with a 12-hour light/dark cycle starting at 7:30 AM.

III – 2. Experimental Protocol

Mice were randomly divided into ten groups, each consisting of six animals. They were given intraperitoneally 0 (saline-vehicle) or 300 mg/kg APAP (Sigma Chemical Co., St. Louis, MO) in 20 ml/kg saline. Animals were fasted overnight before the administration of APAP. Two hours after APAP administration, mice were exposed to 0 (air), 0.25 or 0.5 ppm O3 for 6 h (Figure 1). Mice were killed 9 or 32 h after APAP (1 or

24 h after O3 exposure, respectively). As no significant differences were detected in preliminary studies, no morphological evaluation was conducted at 0.25 ppm for the 9 h time point and at 32 h, data analysis in animals given 0.25 ppm was limited to morphological evaluations (airway epithelial damage and 5-bromo-2-deoxyuridine (BrdU) immunostaining) at the later time (32 h) (Figure 15).

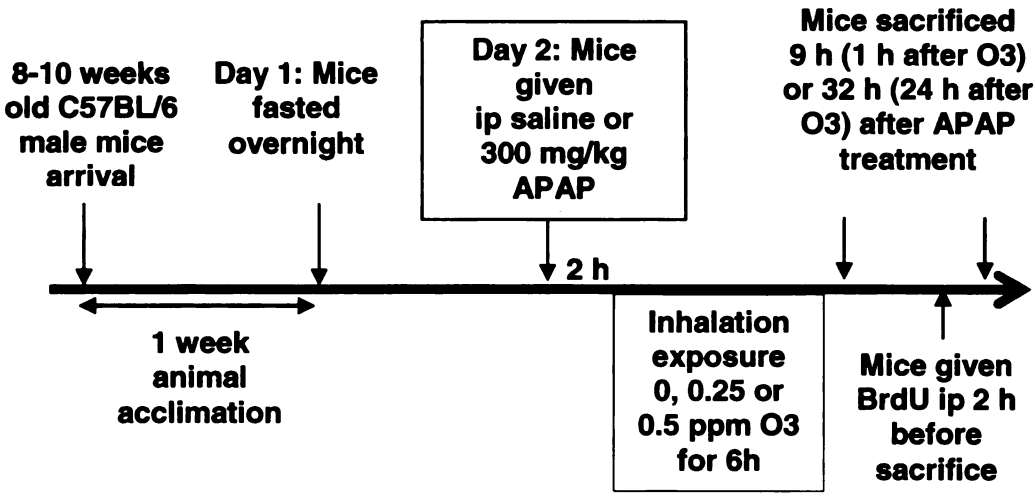

Figure 15. Experimental design of APAP and O3 studies in the lung. (A) Eight to ten weeks old C57BL/6 male mice were given 0 (saline) or 300 mg/kg APAP and then exposed to ozone (0 or air, 0.25 or 0.5 ppm) for 6 h. Mice were euthanized 9 (1 h after O3 exposure) or 32 h (24 h after O3 exposure) after APAP injection.

Mice were housed individually and exposed to O3 in stainless steel wire cage, whole-body inhalation exposure chambers (HC-100, Lab Products, Maywood, NJ). O3 was generated with an OREC 03V1-O ozonizer (O3 Research and Equipment Corp., AZ)

using compressed air as a source of oxygen. Total airflow through the exposure chambers was 250 l/min (15 chamber air changes/hour). The concentration of O3 within chambers was monitored during the exposure using Dasibi 1003 AH ambient air O3 monitors (Dasibi Environmental Corp., Glendale, CA). Two O3 sampling probes were placed in the middle of the O3 chambers, 10-15 cm above cage racks. O3 airborne concentrations during the inhalation exposures were 0.26 +/- 0.02 ppm or 0.53 +/- 0.01 ppm (mean +/- standard error of the mean) for O3 chambers and 0.01 +/- 0.008 or 0.02 +/- 0.009 ppm for air chambers.

III – 3. Animal Necropsy, Bronchoalveolar Lavage, and Tissue Selection for Microscopic and Biochemical Analyses

Two hours prior to scheduled sacrifice, mice were given BrdU intraperitoneally (50 mg/kg, Fisher Scientific, Fair Lawn, NJ) for nuclear incorporation and immunohistochemical detection of airway epithelial cells undergoing DNA synthesis (cycling cells in S phase). At the time of necropsy, mice were anesthetized with an intraperitoneal injection of sodium pentobarbital (50 mg/kg; Fatal Plus, Vortech Pharmaceuticals, Dearborn, MI), the abdominal cavity was opened and blood was collected from the abdominal vena cava in BD Microtainer tubes (Franklin Lakes, NJ). Animals were then killed by exsanguination.

The thoracic cavity was opened by puncturing the hemidiaphragms to allow collapse of lung lobes. After the trachea was cannulated, the heart-lung block was excised and the lung was gently lavaged twice with 0.9 ml of sterile saline. Approximately 75-90% of the intratracheally instilled saline was recovered as BALF from the lavaged lung

lobes and immediately placed on ice until further analysis. The right lung lobes were tied off at the bronchus level and severed from the left lobe. The left lobe attached to the heart bloc was gravity-perfusion inflated at a constant pressure of 25 cm of water for at least 1.5 hour using 10% neutral buffered formalin (NBF) (Fisher Scientific, Fair Lawn, NJ) and then immersed in NBF for light microscopic, morphometric and immunohistochemical analyses. The right cranial lobe was immersed in RNAlater (Qiagen, Valencia, CA), kept at 4°C for 24 h and then transferred to a -20°C freezer for gene expression analyses using real time PCR. The right middle, caudal and accessory lobes were frozen and stored at -80°C for biochemical analysis of glutathione and thiobarbituric acid reactive substances.

III – 4. Cellular Analysis of Bronchoalveolar Lavage Fluid

Total cell counts in the collected BALF from each mouse were determined using a hemocytometer. Cytological slides were prepared using a Shandon cytospin 3 (Shandon Scientific, Sewickley, PA), centrifuged at 600 rpm for 10 minutes and stained with Diff-Quick (Dade Behring, Newark, DE). Differential counts of neutrophils, eosinophils, macrophages and lymphocytes were assessed on a total of 200 cells. Remaining BALF were centrifuged at 1500 rpm for 15 minutes to collect the supernatant fraction that was stored at -80°C for later biochemical analyses.

III – 5. Flow Cytometric Analyses for Inflammatory Cytokines

BALF supernatants were assayed for selected inflammatory cytokines that included interleukin-1beta (IL-1β), tumor necrosis factor-alpha (TNF-α), interferon-gamma (IFN-γ), interleukin-6 (IL-6), monocyte chemoattractant protein-1 (MCP-1), interleukin-12 (IL-12), keratinocyte-derived chemokine (KC) and interleukin-10 (IL-10). Plasma cytokines concentrations for KC, TNF-α, MCP-1 and IL-6 were also determined. All cytokines were purchased as Flex Set reagents or as a preconfigured cytometric bead array kit (BD Biosciences, San Diego, CA). Cytokines analysis was performed using a FACSCalibur flow cytometer (BD Franklin Lakes, NJ). Briefly, 50 µl of BALF or plasma was added to the antibody-coated bead complexes and incubation buffer. Samples were incubated with the beads. Phycoerythrin (PE)-conjugated secondary antibodies were then added to form sandwich complexes. Following acquisition of sample data using the flow cytometer, cytokine concentrations were calculated based on standard curves using FCAP Array software (BD, Franklin Lakes, NJ).

III – 6. Lung Tissue Processing for Light Microscopy and Immunohistochemistry

The left lung lobe was collected as described previously and 2 sections transverse to the axial airway were cut at the level of the fifth (G5) or eleventh generation (G11) from the axial airway (Figure 16). These sections were embedded in paraffin, cut at a thickness of 5 µm and stained with hematoxylin and eosin (H&E) for routine histopathological evaluation.

Routine immunohistochemical techniques were used for detection of airway epithelial cell nuclear BrdU and cytoplasmic CCSP. Neutrophils accumulation in the airway and parenchyma was also detected and quantified using immunohistochemistry. Briefly, lung sections were deparafinized in xylene and rehydrated through descending grades of ethanol and immersed in 3% hydrogen peroxide to block endogenous peroxides. Sections were incubated with normal sera to inhibit nonspecific proteins (normal horse, rabbit or goat sera for BrdU, neutrophils or CCSP immunostaining, respectively, Vector Laboratories Inc., Burlingame, CA) followed by specific dilutions of primary antibodies (1:40, monoclonal mouse anti-BrdU antibody, BD, Franklin Lakes, NJ; 1:2500, monoclonal rat anti-neutrophil antibody, AbD Serotec, Raleigh, NC; 1/1600, polyclonal rabbit anti-CCSP antibody, Seven Hills Bioreagents, Cincinnati, OH). Tissue sections were subsequently covered with secondary biotinylated antibodies and immunostaining was developed with the Vector RTU Elite ABC kit (BrdU and CCSP Vector Laboratories Inc) or the RTU Phosphatase-labeled Streptavidin kit (neutrophils, Kirkegaard Perry Labs, Gaithersburg, MD) and visualized with Vector Red (Vector Laboratories Inc). Slides were counstertained with Gill 2 hematoxylin (Thermo Fisher, Pittsburgh, PA).

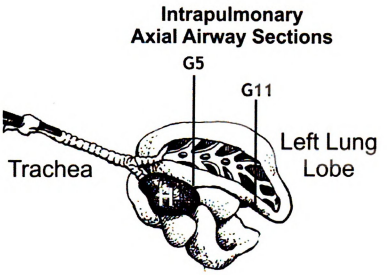

Figure 16. Schematic representation of lung sectioning levels for histology and morphometry. Two transverse sections were taken. One at the level of the fifth generation (G5) from the central airway for analysis of axial airway morphology and morphometry and the other one at the eleventh level (G11) for terminal bronchioles evaluation.

III – 7. Lung Morphometric Analyses

Evaluation of epithelial, inflammatory or proliferation changes in the axial airway or terminal bronchioles in the section taken at at the level of the fifth (G5) and the one taken eleventh (G11) bifurcation showed no differences. Therefore, morphometric evaluation of axial airway changes were conducted at G5 while terminal bronchioles evaluation was done at the level of G11. Evaluation of alveolar septa neutrophils was

conducted at the level of G5 as no differences were detected between sections at G5 and G11.

Bromodeoxyuridine stained and unstained airway epithelial cell nuclei were counted in the axial airway in sections taken at the level of G5 and in all terminal bronchioles in sections taken at the level of G11. The BrdU labeling index for the axial airway (AA) or terminal bronchioles (TBs) was determined by dividing the number of BrdU positive cells by the number of total (stained and unstained) epithelial cells and multiplying by 100 (Cho et al., 1999). Similarly, the CCSP labeling index was determined by dividing the CCSP stained cells (cytoplasmic staining) by the total stained and unstained cells and multiplying by 100. To estimate the amount of the intraepithelial CCSP in the airway epithelium, the volume density (Vs) of CCSP staining was quantified using computerized image analysis and standard morphometric techniques. The area of CCSP staining was calculated from the automatically circumscribed perimeter of stained intraepithelial material using the public domain NIH Image program (written by Wayne Rasband, U.S. National Institutes of Health). The length of the basal lamina underlying the surface epithelium was calculated from the contour length of the digitized image of the basal lamina. The volume of stored CCSP per unit of surface area of epithelial basal lamina was estimated using the method described in detail by Harkema and collaborators (Harkema et al., 1987). The Vs of CCSP is expressed as nanoliters of CCSP per mm^2 of basal lamina.

Proximal or distal airway acute inflammatory cell accumulation was assessed by counting the numbers of immunohistochemically labeled neutrophils (cell membrane labeling) in the axial airway (G5) or terminal bronchioles (G11) surface epithelium,

respectively, divided by the length of the underlying basal lamina (Cho et al., 1999). The length of the basal lamina underlying the surface epithelium was calculated from the contour length of the basal lamina, by using a National Institutes of Health (NIH) image analysis software (NIH Image; written by Wayne Rasband at the U.S. NIH). It is reported as the number of neutrophils per mm of basal lamina. Alveolar septa neutrophil accumulation was assessed by averaging the numbers of neutrophils enumerated in 5 medium power fields (X200) in each slide. Analyzed fields were selected in an unbiased manner with a random start and count of every other field. Fields comprising the axial airway and major pulmonary vessels were excluded from evaluation.

To quantify APAP and/or O3-induced epithelial injury, morphometric analyses were conducted on H&E sections. The numeric epithelial cell density (i.e., number of epithelial cell per mm of basal lamina) was determined by counting the total number of surface epithelial cell nuclear profiles in transverse airway sections normalized to the length of the underlying basal lamina (Cho et al., 1999). Numeric cell densities were evaluated in the axial airway at the level of the fifth generation (Figure 2, G5) and in all terminal bronchioles in the section taken at the level of the eleventh bifurcation from the axial airway (Figure 2, G11). A terminal bronchiole was identified as any airway portion blending into an alveolar bed on one side and connecting to another airway (first junction) on the other side. For the terminal bronchioles, the numeric cell density presented is the mean of numeric densities for each section. The length of the basal lamina was measured using the NIH Image program (Wayne Rasband, U.S. National Institutes of Health).

III – 8. Quantitative Real Time PCR

Total RNA was extracted using RNeasy Mini Kit according to the manufacturer's instructions (Qiagen, Valencia, CA). Briefly, lung tissues were homogenized in RLT buffer containing β-Mercaptoethanol with a 5 mm Rotor-Sator Homogenizer (PRO Scientific, Oxford, CT) and centrifuged at 10,700 rpm for 3 minutes. Samples were then treated with Rnase-Free Dnase set on the column for 30 minutes. Eluted RNA was diluted 1:5 with Rnase free water and quantified using a GeneQuant Pro spectrophotometer (BioCrom, Cambridge, England).

Reverse transcription (RT) reaction was performed using reverse transcription high capacity cDNA reagents (Applied Biosystems, Foster City, CA) and a GeneAmp PCR System 9700 Thermocycler PE (Applied Biosystems). Each RT reaction was run in 5 µl of sample with 20 µl of cDNA Master Mix prepared according to the manufacturer's protocol (Applied Biosystems).

Expression analyses of isolated mRNA were performed by quantitative real-time PCR using individual animals' cDNA with the ABI PRISM 7900 HT Sequence Detection System using Taqman® Gene Expression Assay reagents (Applied Biosystems). The cycling parameters were 48°C for 2 minutes, 95°C for10 minutes, and 40 cycles of 95°C for 15 seconds followed by 60°C for 1 minute. Individual data are reported as fold change of mRNA in experimental samples compared to the saline/air control group. Real-time PCR amplifications were quantified using the comparative Ct method normalized to the mean of 2 endogenous controls (18S and GAPDH). The cycle number at which each amplified product crosses the set threshold represents the Ct value. The amount of target

genes normalized to the mean of the endogenous reference genes was calculated by subtracting the endogenous reference Ct from the target gene Ct (ΔCt). Relative mRNA expression was calculated by subtracting the mean ΔCt of the treated samples from the ΔCt of the control samples (saline-treated, air-exposed) (ΔΔCt). The absolute values of the comparative expression level (fold change) was then calculated by using the formula: Fold change = $2^{-\Delta\Delta CT}$.

III – 9. Glutathione Assay

Lung total (reduced or GSH and oxidized or GSSG) and oxidized glutathione were homogenized in cold MES buffer (0.4 M 2-(N-morpholino)ethanesulfonic acid, 0.1 M phosphate, and 2 mM EDTA, pH = 6). The homogenates were then centrifuged at 9,700 rpm for 15 minutes at 4°C and the supernanant collected and deproteinated. The total glutathione concentration was assayed on the deproteinated samples as recommended by the manufacturer (Cayman Chemical Co., Ann Arbor, MI). GSSG concentration was determined after derivatization of reduced glutathione with vinylpyridine. Sample absorbance was determined at 405 nm, and the total or oxidized glutathione concentration in lung homogenates was assessed by comparison of absorption to standard curves.

III – 10. Thiobarbituric Acid-Reactive Substances Assay (TBARS Assay)

Lipid peroxidation in the lung was estimated using a commercially available kit according to the manufacturer's recommendations and malonaldehyde as a standard (TBARS kit, Cayman Chemical Co., Ann Arbor, MI). Lung tissue was homogenized on ice in RIPA Buffer and Proteases Inhibitor (Thermo Scientific, Rockford, IL). The homogenates were centrifuged at 3,900 rpm, and the supernatant was collected and used to detect malonaldehyde and thiobarbituric acid adducts in acidic conditions and under high temperature (100°C). Absorbance was measured at 530 nm.

III – 11. Statistical Analysis

Data are reported as mean +/- SE. Differences among groups were analysed by a one or two-way ANOVA followed by Student-Newman-keuls post hoc test. When normality or variance equality failed, a Kruskal-Wallis ranked test was conducted. All analyses were performed using a SigmaStat software (SigmaStat; Jandel Scientific, San Rafael, CA). Significance was assigned to p values smaller than or equal to 0.05.

IV. RESULTS

IV – 1. Lung Histopathology and Morphometric Assessment of Epithelial Injury and Inflammation

APAP treatment (APAP alone or APAP/air) or O3 exposure (O3 alone or SAL/O3) were compared to effects of the combined treatment (APAP/O3 or APAP and O3-coexposed groups) or controls (SAL/air). O3 exposure did not induce histopathological changes in the lung airway 9 or 32 h after saline administration (Figure 17A, B). At 9 h, APAP administration caused limited airway epithelial degeneration with very few epithelial necrosis (data not shown). Epithelial degeneration was characterized by cell swelling with cytoplasmic clarification and vacuolation. At 32 h, APAP treatment resulted in epithelial degeneration, necrosis and exfoliation along the entire length of airway epithelia (Figure 17C). Histopathological evaluation also revealed that both Clara and ciliated cells were affected by APAP administration although Clara cells seemed to be predominantly targeted (data not shown). Along the airway tree, APAP-treated animals apparently had more epithelial damage in the axial airway compared to the terminal bronchioles (see below, airway epithelium morphometry results). APAP and O3-coexposed mice had changes similar to the APAP/air group with extension in severity of both degeneration and necrosis of airway epithelial cells (Figure 17D). Very few inflammatory cell were detected in H&E slides in the axial airway or terminal bronchioles epithelium in the combined treatment but not with APAP or O3 alone (data not shown).

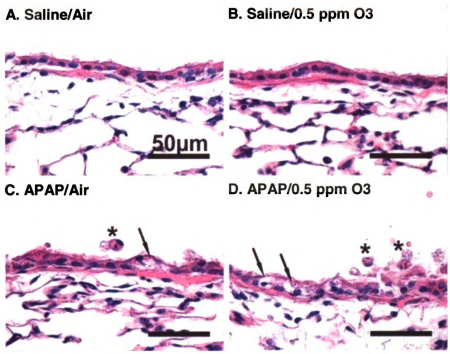

Figure 17. Axial airway epithelial damage induced by APAP and O3 treatment 32 h after APAP. Thirty-two hours after APAP administration, animals were euthanized, left lung lobe was collected and evaluated morphologically. Solid arrow, airway epithelial degeneration; asterisk, airway epithelial necrosis and exfoliation.

Morphometric evaluations showed that O3 alone had no effects on epithelial cell densities at any time (Figure 18A-D). At 9 h, APAP alone caused a slight nonsignificant decrease of epithelial cells in the axial airway but not in terminal bronchioles (Figure 18A, C). At the same time, 0.5 ppm O3 exposure enhanced APAP-induced airway epithelial damage as the APAP/0.5 ppm O3 co-treatment was the only group with significant loss of epithelial cell in the axial airway (Figure 18A, C). At 32 h, the cell loss due to APAP alone treatment in the axial airway reached statistical significance, while in the terminal bronchioles a nonsignificant reduction of the number of epithelial cell was observed (Figure 18B, D). At 32 h, epithelial loss further increased in the axial airway of the APAP/O3 co-treated group in an O3 dose-dependent way, while in the terminal bronchioles APAP and O3 coexposure-induced airway epithelial loss reached statistical significance (Figure 18B, D).

Figure 18. Epithelial numeric cell density in APAP and O3 treated mice 9 and 32 h after APAP in the axial airway (A and C) and terminal bronchioles (B and D). Animals were injected ip with 0 (saline) or 300 mg/kg APAP and 2 h later exposed to 0 (air), 0.25 or 0.5 ppm O3 for 6 h. 9 or 32 h after APAP administration, animals were euthanized and left lung lobe collected, routinely stained and evaluated as described in Material and Methods. Data are expressed as mean ± SE, (n = 6). a, significantly different from saline/0.5 ppm O3 group; b, significantly different from saline/air; c, significantly different from APAP/air group; d, significantly different from saline/0.25 ppm O3 group; ($p \leq 0.05$). BL, Basal lamina.

Figure 18

A. Axial airway epithelial density at 9 h

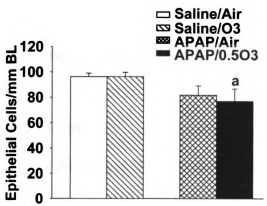

B. Axial airway epithelial density at 32 h

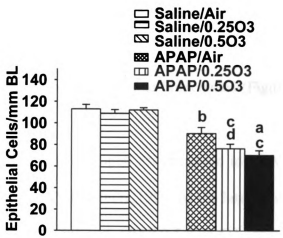

C. Terminal bronchioles epithelial density at 9 h

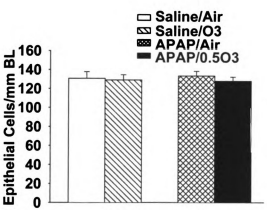

D. Terminal bronchioles epithelial density at 32 h

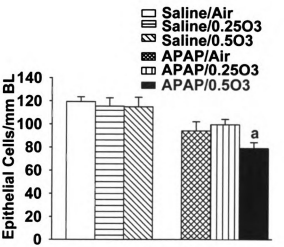

No neutrophil infiltration was seen in the axial airway or terminal bronchioles epithelium with any treatment regimen at 9 h (Figure 19A, C). Later, at 32 h, O3-exposure had no effect on neutrophil numbers in the airways while APAP alone caused neutrophils accumulation that reached statistical significance in the axial airway (Figure 19B, D). O3 at a dose of 0.5 ppm significantly increased APAP-induced neutrophil accumulation in the epithelium of the axial airway but not terminal bronchioles (Figure 19B, D).

Unlike airways, alveolar septa had significant neutrophil accumulation in APAP alone or APAP and O3-coexposed mice 9 h after APAP (Figure 19E). At the later time, neutrophil accumulation progressed in both APAP alone and APAP/0.5 ppm O3 groups but no significant differences were detected between these groups (Figure 19F).

Figure 19. Lung neutrophil infiltration in APAP and O3 treated mice 9 and 32 h after APAP in the axial airway (A and B), terminal bronchioles (C and D) and alveolar septa (E and F). Animals were injected ip with 0 (saline) or 300 mg/kg APAP and 2 h later exposed to 0 (air), 0.25 or 0.5 ppm O3 for 6 h. Lung sections were immunohistochemically stained and neutrophils evaluated in the airways or alveolar septa as described in Material and Methods. Data are expressed as mean ± SE, (n = 6). a, significantly different from saline/air group; b, significantly different from saline/0.25 ppm O3 group; c, significantly different from saline/0.5 ppm O3 group; d, significantly different from APAP/air group; ($p \leq 0.05$). ND, not detected; BL, basal lamina.

Figure 19

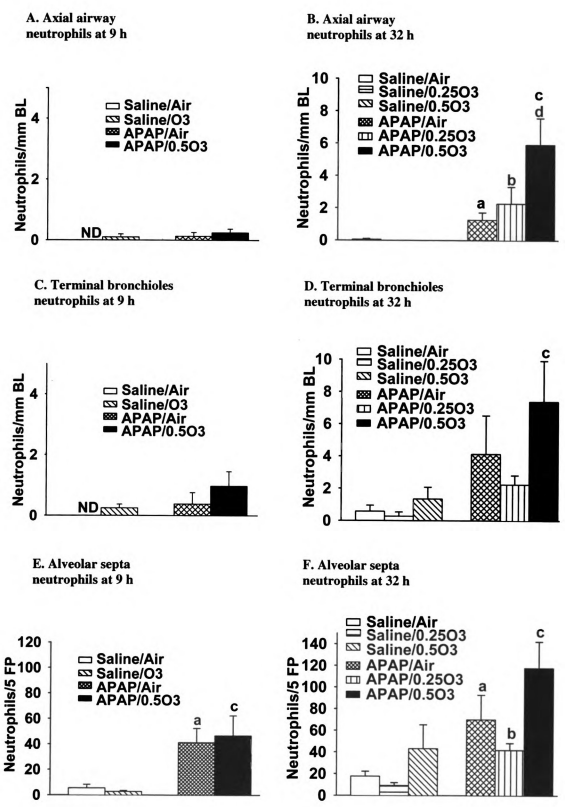
A. Axial airway neutrophils at 9 h
Neutrophils/mm BL
Saline/Air
Saline/O3
APAP/Air
APAP/0.5O3
ND
B. Axial airway neutrophils at 32 h
Neutrophils/mm BL
Saline/Air
Saline/0.25O3
Saline/0.5O3
APAP/Air
APAP/0.25O3
APAP/0.5O3
a
b
c
d
C. Terminal bronchioles neutrophils at 9 h
Neutrophils/mm BL
Saline/Air
Saline/O3
APAP/Air
APAP/0.5O3
ND
D. Terminal bronchioles neutrophils at 32 h
Neutrophils/mm BL
Saline/Air
Saline/0.25O3
Saline/0.5O3
APAP/Air
APAP/0.25O3
APAP/0.5O3
c
E. Alveolar septa neutrophils at 9 h
Neutrophils/5 FP
Saline/Air
Saline/O3
APAP/Air
APAP/0.5O3
a
c
F. Alveolar septa neutrophils at 32 h
Neutrophils/5 FP
Saline/Air
Saline/0.25O3
Saline/0.5O3
APAP/Air
APAP/0.25O3
APAP/0.5O3
a
b
c

IV – 2. Bronchoalveolar Lavage Fluid Inflammatory Accumulation

O3 exposure did not cause changes in BALF total inflammatory cells at any time when compared to control mice (Figure 20A-F). Compared to controls, APAP alone or APAP and O3 coexposure caused a time-dependent, statistical increase in the number of total inflammatory cells in the BALF at 9 and 32 h after APAP administration (Figure 20A, B). Although not significant, there was a trend for greater total inflammatory cells in the lungs of the APAP and O3-coexposed mice compared to APAP alone (Figure 20A, B).

Pulmonary inflammatory cell responses as reflected in the BALF were due to increases in macrophages and/or neutrophils (Figure 20C, D, E, F). O3 alone did not cause changes in neutrophil or macrophages in BALF at any time (Figure 20C, D, E, F). At 9 and 32 h, mice exposed to APAP alone or APAP and O3-coexposed mice had a time-dependent increase of macrophages and neutrophils (Figure 20C, D, E, F). APAP alone and APAP/O3 groups were the only ones with detectable levels of neutrophil infiltrates in the BALF at 9 h (Figure 20E). At the later time, APAP and O3-coexposed mice had marked, O3 dose-dependent increase in neutrophil numbers in BALF (Figure 20F), indicating a synergistic neutrophil effect of APAP and O3 coexposure.

Figure 20. Inflammatory cell accumulation in bronchoalveolar lavage (BALF) in APAP and O3 treated mice. Total inflammatory cells (A and B), macrophages (C and D) and neutrophils (E and F) per ml of BALF 9 and 32 h after APAP administration. Animals were injected ip with 0 (saline) or 300 mg/kg APAP and 2 hours later exposed to 0 (air), 0.25 or 0.5 ppm O3 for 6 h. 9 or 32 h after APAP administration, animals were euthanized and BALF harvested and analyzed as described in Material and Methods. Data are expressed as mean ± SE, (n = 6). a, significantly different from saline/air group; b, significantly different from saline/ 0.5 ppm O3; c, significantly different from saline/0.25 ppm O3; ($p \leq 0.05$). ND, not detected.

Figure 20

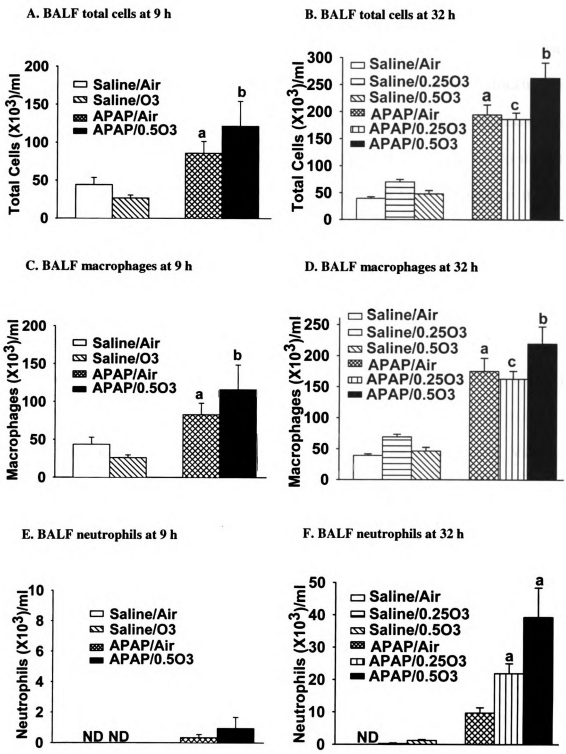
A. BALF total cells at 9 h
Total Cells (X10^3)/ml
Saline/Air
Saline/O3
APAP/Air
APAP/0.5O3
a
b
B. BALF total cells at 32 h
Total Cells (X10^3)/ml
Saline/Air
Saline/0.25O3
Saline/0.5O3
APAP/Air
APAP/0.25O3
APAP/0.5O3
a
c
b
C. BALF macrophages at 9 h
Macrophages (X10^3)/ml
Saline/Air
Saline/O3
APAP/Air
APAP/0.5O3
a
b
D. BALF macrophages at 32 h
Macrophages (X10^3)/ml
Saline/Air
Saline/0.25O3
Saline/0.5O3
APAP/Air
APAP/0.25O3
APAP/0.5O3
a
c
b
E. BALF neutrophils at 9 h
Neutrophils (X10^3)/ml
Saline/Air
Saline/O3
APAP/Air
APAP/0.5O3
ND ND
F. BALF neutrophils at 32 h
Neutrophils (X10^3)/ml
Saline/Air
Saline/0.25O3
Saline/0.5O3
APAP/Air
APAP/0.25O3
APAP/0.5O3
ND
a
a

IV – 3. Relative Genes Expression and Protein Concentrations of Inflammatory Cytokines in the Lung and BALF

In order to investigate factors responsible for the acute pulmonary inflammation in the coexposure group, several chemokines involved in neutrophil trafficking were evaluated in lung tissues. Neutrophils chemoattractants KC and MIP-2 expression were significantly elevated with O3 but not with APAP at 9 h (Figure 21A, C). At this early time, APAP and O3-coexposed animals had 3 times more MIP-2 expression than O3-exposed mice, although significance was not observed (Figure 21A, C). At 32 h post-APAP, KC and MIP-2 expressions declined in O3 or APAP/O3 groups from expression levels seen at 9 h and no differences were present between SAL/O3, APAP/air or APAP/O3 groups (Figure 21B, D).

Macrophages infiltration was not evaluated at the tissue level. However, in the BALF of APAP alone or APAP and O3-coexposed mice, there was an increase of macrophages accumulation compared to controls (Figure 20C, D). At 9 h, MCP-1, a monocyte chemokine, had increased relative expression in APAP or O3 alone groups but was greatest in the coexposed group compared to either substance alone (Figure 21E). At 32 h, mRNA expression of MCP-1 in the APAP and O3-coexposed group slightly declined but was still above APAP or O3 alone group expression level (Figure 21F).

Figure 21. KC (A and B), MIP-2 (C and D) and MCP-1 (E and F) genes expression in the lung of APAP and O3 treated mice. Animals were injected ip with 0 (saline) or 300 mg/kg APAP and 2 h later exposed to 0 (air) or 0.5 ppm O3 for 6 h. 9 or 32 h after APAP administration, animals were euthanized and lung samples collected in RNAlater. Data are expressed as mean ± SE, (n = 6). a, significantly different from saline/air group; b, significantly different from APAP/air group; c, significantly different from saline/O3 group; ($p \leq 0.05$). FC, fold change.

Fig

Figure 21

A. Lung KC expression at 9 h

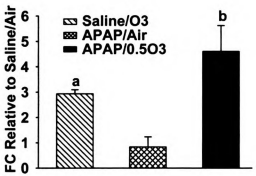

B. Lung KC expression at 32 h

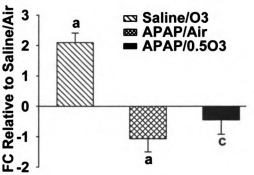

C. Lung MIP-2 expression at 9 h

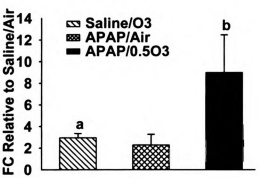

D. Lung MIP-2 expression at 32 h

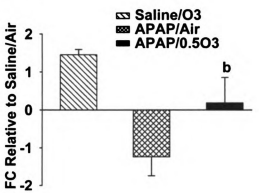

E. Lung MCP-1 expression at 9 h

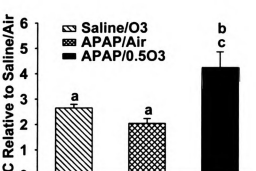

F. Lung MCP-1 expression at 32 h

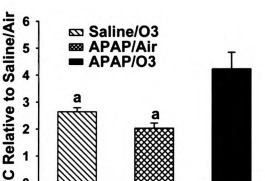

Two other markers of inflammation were evaluated in the lung tissue. These include a pro-inflammatory cytokine, IL-6, and an enzyme involved in the generation of inflammatory mediators, cyclooxygenase 2 (COX-2). At 9 h, IL-6 but not COX-2 expression was elevated in APAP or O3 alone over controls (Figure 22A, C). At the same time, APAP and O3-coexposed mice had significant elevation of IL-6 and COX-2 expression compared to either APAP or O3 alone (Figure 22A, C). At 32 h, APAP alone, O3 alone or APAP/O3 had similar mRNA expressions of IL-6 or COX-2 (Figure 22B, D).

Figure 22. IL-6 (A and B), and COX-2 (C and D) genes expression in the lung of APAP and O3 treated mice. Animals were injected ip with 0 (saline) or 300 mg/kg APAP and 2 h later exposed to 0 (air) or 0.5 ppm O3 for 6 h. 9 or 32 h after APAP administration, animals were euthanized and lung samples collected in RNAlater. Samples were evaluated as described in Materials and Methods. Data are expressed as mean ± SE, (n = 6). a, significantly different from saline/air group; b, significantly different from saline/O3 group; c, significantly different from APAP/air group; ($p \leq 0.05$). FC, fold change.

Figu

FC Relative to Saline/Air

Figure 22

A. Lung IL-6 expression at 9 h

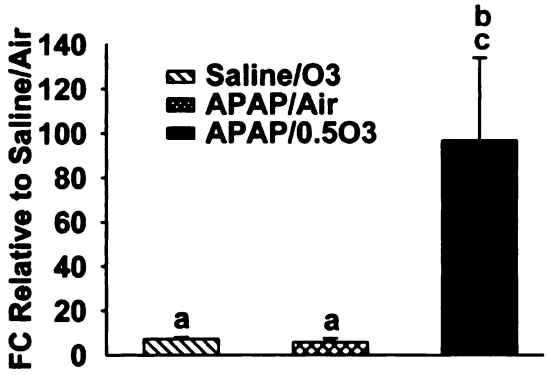

B. Lung IL-6 expression at 32 h

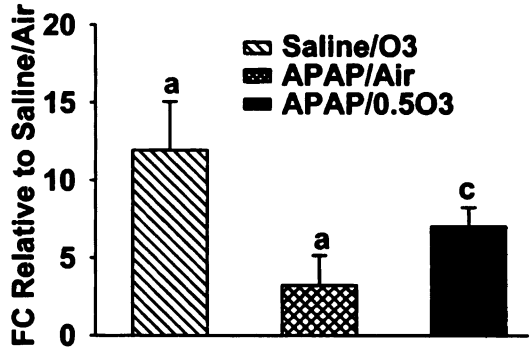

C. Lung COX-2 expression at 9 h

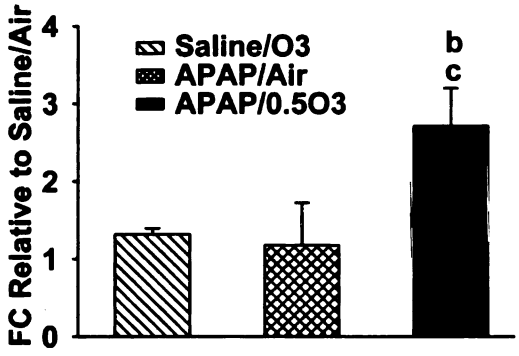

D. Lung COX-2 expression at 32 h

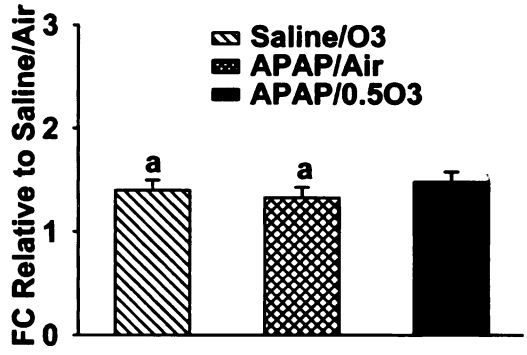

IL-6 protein concentration was significantly elevated in the BALF of APAP/O3-coexposed mice 9 h post-APAP when compared to APAP or O3 alone (Figure 23A). At 32 h, IL-6 protein concentration was slightly above control concentration in APAP alone-treated mice and no change was detected in other groups compared to SAL/air control animals (Figure 23B). MCP-1 was not detected at the protein level in the BALF of any group including control mice at 9 h (Figure 23C). At 32 h, APAP or O3 alone and APAP and O3-coexposed groups had significantly increased concentrations of MCP-1 compared to controls (Figure 23D). Although not significant, APAP alone and APAP/O3 groups had approximately 3 times the concentration of MCP-1 measured in the BALF of O3-exposed mice (Figure 23D).

Figure 23. IL-6 (A and B) and MCP-1 (C and D) protein concentrations in the BALF of APAP and O3 treated mice. Animals were injected ip with 0 (saline) or 300 mg/kg APAP and 2 h later exposed to 0 (air) or 0.5 ppm O3 for 6 h. 9 or 32 h after APAP administration, animals were euthanized, BALF harvested and cytokines evaluated by flow cytometry as described in Material and Methods. Data are expressed as mean ± SE, (n = 6). a, significantly different from saline/O3 group; b, significantly different from APAP/air group; c, significantly different from saline/air group; ($p \leq 0.05$). ND, not detected.

Figure 23

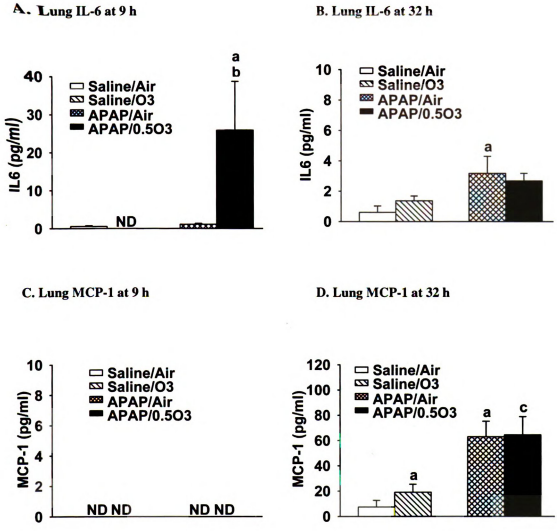
A. Lung IL-6 at 9 h
IL6 (pg/ml)
Saline/Air
Saline/O3
APAP/Air
APAP/0.5O3
ND
a
b
B. Lung IL-6 at 32 h
IL6 (pg/ml)
Saline/Air
Saline/O3
APAP/Air
APAP/0.5O3
a
C. Lung MCP-1 at 9 h
MCP-1 (pg/ml)
Saline/Air
Saline/O3
APAP/Air
APAP/0.5O3
ND ND
ND ND
D. Lung MCP-1 at 32 h
MCP-1 (pg/ml)
Saline/Air
Saline/O3
APAP/Air
APAP/0.5O3
a
a
c

IV - 4. Airway Epithelial Regeneration and Related Genes Expression

Administration of APAP in mice caused an elevation in the number of cycling airway epithelial cells in the axial airway and terminal bronchioles 32 h after treatment (Figure 24C, E, F). Compared to control mice, O3 alone resulted in an increase of BrdU positive cells in the terminal bronchioles but did not change the number of cycling epithelial cell in the axial airway (Figure 24A, B, E, F). In either location, O3 exposure caused a dose-dependent reduction of APAP-induced epithelial cell proliferation (Figure 24D, E, F). This effect seemed to be more pronounced in the axial airway compared to the terminal bronchioles and coexposure of APAP and 0.5 ppm O3 almost completely suppressed the number of cycling epithelial cells (Figure 24E, F).

Regeneration of pulmonary airway epithelia is a very slow process compared to rapidly cycling other epithelia (Rawlins and Hogan, 2006) and proceeds in mice airways from Clara cells among other cells (Giangreco et al., 2002; Hong et al., 2001). We therefore decided to evaluate Clara cells damage within the axial airway and terminal bronchioles at the time where statistical differences were present (32 h). At this time, APAP or O3 alone caused reduction of CCSP immunostaining in the axial airway compared to control animals (Figure 25A, B, C). At the same location, APAP/O3-coexposed mice had further reduction of CCSP immunostaining compared to animals given either substance alone (Figure 25B, C, D).

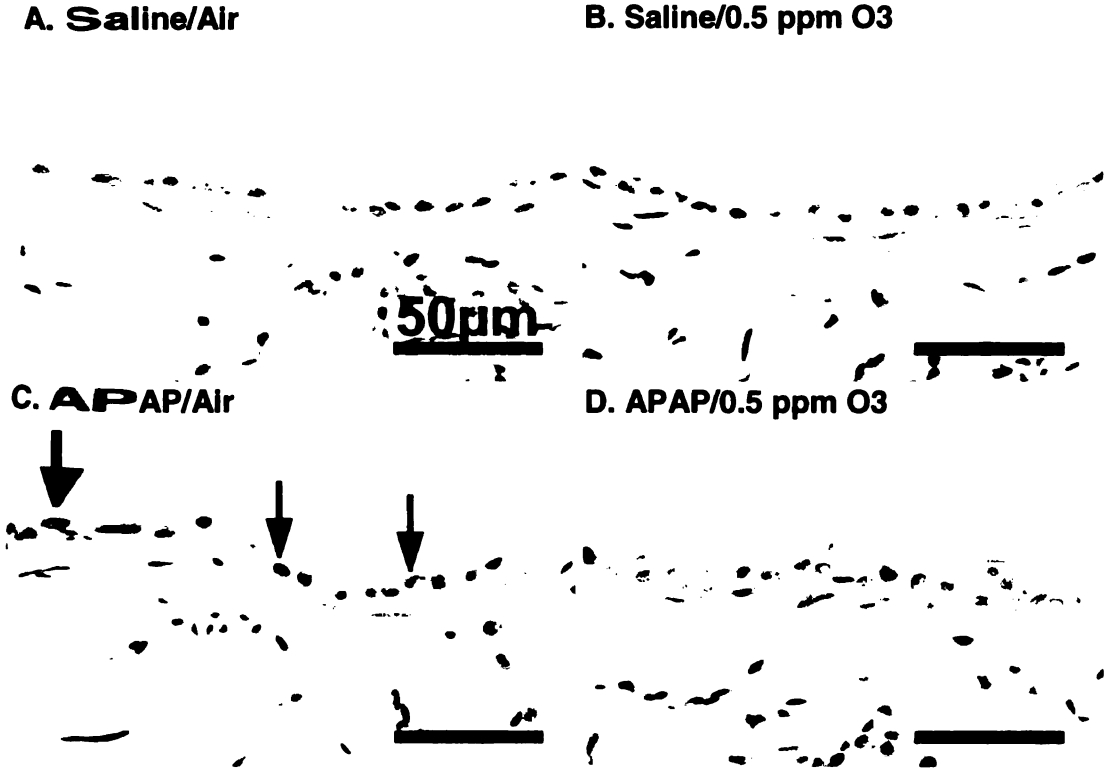

Figure 24. Airway epithelium cell proliferation in APAP and O3 treated mice 32 h after APAP. BrdU-labeled epithelial cells were evaluated in the axial airway (A-D and E) and in terminal bronchioles (F). Animals were injected ip with 0 (saline) or 300 mg/kg APAP and 2 h later exposed to 0 (air), 0.25 or 0.5 ppm O3 for 6 h. Thirty two hours after APAP administration, animals were euthanized and left lung lobes collected. Lung sections were immunohistochemically stained and evaluated as described in Materials and Methods. Data are expressed as mean ± SE, (n = 6). a, significantly different from saline/air group; b, significantly different from APAP/air group; c, significantly different from saline/O3 groups; ($p \leq 0.05$). Black arrowS indicate cells in S phase.

Figure 24 (cont'd)

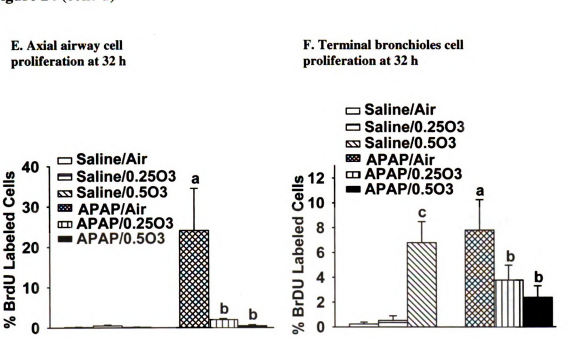

These morphologic changes were confirmed when Clara cell density (number of Clara cell per mm of basal lamina) and CCSP volume density (amount in nanoliters of intracytoplasmic CCSP in epithelial cells per mm^2 of basal lamina) were evaluated in the airway surface epithelium. O3 exposure resulted in a slight but significant reduction of Clara cell number in the terminal bronchioles but not axial airway (Figure 26A, B). In either location, O3 alone caused a significant reduction of CCSP content in Clara cell (Figure 26C, D). On the other hand, APAP alone caused significant loss of Clara cell as well as loss of CCSP content in the axial airway and terminal bronchioles (Figure 26A-D). In either location, O3 exposure dose-dependently enhanced APAP-induced loss of Clara cell, reaching significance at the high dose of O3 (Figure 26A, B). Coexposure of

these substances resulted in a slight nonsignificant trend toward a smaller content of CCSP in Clara cells as compared to APAP or O3 alone (Figure 26C, D).

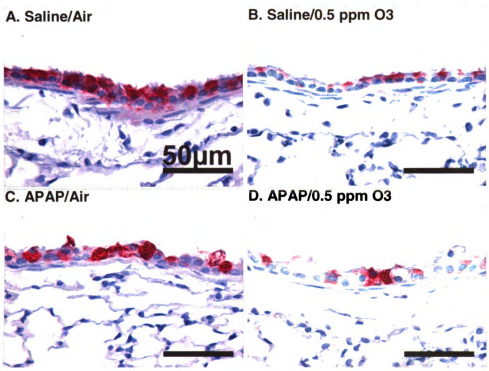

Figure 25. CCSP immunolabeling in the axial airway of APAP and O3 treated mice. Thirty-two hours after APAP administration, animals were euthanized, left lung lobe was collected and immunohistochemically stained and evaluated. Red staining represents CCSP protein immunolocalization in the cytoplasm of airway epithelial cells.

CCSP gene expression in the lung tissue was decreased in all treatment groups and reached statistical significance in the APAP alone or the APAP/O3 group at the 9 h time point (Figure 27A). At 32 h, mRNA expression of CCSP was still lower than baseline in APAP and APAP/O3-coexposed groups (Figure 27B). In relation with the regeneration and repair of airway epithelia, the cell cycle-dependent kinase inhibitor P21 expression was significantly upregulated in APAP or O3 alone 9 h post-APAP (Figure 27C). At the same time, APAP/O3 mice, the group with deficient epithelial proliferation had greater P21 mRNA expression compared to APAP or O3 alone (Figure 27C). At 32 h, relative P21 expression was still elevated in APAP/air, SAL/O3 and APAP/O3 but no differences were detected between these groups (Figure 27D).

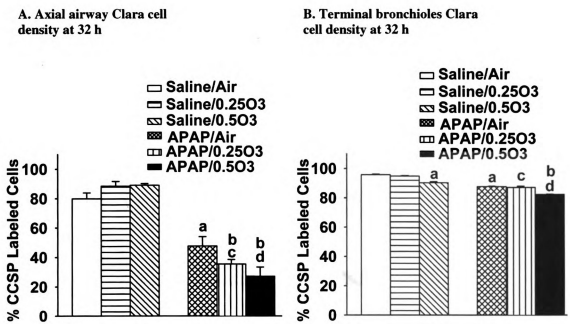

Figure 26. Clara cell density (A and B) and CCSP volume density (C and D) in the axial airway (A and C) and terminal bronchioles (B and D) 32 h after APAP. Animals were injected ip with 0 (saline) or 300 mg/kg APAP and 2 h later exposed to 0 (air), 0.25 or 0.5 ppm O3 for 6 h. Thirty-two hours after APAP administration, animals were euthanized, left lung lobe was collected and immunohistochemically stained. Data are expressed as mean ± SE, (n = 6). a, significantly different from saline/air group; b, significantly different from APAP/air group(s); c, significantly different from saline/0.25 ppm O3 group; d, significantly different from saline/0.5 ppm O3; ($p \leq 0.05$).

Figure 26 (cont'd)

C. Axial airway CCSP volume density at 32 h

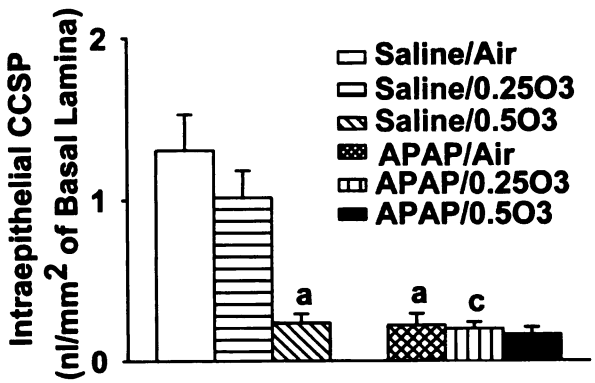

D. Terminal bronchioles CCSP volume density at 32 h

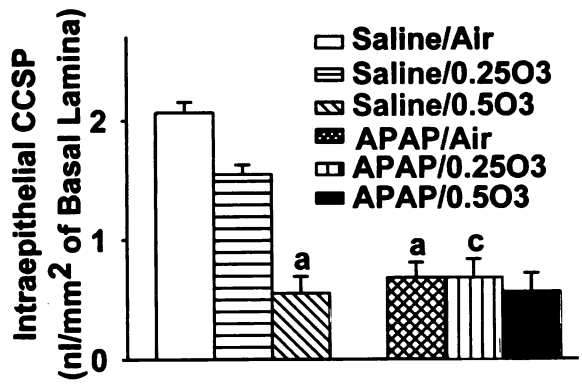

Figure 27. CCSP (A and B) and cyclin-dependent kinase inhibitor P21 (C and D) genes expression in the lung of APAP and O3 treated mice. Animals were injected ip with 0 (saline) or 300 mg/kg APAP and 2 h later exposed to 0 (air) or 0.5 ppm O3 for 6 h. 9 or 32 h after APAP administration, animals were euthanized and lung samples collected in RNAlater. Samples were evaluated as described in Materials and Methods. Data are expressed as mean ± SE, (n = 6). a, significantly different from saline/air group; b, significantly different from saline/O3 groups; c, significantly different from APAP/air group; ($p \leq 0.05$). FC, fold change.

Figure 27

A. Lung CCSP expression at 9 h

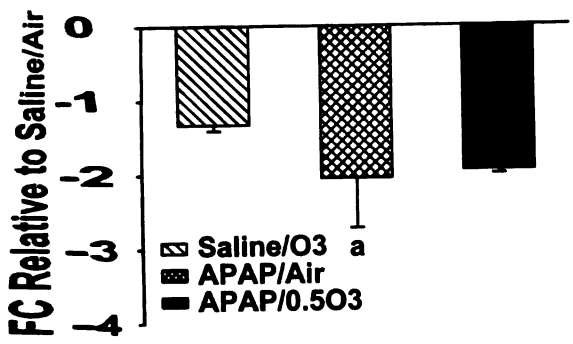

B. Lung CCSP expression at 32 h

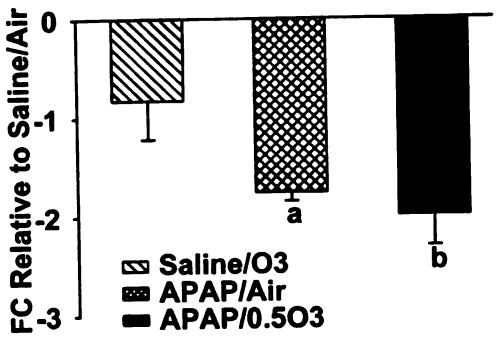

C. Lung P21 expression at 9 h

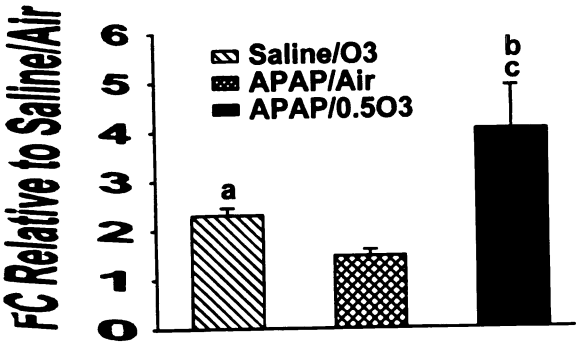

D. Lung P21 expression at 32 h

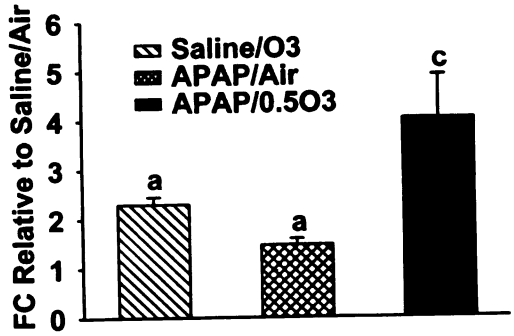

IV - 5. Pulmonary Oxidative Stress

Several oxidative stress responsive genes as well as glutathione concentrations were evaluated in control and treated mice to assess a potential contributory role of oxidative stress in the O3 enhancement of APAP-induced lung airway injury. At 9 h post-APAP, O3 but not APAP caused greater expression of metallothionein 1 (MT-1) compared to controls (Figure 28A). At the same time, APAP/O3 coexposure resulted in significantly greater MT-1 expression compared to O3 alone (Figure 28A). At 9 h, heme oxygenase 1 (HO-1), another oxidative stress responsive gene had significantly elevated expression in APAP alone or APAP/O3-coexposed mice compared to control mice (Figure 28C). At 32 h, MT-1 and HO-1 had slightly above or comparable expression in APAP and /or O3-treated groups compared to controls (Figure 28B, D).

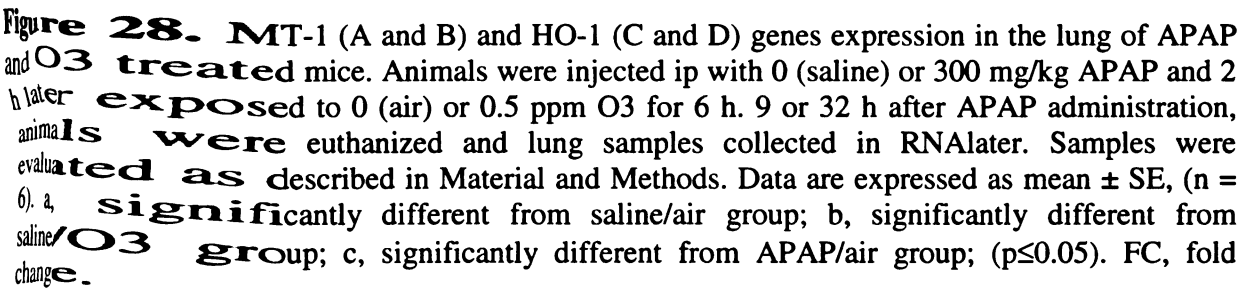

Figure 28. MT-1 (A and B) and HO-1 (C and D) genes expression in the lung of APAP and O3 treated mice. Animals were injected ip with 0 (saline) or 300 mg/kg APAP and 2 h later exposed to 0 (air) or 0.5 ppm O3 for 6 h. 9 or 32 h after APAP administration, animals were euthanized and lung samples collected in RNAlater. Samples were evaluated as described in Material and Methods. Data are expressed as mean ± SE, (n = 6). a, significantly different from saline/air group; b, significantly different from saline/O3 group; c, significantly different from APAP/air group; ($p \leq 0.05$). FC, fold change.

Figure 28

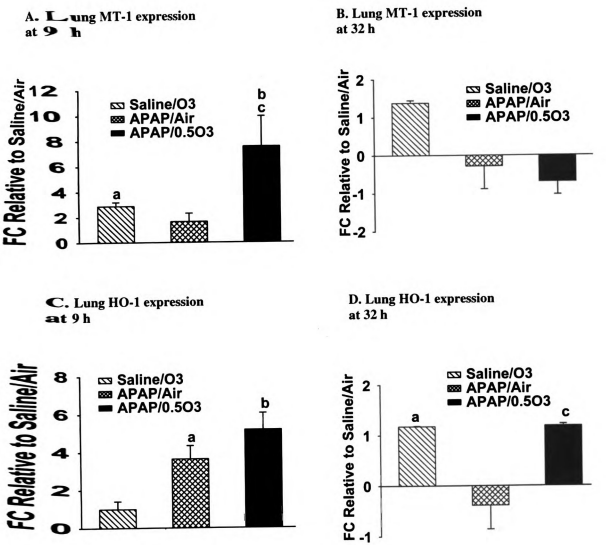
A. Lung MT-1 expression at 9 h
FC Relative to Saline/Air
Saline/O3
APAP/Air
APAP/0.5O3
a
b
c
B. Lung MT-1 expression at 32 h
FC Relative to Saline/Air
Saline/O3
APAP/Air
APAP/0.5O3
C. Lung HO-1 expression at 9 h
FC Relative to Saline/Air
Saline/O3
APAP/Air
APAP/0.5O3
a
b
D. Lung HO-1 expression at 32 h
FC Relative to Saline/Air
Saline/O3
APAP/Air
APAP/0.5O3
a
c

An additional evidence for a role of oxidative stress in APAP/O3 enhanced toxicity came from the gene expression analysis of the catalytic subunit of glutamate-cysteine ligase (GCLC) involved in the synthesis of glutathione. At 9 h, GCLC was significantly greater in the APAP/O3-coexposed group compared to APAP treatment or O3 exposure (Figure 29A). No differences in GCLC expression were detected between APAP alone, O3 alone or APAP/O3 groups 32 h after APAP administration (Figure 29B). Evaluation of glutathione in lung tissue 9 h after APAP administration showed that the ratio of oxidized glutathione (GSSG) to total oxidized and reduced (GSH) glutathione was significantly elevated in animals exposed to O3 associated or not to APAP treatment (SAL/O3 and APAP/O3 groups) (Figure 29C).

The thiobarbituric acid-reactive substance assay did not show differences between the treatment and control groups at any time post-APAP (data not shown).

Figure 29. GCLC (A and B) gene expression and oxidized/total glutathione ratio (C) in the lung of APAP and O3 treated mice. Animals were injected ip with 0 (saline) or 300 mg/kg APAP and 2 h later exposed to 0 (air) or 0.5 ppm O3 for 6 h. 9 and 32 h (B) after APAP administration, animals were euthanized and lung samples collected in RNAlater. Data are expressed as mean ± SE, (n = 6). a, significantly different from saline/air group; b, significantly different from saline/O3 group; c, significantly different from APAP/air group; ($p \leq 0.05$). FC, fold change.

Figure 29

A. Lung GCLC expression at 9 h

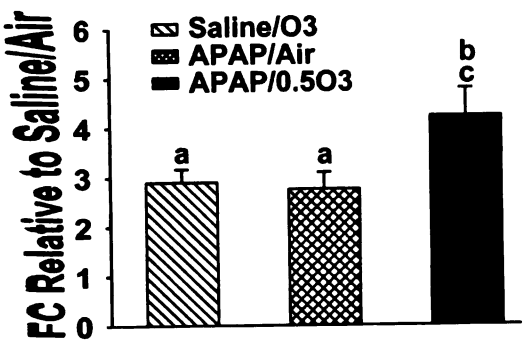

B. Lung GCLC expression at 32 h

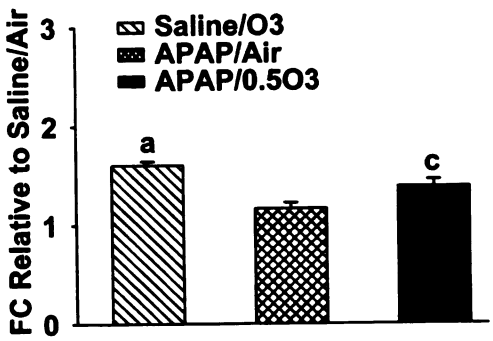

C. Lung oxidized to total GSH ratio at 9 h

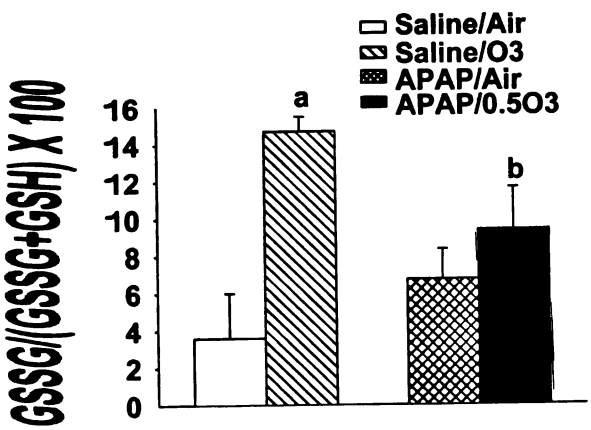

V. DISCUSSION

We report in this study that 0.5 ppm O3 did not cause epithelial damage or inflammatory cell accumulation in the axial airway, terminal bronchioles or BALF at 1 or 24 h after exposure (9 or 32 h after saline administration, respectively). APAP at a dose of 300 mg/kg caused epithelial damage in the axial airway and terminal bronchioles. At this dose, APAP caused a time-dependent airway epithelial cell loss and inflammatory cell accumulation composed of macrophages and neutrophils at 9 and 32 h. APAP and O3 coexposure caused greater airway epithelial damage and neutrophil accumulation as well as greater neutrophil exudation in the BALF compared to APAP alone.

In the axial airway and terminal bronchioles, APAP alone increased the number of proliferating epithelial cells 32 h after its administration. O3 exposure resulted in inhibition of APAP-induced epithelial cell proliferation in the axial airway and terminal bronchioles. Early in the course of toxicity, several oxidative stress responsive genes (MT-1, GCLC) and a cyclin-dependent kinase inhibitor (P21) expressions were elevated in the APAP/O3 group compared to APAP or O3 alone. O3 an hour after the end of the 6 h exposure period (9 h after saline or APAP administration) resulted in increased oxidized to total glutathione ratio.

APAP at high doses causes airway epithelial damage as shown by several studies (Baudouin et al., 1995; Genter et al., 1998; Jeffery and Haschek, 1988; Placke et al., 1987a; Placke et al., 1987b). In mice, APAP administration resulted in bronchiolar epithelial degeneration 4 h after injection while necrosis was evident 8 h after administration (Placke et al., 1987b). In our study, we observed degeneration of airway epithelial cells 9 h after APAP with very few necrotic cells. Frank necrosis was evident at

32 h after APAP injection. Clara cells are present within the entire length of the pulmonary airway epithelium and are sensitive to the toxic effects of APAP (Amatya et al., 2002; Jeffery and Haschek, 1988; Pack et al., 1980). We observed APAP-induced damage in both Clara and ciliated cells in airway epithelia. APAP induced greater total epithelial cell or Clara cell damage in the axial airway compared to the terminal bronchioles. The reasons for this gradient of toxicity are not clear but could be related to Clara cell number or content.

APAP is metabolized in the liver through the cytochrome P450 monooxygenases (Dahlin et al., 1984; Jollow et al., 1973; Mitchell et al., 1973a; Mitchell et al., 1973b). In the lung, Clara cells have the highest level of cytochrome P450s among all resident lung cells (Devereux et al., 1989; Massaro et al., 1994) and are therefore potential sites for APAP bioactivation. In mice deficient in liver specific NADPH-cytochrome P450 reductase (cpr), the electron donor of microsomal P450s, the severity of lung lesions was decreased while liver toxicity was abrogated suggesting that liver metabolism was only partially involved in APAP-induced airway epithelial damage (Gu et al., 2005). This result also suggests that APAP bioactivation also occurred in the lung as lung toxicity was not completely eliminated in those cpr null mice. In the lung, at least two isoforms responsible for hepatic APAP bioactivation, namely CYP2E1 and CYP1A2, or their activity are involved in xenobiotics metabolism (Dey et al., 1999; Forkert et al., 2001; Stoilov et al., 2006). The greater APAP lung toxicity in the axial airway compared to the terminal bronchioles could be related to site-specific differences in Clara cell functional properties including bioactivation (pool of cytochrome P450s expressed and activity, etc) in the different airway subcompartments. One of the few studies comparing axial airway

and terminal bronchioles xenobiotics toxication capabilities showed that mice treated ip with naphthalene, a Clara cell toxicant, dependent upon specific cytochrome P450 isoforms bioactivation, resulted in more distal damage compared to the proximal airway epithelium (Plopper et al., 1992a; Plopper et al., 1992b). For APAP itself, isoforms responsible of its bioactivation in the different lung subcompartments are not known and could be an important factor in the differential toxicity between the proximal and distal airway regions.

Clara cell antioxidants (e.g., GSH, CCSP, etc) content is also another important factor to consider in APAP-induced airway proximal and distal toxicity. Clara cells in the axial airway epithelium had higher content of GSH and fewer cells with low GSH content compared to terminal bronchioles (West et al., 2000). The relative abundance of Clara cells (containing the antioxidant CCSP) in distal areas compared to proximal locations may have been an important contributor to the lesser toxicity seen in the former areas (Plopper and Hyde, 2008; Plopper et al., 2006). Our results are showing that the distal region in the control mice had a slightly greater proportion of Clara cells and CCSP volume density than the proximal airway. It is possible that this greater content in CCSP in the distal bronchioles had a protective effect on the smaller number of associated ciliated cells. From these studies we can conclude that APAP bioactivation and the abundance of Clara cells as well as their content in antioxidants could be potential factors responsible for differences in APAP toxicity in the axial airway compared to the terminal bronchioles.

Acute exposures to 1 ppm O3 caused centriacinar epithelial cell damage and inflammation as early as 4 h after the initiation of exposure in rodents (Boorman et al.,

1980; Dungworth et al., 1975; Mellick et al., 1975; Pino et al., 1992a; Stephens et al., 1974; Sterner-Kock et al., 2000). In those regions, ciliated cells and type I pneumocytes are the most susceptible cells although Clara cells are also affected by O3 exposure (Dormans et al., 1999; Schwartz et al., 1976). In our study, O3 exposure at the dose of 0.5 ppm for 6 h did not cause airways epithelial damage or inflammation. O3, however, enhanced APAP-induced epithelial cell loss and inflammation in both the axial airway and terminal bronchioles. Mechanisms behind O3 potentiation of APAP injury are not clear, however O3 modulation of APAP bioactivation, enhanced neutrophil accumulation or greater oxidative stress in the coexposure group as well as O3 suppression of APAP-induced epithelial regeneration might have had a role in this process.

In early reports of O3 systemic effects, O3 inhalation prolonged pentobarbital sleeping time in mice, rats and hamsters (Graham et al., 1981). These results led to the hypothesis that O3 could modulate enzymes involved in the metabolism of pentobarbital (Graham et al., 1981). Recent studies in mice showed that O3 inhalation downregulated expression of several cytochrome P450s in the lung (CYP2E1) and in the liver (several isoforms including CYP2E1 and 3A11) (Gohil et al., 2003; Last et al., 2005) while others reported an increase or decrease of CYP2E1 in rats exposed to O3 (Watt et al., 1997). In our study, no change in CYP2E1 gene expression was detected in the lung of 0.5 ppm O3-exposed mice 1 or 24 h after exposure (data not shown). Moreover, APAP was given 2 h before O3 and APAP metabolism is a fast process almost complete in an hour or so as suggested by GSH depletion 2 h after administration (Dai et al., 2006; Jollow et al., 1973). Therefore, it is unlikely that O3 modulation of cytochromes P450 isoforms played a major role in the APAP/O3 toxic synergy.

Neutrophil infiltration of higher magnitude was detected in mice exposed to APAP and O3 compared to APAP or O3 alone-treated mice 32 h after APAP. It is not clear whether neutrophil infiltration in animals given both APAP and O3 had a role in the greater epithelial damage or was rather a consequence associated with the scavenging of damaged epithelial cells. Neutrophils usually contribute to epithelial injury through generation and release of reactive oxygen species and specific proteases (Ho et al., 1996; Jaeschke, 2000). Neutrophil infiltration due to bacterial or viral stimuli shifted to the left the dose-response curve of low non-toxic doses of several drugs including APAP (Maddox et al., ; Roth et al., 1997; Shaw et al., 2009). Therefore, enhanced neutrophil accumulation in APAP and O3-coexposed mice might have had a contributory role in the greater airway epithelial toxicity. Neutrophil accumulation in the alveolar septa in APAP or APAP/O3 groups 9 h post-APAP are most likely located in the alveolar capillaries that are sites of neutrophils extravasation into the alveolar spaces (Wagner and Roth, 2000). This was interpreted as an APAP-related increase in neutrophil trafficking as no injury was detected in these sites by light microscopy.

APAP and O3 coexposed animals had greater induction of oxidative stress responsive genes (MT-1 and GCLC) compared to either substance alone. Oxidative stress plays a role in APAP-induced liver toxicity, particularly through mitochondrial proteins covalent binding (Jaeschke et al., 2003; James et al., 2003). Furthermore, APAP depletes antioxidant small molecules in both liver and lung, particularly GSH. APAP-treated mice (375 mg/kg ip) for instance had their lowest level of GSH 2-4 h after injection in both liver and lung, liver depletion being of higher magnitude compared to lung depletion (Chen et al., 1990). O3 on the other hand reacts with epithelial lining fluid and cell

membranes to yield secondary reactive hydroxyl and lipid radicals (Pryor, 1994; Pryor et al., 1995a, b). Subsequently, these secondary products lead to consumption of antioxidant molecules including GSH and unbalance the pro/antioxidant equilibrium toward an oxidative state (Kirichenko et al., 1996; Li et al., 1996; Menzel, 1994). We report here that O3 alone at the high dose caused increased oxidized (GSSG) to total glutathione ratio (GSH + GSSG). APAP or O3 individually induces oxidative stress in the lung and the increased toxicity observed in the combination of these substances may have been the results of elevated consumption of anti-oxidants and greater oxidative damage.

Metallothionein is a cysteine-rich small molecular weight protein which has radicals scavenging and antioxidant properties (Coyle et al., 2002; Kang, 2006; Kumari et al., 1998; Sato and Kondoh, 2002). In our study, MT-1 had the greatest level of mRNA expression in the coexposure group compared to either APAP or O3 alone. Others reported that APAP treatment upregulated hepatic expression of MT-1 in mice (Last et al., 2005; Liu et al., 1999). O3 exposure (at doses of 0.5, 1 or 2.5 ppm for 4 h) was also responsible for increased expression of MT expression in the lung of exposed mice (Johnston et al., 1999; Mango et al., 1998). In this last study, mice deficient in CCSP had greater MT mRNA expression by 2 h of exposure. Mice deficient in MT-1 and MT-2 exposed to O3 had greater epithelial damage and inflammatory changes than wild type mice. Metallothioneins deficient mice exposed to O3 also exhibited greater inflammation and oxidative stress as shown by higher levels of IL-6, HO-1, 8-hydroxy-deoxyguanosine and nitrotyrosine (Inoue et al., 2008). Overall, these studies demonstrated that metallothioneins are protective from APAP or O3 oxidative stress, particularly in the absence of other anti-oxidant molecules (e.g., CCSP). Therefore, APAP/O3-induced

greater MT-1 expression in our study could be interpreted as a response to an ongoing greater oxidative damage.

Clara cell secretory protein (CCSP) represents a protein secreted by Clara cells in airways of mammalian species including mice (Hermans and Bernard, 1999). Various roles have been ascribed to CCSP including anti-inflammatory and antioxidant activities and binding of lipophilic xenobiotics and other chemicals (Hermans and Bernard, 1999; Plopper et al., 2006). In our study, APAP or O3 alone caused a significant reduction of CCSP in the axial airway and terminal bronchioles. APAP/O3 animals had a slight but not significant trend toward a reduction of CCSP in either location suggesting that APAP or O3 alone induced substantial reduction of cytoplasmic CCSP and that further reduction in coexposed animals probably extended beyond the sensitivity of the detection method. This loss of CCSP detected in treated animals is probably due to increased secretion of CCSP into the epithelial lining fluid but also to decreased synthesis as shown by the CCSP gene expresssion analysis. Exposure to high concentration of oxygen in mice resulted in decreased Clara cell number and CCSP content of these cells (Johnston et al., 1998). Exposure of CCSP deficient or sufficient mice to 1 ppm O3 for 8 h resulted in epithelial injury in both the proximal airway and terminal bronchioles in either genotype (Plopper et al., 2006). In this study, CCSP deficient mice had increased susceptibility of ciliated cells and Clara cells to O3 effects and in deficient mice, O3 damage extended to more proximal airway sites not affected in the wild type CCSP sufficient animals. As described previously, mice deficient in CCSP had greater expression of MT-1 when exposed to O3, suggesting that these 2 proteins might act as a back up for each other (Mango et al., 1998). Taken together, these studies suggest that O3 exacerbation of

APAP toxicity could be partially explained by greater oxidative injury due to O3 depletion of CCSP from APAP sensitized Clara cell. In this scenario, a potentiation by O3-induced inflammatory cell oxidative activity is also plausible.

Exposure of O3 in mice treated with APAP resulted in significant decrease of airway epithelial cell proliferation induced by APAP. Various populations of adult stem cell responsible for epithelial regeneration have been identified within different compartments of the lung. In the axial airway area of rodents, Clara cells and basal cells are considered having stem cell potential (Boers et al., 1998; Breuer et al., 1990; Liu et al., 2006; Plopper and Dungworth, 1987). Clara cells have been shown to dedifferentiate into immature cells upon O3 exposure in rat and then able to generate mature Clara or ciliated cells (Evans et al., 1976). Those immature cells were also able to produce undifferentiated Clara cells known as facultative progenitor cells (to distinguish them from 'professional' progenitor) (Evans et al., 1978; Stripp, 2008). A variant of Clara cells, immunohistochemically positive for CCSP with a resistant phenotype to naphthalene injury have been shown to be true ('professional') stem cell and to localize in neuroepithelial niches or bronchioloalveolar junction (Giangreco et al., 2002; Hong et al., 2001). In case of severe airway epithelial damage, both progenitor and true stem cells participated in epithelial reconstruction while only the progenitor cell population maintained homeostatic epithelial regeneration or epithelial renewal following less severe injury (Giangreco et al., 2009). It is therefore possible that the absence of regeneration in APAP/O3 animals is related to a greater depletion of progenitor-based repair.

APAP and O3 coexposure resulted in greater expression of P21 compared to either substance alone. The cyclin-dependent kinase inhibitor P21 blocks cells in G1

phase to allow repair (Weinberg and Denning, 2002). DNA damage from oxidative stress or other causes induces P21 which then arrest the cell cycle in G1 (Clement et al., 2001). Indeed, under hyperoxic conditions, lung epithelial cells exhibited upregulation of P21 mRNA and protein concentration, DNA fragmentation and inhibition of epithelial cell proliferation (Clement et al., 2001; Corroyer et al., 1996; O'Reilly et al., 1998; O'Reilly et al., 2001). Interestingly, APAP or O3 have both been reported to cause DNA damage. APAP genotoxic activity at high doses has been related to 3 main mechanisms, namely inhibition of ribonucleotide reductase, direct DNA damage by the reactive metabolite of APAP and APAP-induced increase of intracellular calcium (Bergman et al., 1996). Inhalation of O3 caused oxidative DNA damage in BALF cells, double strand break through generation of hydroxyl radical or direct base modification (Haney et al., 1999; Ito et al., 2005). Assessment of DNA damage for strand breaks (Comet assay, 8-oxo-dG evaluation, etc) or DNA base modifications could therefore shed some light on the impaired regeneration observed in APAP/O3 animals as compared to APAP alone-treated or O3 alone-exposed animals.

In neutrophil depleted rats (using a rabbit antirat neutrophil antibody), O3 inhalation resulted in the presence of less BrdU-labeled cells in the terminal bronchioles. This led to the conclusion that neutrophils had an important role in cleaning up the distal bronchioles and by doing so contribute to the epithelial repair process (Vesely et al., 1999). In our study, APAP and 0.5 ppm O3 coexposure resulted in more neutrophils associated to almost completely nonexistant BrdU-labeled cells which is in contradiction with the results of Vesely and collaborators (1999). Furthermore, in the nasal cavity of

rats exposed to O3, the presence of neutrophils was reported to be important for mucus cell metaplasia but not for nasal epithelial repair after O3 injury (Cho et al., 2000).

In conclusion, APAP and O3 coexposure in mice resulted in greater airway epithelial damage in the axial airway and terminal bronchioles as well as greater BALF and airways neutrophil accumulation. APAP administration alone resulted in greater number of cycling airway epithelial cells. O3 exposure following APAP treatment resulted in inhibition of APAP-induced epithelial proliferation. APAP/O3 mice also had greater loss of Clara cell in the airways and greater expression of the cyclin dependent kinase inhibitor P21. O3 alone or APAP/O3-coexposed mice had greater lung GSSG to total glutathione ratio compared to controls or APAP alone. Finally, APAP and O3-coexposed mice had greater induction of several oxidant responsive genes (MT-1, GCLC) compared to either substance.

VI. REFERENCES

Amatya, B.M., Kimula, Y., Koike, M., 2002. The Clara cells activated by acetaminophen. J Med Dent Sci 49, 103-108.

Balmes, J.R., Aris, R.M., Chen, L.L., Scannell, C., Tager, I.B., Finkbeiner, W., Christian, D., Kelly, T., Hearne, P.Q., Ferrando, R., Welch, B., 1997. Effects of ozone on normal and potentially sensitive human subjects. Part I: Airway inflammation and responsiveness to ozone in normal and asthmatic subjects. Res Rep Health Eff Inst, 1-37; discussion 81-99.

Baudouin, S.V., Howdle, P., O'Grady, J.G., Webster, N.R., 1995. Acute lung injury in fulminant hepatic failure following paracetamol poisoning. Thorax 50, 399-402.

Bergman, K., Muller, L., Teigen, S.W., 1996. Series: current issues in mutagenesis and carcinogenesis, No. 65. The genotoxicity and carcinogenicity of paracetamol: a regulatory (re)view. Mutat Res 349, 263-288.

Bhalla, D.K., Gupta, S.K., 2000. Lung injury, inflammation, and inflammatory stimuli in rats exposed to ozone. J Toxicol Environ Health A 59, 211-228.

Boers, J.E., Ambergen, A.W., Thunnissen, F.B., 1998. Number and proliferation of basal and parabasal cells in normal human airway epithelium. Am J Respir Crit Care Med 157, 2000-2006.

Boorman, G.A., Schwartz, L.W., Dungworth, D.L., 1980. Pulmonary effects of prolonged ozone insult in rats. Morphometric evaluation of the central acinus. Lab Invest 43, 108-115.

Breuer, R., Zajicek, G., Christensen, T.G., Lucey, E.C., Snider, G.L., 1990. Cell kinetics of normal adult hamster bronchial epithelium in the steady state. Am J Respir Cell Mol Biol 2, 51-58.

Carey, S.A., Minard, K.R., Trease, L.L., Wagner, J.G., Garcia, G.J., Ballinger, C.A., Kimbell, J.S., Plopper, C.G., Corley, R.A., Postlethwait, E.M., Harkema, J.R., Einstein, D.R., 2007. Three-dimensional mapping of ozone-induced injury in the nasal airways of monkeys using magnetic resonance imaging and morphometric techniques. Toxicol Pathol 35, 27-40.

Cassee, F.R., Boere, A.J., Bos, J., Fokkens, P.H., Dormans, J.A., van Loveren, H., 2002. Effects of diesel exhaust enriched concentrated PM2.5 in ozone preexposed or monocrotaline-treated rats. Inhal Toxicol 14, 721-743.

Chen, T.S., Richie, J.P., Jr., Lang, C.A., 1990. Life span profiles of glutathione and acetaminophen detoxification. Drug Metab Dispos 18, 882-887.

Cho, H.-Y., Hotchkiss, J.A., Bennett, C.B., Harkema, J.R., 2000. Neutrophil-dependent and neutrophil-independent alterations in the nasal epithelium of ozone-exposed rats. Am J Respir Crit Care Med 162, 629-636.

Cho, H.-Y., Hotchkiss, J.A., Harkema, J.R., 1999. Inflammatory and epithelial responses during the development of ozone-induced mucous cell metaplasia in the nasal epithelium of rats. Toxicol Sci 51, 135-145.

Churg, A., 2003. Interactions of exogenous or evoked agents and particles: the role of reactive oxygen species. Free Radic Biol Med 34, 1230-1235.

Clement, A., Henrion-Caude, A., Besnard, V., Corroyer, S., 2001. Role of cyclins in epithelial response to oxidants. Am J Respir Crit Care Med 164, S81-84.

Corroyer, S., Maitre, B., Cazals, V., Clement, A., 1996. Altered regulation of G1 cyclins in oxidant-induced growth arrest of lung alveolar epithelial cells. Accumulation of inactive cyclin E-DCK2 complexes. J Biol Chem 271, 25117-25125.

Coyle, P., Philcox, J.C., Carey, L.C., Rofe, A.M., 2002. Metallothionein: the multipurpose protein. Cell Mol Life Sci 59, 627-647.

Dahlin, D.C., Miwa, G.T., Lu, A.Y., Nelson, S.D., 1984. N-acetyl-p-benzoquinone imine: a cytochrome P-450-mediated oxidation product of acetaminophen. Proc Natl Acad Sci U S A 81, 1327-1331.

Dai, G., He, L., Chou, N., Wan, Y.J., 2006. Acetaminophen metabolism does not contribute to gender difference in its hepatotoxicity in mouse. Toxicol Sci 92, 33-41.

Depuydt, P., Joos, G.F., Pauwels, R.A., 1999. Ambient ozone concentrations induce airway hyperresponsiveness in some rat strains. Eur Respir J 14, 125-131.

Depuydt, P.O., Lambrecht, B.N., Joos, G.F., Pauwels, R.A., 2002. Effect of ozone exposure on allergic sensitization and airway inflammation induced by dendritic cells. Clin Exp Allergy 32, 391-396.

Devereux, T.R., Domin, B.A., Philpot, R.M., 1989. Xenobiotic metabolism by isolated pulmonary cells. Pharmacol Ther 41, 243-256.

Dey, A., Jones, J.E., Nebert, D.W., 1999. Tissue- and cell type-specific expression of cytochrome P450 1A1 and cytochrome P450 1A2 mRNA in the mouse localized in situ hybridization. Biochem Pharmacol 58, 525-537.

Dinnova, S., Hoet, P.H., Dinsdale, D., Nemery, B., 2005. Acetaminophen decreases intracellular glutathione levels and modulates cytokine production in human alveolar macrophages and type II pneumocytes in vitro. Int J Biochem Cell Biol 37, 1727-1737.

Dormans, J.A., van Bree, L., Boere, A.J., Marra, M., Rombout, P.J., 1999. Interspecies differences in time course of pulmonary toxicity following repeated exposure to ozone. Inhal Toxicol 11, 309-329.

Dungworth, D.L., Castleman, W.L., Chow, C.K., Mellick, P.W., Mustafa, M.G., Tarkington, B., Tyler, W.S., 1975. Effect of ambient levels of ozone on monkeys. Fed Proc 34, 1670-1674.

Dye, J.A., Madden, M.C., Richards, J.H., Lehmann, J.R., Devlin, R.B., Costa, D.L., 1999. Ozone effects on airway responsiveness, lung injury, and inflammation. Comparative rat strain and in vivo/in vitro investigations. Inhal Toxicol 11, 1015-1040.

Eneli, I., Sadri, K., Camargo, C., Jr., Barr, R.G., 2005. Acetaminophen and the risk of asthma: the epidemiologic and pathophysiologic evidence. Chest 127, 604-612.

EPA, U.S., 2008. Air Quality Criteria for O3 and Related Photochemical Oxidants (Final) - EPA 600/R-05/004-aF-cF. In: EPA, U.S. (Ed.), vol. I, Research Triagle Park.

Evans, M.J., Cabral-Anderson, L.J., Freeman, G., 1978. Role of the Clara cell in renewal of the bronchiolar epithelium. Lab Invest 38, 648-653.

Evans, M.J., Johnson, L.V., Stephens, R.J., Freeman, G., 1976. Renewal of the terminal bronchiolar epithelium in the rat following exposure to NO2 or O3. Lab Invest 35, 246-257.

Fogarty, A., Davey, G., 2005. Paracetamol, antioxidants and asthma. Clin Exp Allergy 35, 700-702.

Forkert, P.G., Boyd, S.M., Ulreich, J.B., 2001. Pulmonary bioactivation of 1,1-dichloroethylene is associated with CYP2E1 levels in A/J, CD-1, and C57BL/6 mice. J Pharmacol Exp Ther 297, 1193-1200.

Genter, M.B., Liang, H.C., Gu, J., Ding, X., Negishi, M., McKinnon, R.A., Nebert, D.W., 1998. Role of CYP2A5 and 2G1 in acetaminophen metabolism and toxicity in the olfactory mucosa of the Cyp1a2(-/-) mouse. Biochem Pharmacol 55, 1819-1826.

Giangreco, A., Arwert, E.N., Rosewell, I.R., Snyder, J., Watt, F.M., Stripp, B.R., 2009. Stem cells are dispensable for lung homeostasis but restore airways after injury. Proc Natl Acad Sci U S A 106, 9286-9291.

Giangreco, A., Reynolds, S.D., Stripp, B.R., 2002. Terminal bronchioles harbor a unique airway stem cell population that localizes to the bronchoalveolar duct junction. Am J Pathol 161, 173-182.

Gohil, K., Cross, C.E., Last, J.A., 2003. Ozone-induced disruptions of lung transcriptomes. Biochem Biophys Res Commun 305, 719-728.

Goldsmith, C.A., Ning, Y., Qin, G., Imrich, A., Lawrence, J., Murthy, G.G., Catalano, P.J., Kobzik, L., 2002. Combined air pollution particle and ozone exposure increases airway responsiveness in mice. Inhal Toxicol 14, 325-347.

Graham, J.A., Menzel, D.B., Miller, F.J., Illing, J.W., Gardner, D.E., 1981. Influence of ozone on pentobarbital-induced sleeping time in mice, rats, and hamsters. Toxicol Appl Pharmacol 61, 64-73.

Gu, J., Cui, H., Behr, M., Zhang, L., Zhang, Q.Y., Yang, W., Hinson, J.A., Ding, X., 2005. In vivo mechanisms of tissue-selective drug toxicity: effects of liver-specific knockout of the NADPH-cytochrome P450 reductase gene on acetaminophen toxicity in kidney, lung, and nasal mucosa. Mol Pharmacol 67, 623-630.

Han, S.-G., Andrews, R., Gairola, C.G., Bhalla, D.K., 2008. Acute pulmonary effects of combined exposure to carbon nanotubes and ozone in mice. Inhal Toxicol 20, 391-398.

Haney, J.T., Jr., Connor, T.H., Li, L., 1999. Detection of ozone-induced DNA single strand breaks in murine bronchoalveolar lavage cells acutely exposed in vivo. Inhal Toxicol 11, 331-341.

Harkema, J.R., Plopper, C.G., Hyde, D.M., St George, J.A., Dungworth, D.L., 1987. Effects of an ambient level of ozone on primate nasal epithelial mucosubstances. Quantitative histochemistry. Am J Pathol 127, 90-96.

Harkema, J.R., Plopper, C.G., Hyde, D.M., St George, J.A., Wilson, D.W., Dungworth, D.L., 1993. Response of macaque bronchiolar epithelium to ambient concentrations of ozone. Am J Pathol 143, 857-866.

Harkema, J.R., Wagner, J.G., 2005. Epithelial and inflammatory responses in the airways of laboratory rats coexposed to ozone and biogenic substances: enhancement of toxicant-induced airway injury. Exp Toxicol Pathol 57 Suppl 1, 129-141.

Hermans, C., Bernard, A., 1999. Lung epithelium-specific proteins: characteristics and potential applications as markers. Am J Respir Crit Care Med 159, 646-678.

Ho, J.S., Buchweitz, J.P., Roth, R.A., Ganey, P.E., 1996. Identification of factors from rat neutrophils responsible for cytotoxicity to isolated hepatocytes. J Leukoc Biol 59, 716-724.

Hong, K.U., Reynolds, S.D., Giangreco, A., Hurley, C.M., Stripp, B.R., 2001. Clara cell secretory protein-expressing cells of the airway neuroepithelial body microenvironment include a label-retaining subset and are critical for epithelial renewal after progenitor cell depletion. Am J Respir Cell Mol Biol 24, 671-681.

Hotchkiss, J.A., Harkema, J.R., Johnson, N.F., 1997. Kinetics of nasal epithelial cell loss and proliferation in F344 rats following a single exposure to 0.5 ppm ozone. Toxicol Appl Pharmacol 143, 75-82.

Hotchkiss, J.A., Harkema, J.R., Sun, J.D., Henderson, R.F., 1989. Comparison of acute ozone-induced nasal and pulmonary inflammatory responses in rats. Toxicol Appl Pharmacol 98, 289-302.

Inoue, K., Takano, H., Kaewamatawong, T., Shimada, A., Suzuki, J., Yanagisawa, R., Tasaka, S., Ishizaka, A., Satoh, M., 2008. Role of metallothionein in lung inflammation induced by ozone exposure in mice. Free Radic Biol Med 45, 1714-1722.

Ito, K., Inoue, S., Hiraku, Y., Kawanishi, S., 2005. Mechanism of site-specific DNA damage induced by ozone. Mutat Res 585, 60-70.

Jaeschke, H., 2000. Reactive oxygen and mechanisms of inflammatory liver injury. J Gastroenterol Hepatol 15, 718-724.

Jaeschke, H., Knight, T.R., Bajt, M.L., 2003. The role of oxidant stress and reactive nitrogen species in acetaminophen hepatotoxicity. Toxicol Lett 144, 279-288.

Jakab, G.J., Hemenway, D.R., 1994. Concomitant exposure to carbon black particulates enhances ozone-induced lung inflammation and suppression of alveolar macrophage phagocytosis. J Toxicol Environ Health 41, 221-231.

James, L.P., Mayeux, P.R., Hinson, J.A., 2003. Acetaminophen-induced hepatotoxicity. Drug Metab Dispos 31, 1499-1506.

Jeffery, E.H., Haschek, W.M., 1988. Protection by dimethylsulfoxide against acetaminophen-induced hepatic, but not respiratory toxicity in the mouse. Toxicol Appl Pharmacol 93, 452-461.

Johnston, C.J., Finkelstein, J.N., Oberdorster, G., Reynolds, S.D., Stripp, B.R., 1999. Clara cell secretory protein-deficient mice differ from wild-type mice in inflammatory chemokine expression to oxygen and ozone, but not to endotoxin. Exp Lung Res 25, 7-21.

Johnston, C.J., Stripp, B.R., Piedbeouf, B., Wright, T.W., Mango, G.W., Reed, C.K., Finkelstein, J.N., 1998. Inflammatory and epithelial responses in mouse strains that differ in sensitivity to hyperoxic injury. Exp Lung Res 24, 189-202.

Jollow, D.J., Mitchell, J.R., Potter, W.Z., Davis, D.C., Gillette, J.R., Brodie, B.B., 1973. Acetaminophen-induced hepatic necrosis. II. Role of covalent binding in vivo. J Pharmacol Exp Ther 187, 195-202.

Kang, Y.J., 2006. Metallothionein redox cycle and function. Exp Biol Med (Maywood) 231, 1459-1467.

Kirichenko, A., Li, L., Morandi, M.T., Holian, A., 1996. 4-hydroxy-2-nonenal-protein adducts and apoptosis in murine lung cells after acute ozone exposure. Toxicol Appl Pharmacol 141, 416-424.

Kobzik, L., Goldsmith, C.A., Ning, Y.Y., Qin, G., Morgan, B., Imrich, A., Lawrence, J., Murthy, G.G., Catalano, P.J., 2001. Effects of combined ozone and air pollution particle exposure in mice. Res Rep Health Eff Inst, 5-29; discussion 31-28.

Kumari, M.V., Hiramatsu, M., Ebadi, M., 1998. Free radical scavenging actions of metallothionein isoforms I and II. Free Radic Res 29, 93-101.

Larson, A.M., Polson, J., Fontana, R.J., Davern, T.J., Lalani, E., Hynan, L.S., Reisch, J.S., Schiodt, F.V., Ostapowicz, G., Shakil, A.O., Lee, W.M., 2005. Acetaminophen-induced acute liver failure: results of a United States multicenter, prospective study. Hepatology 42, 1364-1372.

Last, J.A., Gohil, K., Mathrani, V.C., Kenyon, N.J., 2005. Systemic responses to inhaled ozone in mice: cachexia and down-regulation of liver xenobiotic metabolizing genes. Toxicol Appl Pharmacol 208, 117-126.

Last, J.A., Pinkerton, K.E., 1997. Chronic exposure of rats to ozone and sulfuric acid aerosol: biochemical and structural responses. Toxicology 116, 133-146.

Last, J.A., Ward, R., Temple, L., Kenyon, N.J., 2004a. Ovalbumin-induced airway inflammation and fibrosis in mice also exposed to ozone. Inhal Toxicol 16, 33-43.

Last, J.A., Ward, R., Temple, L., Pinkerton, K.E., Kenyon, N.J., 2004b. Ovalbumin-induced airway inflammation and fibrosis in mice also exposed to ultrafine particles. Inhal Toxicol 16, 93-102.

Li, L., Hamilton, R.F., Jr., Kirichenko, A., Holian, A., 1996. 4-Hydroxynonenal-induced cell death in murine alveolar macrophages. Toxicol Appl Pharmacol 139, 135-143.

Liu, J., Liu, Y., Hartley, D., Klaassen, C.D., Shehin-Johnson, S.E., Lucas, A., Cohen, S.D., 1999. Metallothionein-I/II knockout mice are sensitive to acetaminophen-induced hepatotoxicity. J Pharmacol Exp Ther 289, 580-586.

Liu, X., Driskell, R.R., Engelhardt, J.F., 2006. Stem cells in the lung. Methods Enzymol 419, 285-321.

Maddox, J.F., Amuzie, C.J., Li, M., Newport, S.W., Sparkenbaugh, E., Cuff, C.F., Pestka, J.J., Cantor, G.H., Roth, R.A., Ganey, P.E., Bacterial- and viral-induced inflammation increases sensitivity to acetaminophen hepatotoxicity. J Toxicol Environ Health A 73, 58-73.

Mango, G.W., Johnston, C.J., Reynolds, S.D., Finkelstein, J.N., Plopper, C.G., Stripp, B.R., 1998. Clara cell secretory protein deficiency increases oxidant stress response in conducting airways. Am J Physiol 275, L348-356.

Massaro, G.D., Singh, G., Mason, R., Plopper, C.G., Malkinson, A.M., Gail, D.B., 1994. Biology of the Clara cell. Am J Physiol 266, L101-106.

Mellick, P.W., Schwartz, L.W., Dungworth, D.L., 1975. Ozone-induced pulmonary lesions in rats and rhesus monkeys. Vet Pathol 12, 61-62.

Menzel, D.B., 1994. The toxicity of air pollution in experimental animals and humans: the role of oxidative stress. Toxicol Lett 72, 269-277.

Micheli, L., Cerretani, D., Fiaschi, A.I., Giorgi, G., Romeo, M.R., Runci, F.M., 1994. Effect of acetaminophen on glutathione levels in rat testis and lung. Environ Health Perspect 102 Suppl 9, 63-64.

Miller, L.A., Gerriets, J.E., Tyler, N.K., Abel, K., Schelegle, E.S., Plopper, C.G., Hyde, D.M., 2009. Ozone and allergen exposure during postnatal development alters the frequency and airway distribution of CD25+ cells in infant rhesus monkeys. Toxicol Appl Pharmacol 236, 39-48.

Mitchell, J.R., Jollow, D.J., Potter, W.Z., Davis, D.C., Gillette, J.R., Brodie, B.B., 1973a. Acetaminophen-induced hepatic necrosis. I. Role of drug metabolism. J Pharmacol Exp Ther 187, 185-194.

Mitchell, J.R., Jollow, D.J., Potter, W.Z., Gillette, J.R., Brodie, B.B., 1973b. Acetaminophen-induced hepatic necrosis. IV. Protective role of glutathione. J Pharmacol Exp Ther 187, 211-217.

Newson, R.B., Shaheen, S.O., Chinn, S., Burney, P.G., 2000. Paracetamol sales and atopic disease in children and adults: an ecological analysis. Eur Respir J 16, 817-823.

O'Reilly, M.A., Staversky, R.J., Watkins, R.H., Maniscalco, W.M., 1998. Accumulation of p21(Cip1/WAF1) during hyperoxic lung injury in mice. Am J Respir Cell Mol Biol 19, 777-785.

O'Reilly, M.A., Staversky, R.J., Watkins, R.H., Reed, C.K., de Mesy Jensen, K.L., Finkelstein, J.N., Keng, P.C., 2001. The cyclin-dependent kinase inhibitor p21 protects the lung from oxidative stress. Am J Respir Cell Mol Biol 24, 703-710.

Osebold, J.W., Zee, Y.C., Gershwin, L.J., 1988. Enhancement of allergic lung sensitization in mice by ozone inhalation. Proc Soc Exp Biol Med 188, 259-264.

Oyarzun, M., Dussaubat, N., Gonzalez, S., 2005. Effect of 0.25 ppm ozone exposure on pulmonary damage induced by bleomycin. Biol Res 38, 353-358.

Pack, R.J., Al-Ugaily, L.H., Morris, G., Widdicombe, J.G., 1980. The distribution and structure of cells in the tracheal epithelium of the mouse. Cell Tissue Res 208, 65-84.

Persky, V., Piorkowski, J., Hernandez, E., Chavez, N., Wagner-Cassanova, C., Vergara, C., Pelzel, D., Enriquez, R., Gutierrez, S., Busso, A., 2008. Prenatal exposure to acetaminophen and respiratory symptoms in the first year of life. Ann Allergy Asthma Immunol 101, 271-278.

Pino, M.V., Levin, J.R., Stovall, M.Y., Hyde, D.M., 1992a. Pulmonary inflammation and epithelial injury in response to acute ozone exposure in the rat. Toxicol Appl Pharmacol 112, 64-72.

Pino, M.V., Stovall, M.Y., Levin, J.R., Devlin, R.B., Koren, H.S., Hyde, D.M., 1992b. Acute ozone-induced lung injury in neutrophil-depleted rats. Toxicol Appl Pharmacol 114, 268-276.

Placke, M.E., Ginsberg, G.L., Wyand, D.S., Cohen, S.D., 1987a. Ultrastructural changes during acute acetaminophen-induced hepatotoxicity in the mouse: a time and dose study. Toxicol Pathol 15, 431-438.

Placke, M.E., Wyand, D.S., Cohen, S.D., 1987b. Extrahepatic lesions induced by acetaminophen in the mouse. Toxicol Pathol 15, 381-387.

Plopper, C.G., Dungworth, D.L., 1987. Structure, function, cell injury and cell renewal of bronchiolar and alveolarepithelium. In: EM, M. (Ed.) Lung Carcinoma. Churchill Livingstone., London.

Plopper, C.G., Hatch, G.E., Wong, V., Duan, X., Weir, A.J., Tarkington, B.K., Devlin, R.B., Becker, S., Buckpitt, A.R., 1998. Relationship of inhaled ozone concentration to acute tracheobronchial epithelial injury, site-specific ozone dose, and glutathione depletion in rhesus monkeys. Am J Respir Cell Mol Biol 19, 387-399.

Plopper, C.G., Hyde, D.M., 2008. The non-human primate as a model for studying COPD and asthma. Pulm Pharmacol Ther 21, 755-766.

Plopper, C.G., Macklin, J., Nishio, S.J., Hyde, D.M., Buckpitt, A.R., 1992a. Relationship of cytochrome P-450 activity to Clara cell cytotoxicity. III. Morphometric comparison of changes in the epithelial populations of terminal bronchioles and lobar bronchi in mice, hamsters, and rats after parenteral administration of naphthalene. Lab Invest 67, 553-565.

Plopper, C.G., Mango, G.W., Hatch, G.E., Wong, V.J., Toskala, E., Reynolds, S.D., Tarkington, B.K., Stripp, B.R., 2006. Elevation of susceptibility to ozone-induced acute tracheobronchial injury in transgenic mice deficient in Clara cell secretory protein. Toxicol Appl Pharmacol 213, 74-85.

Plopper, C.G., Suverkropp, C., Morin, D., Nishio, S., Buckpitt, A., 1992b. Relationship of cytochrome P-450 activity to Clara cell cytotoxicity. I. Histopathologic comparison of the respiratory tract of mice, rats and hamsters after parenteral administration of naphthalene. J Pharmacol Exp Ther 261, 353-363.

Pryor, W.A., 1994. Mechanisms of radical formation from reactions of ozone with target molecules in the lung. Free Radic Biol Med 17, 451-465.

Pryor, W.A., Squadrito, G.L., Friedman, M., 1995a. The cascade mechanism to explain ozone toxicity: the role of lipid ozonation products. Free Radic Biol Med 19, 935-941.
Pryor, W.A., Squadrito, G.L., Friedman, M., 1995b. A new mechanism for the toxicity of ozone. Toxicol Lett 82-83, 287-293.

Rawlins, E.L., Hogan, B.L., 2006. Epithelial stem cells of the lung: privileged few or opportunities for many? Development 133, 2455-2465.

Roth, R.A., Harkema, J.R., Pestka, J.P., Ganey, P.E., 1997. Is exposure to bacterial endotoxin a determinant of susceptibility to intoxication from xenobiotic agents? Toxicol Appl Pharmacol 147, 300-311.

Sato, M., Kondoh, M., 2002. Recent studies on metallothionein: protection against toxicity of heavy metals and oxygen free radicals. Tohoku J Exp Med 196, 9-22.

Schwartz, L.W., Dungworth, D.L., Mustafa, M.G., Tarkington, B.K., Tyler, W.S., 1976. Pulmonary responses of rats to ambient levels of ozone: effects of 7-day intermittent or continuous exposure. Lab Invest 34, 565-578.

Shaheen, S.O., Newson, R.B., Henderson, A.J., Headley, J.E., Stratton, F.D., Jones, R.W., Strachan, D.P., 2005. Prenatal paracetamol exposure and risk of asthma and elevated immunoglobulin E in childhood. Clin Exp Allergy 35, 18-25.

Shaheen, S.O., Sterne, J.A., Songhurst, C.E., Burney, P.G., 2000. Frequent paracetamol use and asthma in adults. Thorax 55, 266-270.

Shaw, P.J., Ganey, P.E., Roth, R.A., 2009. Trovafloxacin enhances the inflammatory response to a Gram-negative or a Gram-positive bacterial stimulus, resulting in neutrophil-dependent liver injury in mice. J Pharmacol Exp Ther 330, 72-78.

Stephens, R.J., Sloan, M.F., Evans, M.J., Freeman, G., 1974. Early response of lung to low levels of ozone. Am J Pathol 74, 31-58.

Sterner-Kock, A., Kock, M., Braun, R., Hyde, D.M., 2000. Ozone-induced epithelial injury in the ferret is similar to nonhuman primates. Am J Respir Crit Care Med 162, 1152-1156.

Stoilov, I., Krueger, W., Mankowski, D., Guernsey, L., Kaur, A., Glynn, J., Thrall, R.S., 2006. The cytochromes P450 (CYP) response to allergic inflammation of the lung. Arch Biochem Biophys 456, 30-38.

Stripp, B.R., 2008. Hierarchical organization of lung progenitor cells: is there an adult lung tissue stem cell? Proc Am Thorac Soc 5, 695-698.

Stripp, B.R., Reynolds, S.D., Plopper, C.G., Boe, I.M., Lund, J., 2000. Pulmonary phenotype of CCSP/UG deficient mice: a consequence of CCSP deficiency or altered Clara cell function? Ann N Y Acad Sci 923, 202-209.

Vesely, K.R., Schelegle, E.S., Stovall, M.Y., Harkema, J.R., Green, J.F., Hyde, D.M., 1999. Breathing pattern response and epithelial labeling in ozone-induced airway injury in neutrophil-depleted rats. Am J Respir Cell Mol Biol 20, 699-709.

Vincent, R., Bjarnason, S.G., Adamson, I.Y., Hedgecock, C., Kumarathasan, P., Guenette, J., Potvin, M., Goegan, P., Bouthillier, L., 1997. Acute pulmonary toxicity of urban particulate matter and ozone. Am J Pathol 151, 1563-1570.

Wagner, J.G., Jiang, Q., Harkema, J.R., Illek, B., Patel, D.D., Ames, B.N., Peden, D.B., 2007. Ozone enhancement of lower airway allergic inflammation is prevented by gamma-tocopherol. Free Radic Biol Med 43, 1176-1188.

Wagner, J.G., Roth, R.A., 2000. Neutrophil migration mechanisms, with an emphasis on the pulmonary vasculature. Pharmacol Rev 52, 349-374.

Wagner, J.G., Van Dyken, S.J., Wierenga, J.R., Hotchkiss, J.A., Harkema, J.R., 2003. Ozone exposure enhances endotoxin-induced mucous cell metaplasia in rat pulmonary airways. Toxicol Sci 74, 437-446.

Watt, K.C., Plopper, C.G., Buckpitt, A.R., 1997. Measurement of cytochrome P450 2E1 activity in rat tracheobronchial airways using high-performance liquid chromatography with electrochemical detection. Anal Biochem 248, 26-30.

Weinberg, W.C., Denning, M.F., 2002. P21Waf1 control of epithelial cell cycle and cell fate. Crit Rev Oral Biol Med 13, 453-464.

Wenzel, D.G., Morgan, D.L., 1983. Interactions of ozone and antineoplastic drugs on rat lung fibroblasts and Walker rat carcinoma cells. Res Commun Chem Pathol Pharmacol 40, 279-287.

West, J.A., Chichester, C.H., Buckpitt, A.R., Tyler, N.K., Brennan, P., Helton, C., Plopper, C.G., 2000. Heterogeneity of clara cell glutathione. A possible basis for differences in cellular responses to pulmonary cytotoxicants. Am J Respir Cell Mol Biol 23, 27-36.

Yu, M., Pinkerton, K.E., Witschi, H., 2002. Short-term exposure to aged and diluted sidestream cigarette smoke enhances ozone-induced lung injury in B6C3F1 mice. Toxicol Sci 65, 99-106.

CHAPTER 4

ROLE OF INTERLEUKIN-6 IN ACETAMINOPHEN AND OZONE HEPATIC AND PULMONARY TOXICITY

I. ABSTRACT

In APAP alone-treated mice, Interleukin-6 (IL-6) expression and protein concentration were elevated 9 h after administration while no changes in gene expression or protein concentration were detected in APAP and O3 co-treated mice. IL-6 is involved in initial phases of hepatocellular regeneration and has been shown to release cells from interphase to enter the cell cycle after injury or hepatectomy. In addition, mice lacking IL-6 had deficient hepatocellular regeneration and were more susceptible to chemical injury. We therefore hypothesized that in APAP and O3-coexposed mice, the lack of IL-6 induction was responsible for the impaired hepatocellular regeneration and for the greater toxicity. IL-6 sufficient and deficient mice were given APAP or O3 alone or sequentially treated with APAP and then O3. IL-6 sufficient mice recapitulated previous results where APAP alone induced hepatocellular proliferation but not APAP and O3 coexposure at 32 h after APAP. At the same time, the APAP/ O3 group had greater toxicity compared to APAP alone. In IL-6 deficient mice, APAP alone or APAP/O3 groups had no changes in hepatocellular proliferation compared to control mice 32 h after APAP administration. However, APAP and O3-coexposed IL-6 deficient mice had greater hepatocellular toxicity compared to APAP-treated deficient mice. These results suggest that IL-6 is important in hepatocellular regeneration after APAP-related liver injury but not involved

in O3 inhibition of APAP-induced hepatocellular proliferation or toxicity. In the same study, IL-6 knock-out mice given APAP alone or APAP and O3 sequentially also had deficient lung airway epithelial regeneration suggesting that IL-6 is also involved in airway epithelial regeneration. At the same time, APAP and O3 coexposure resulted in greater airway epithelial toxicity compared to APAP alone. This study demonstrates that IL-6 is important in hepatocellular and pulmonary airway epithelial regeneration after APAP or APAP and O3 injury but not in O3 inhibition of APAP-induced cell proliferation nor in the exacerbation by O3 of APAP-induced liver or airway toxicity.

II. INTRODUCTION

In our previous chapters, we reported the effects of APAP and O3 coexposure in the liver and lung of C57BL/6 male mice 9 or 32 h after APAP administration. In the liver, APAP/O3-coexposed mice had greater parenchymal damage but significantly smaller reparative hepatocellular regeneration compared to APAP alone-treated mice. O3 alone had no effect in the liver of mice. In the liver of APAP alone-treated mice, interleukin-6 (IL-6) expression and protein concentration were elevated compared to control mice. At the same time, APAP/O3-coexposed mice with defective regeneration had levels of IL-6 similar to control animals. We also found that APAP/O3 coexposure caused greater airway epithelial damage compared to APAP alone. O3 alone did not cause airway injury at the dose used in these studies. Similar to the liver, airway regeneration was also impaired in the APAP and O3-coexposed group compared to APAP alone-treated mice.

IL-6 is a cytokine produced by a variety of cells including macrophages, T and B cells, fibroblasts and endothelial cells among others (Naka et al., 2002). This cytokine has pleiotropic effects including roles in the immune system (B cell differentiation and maturation), in the acute phase response and in hematopoiesis where it releases blast cells from the interphase to divide into functional cell lines (Kishimoto, 1989). In the liver, IL-6 is mainly derived from non-parenchymal cells including Kupffer and endothelial cells and has many roles including induction of liver regeneration (Fausto et al., 2006; Klein et al., 2005; Taub, 2004; Zimmermann, 2004). IL-6 is involved in the initial phases of liver regeneration where hepatocytes transition from the interphase (G0) to the first phase of the cell cycle (G1) to replace necrotic hepatocytes (Fausto et al., 2006; Taub, 2004). In this process, this cytokine is thought to increase the sensitivity of hepatocytes to the effect of growth factors that lead hepatocytes through subsequent steps of the cell cycle (Zimmermann, 2004). IL-6 is produced in the liver in response to APAP injury (Bourdi et al., 2002; James et al., 2003b). Additionally, mice lacking IL-6 had defective regeneration after partial hepatectomy, chemical injury or ischemia (Camargo et al., 1997; Cressman et al., 1996; Kovalovich et al., 2000; Sakamoto et al., 1999). For instance, IL-6 deficient mice with impaired regeneration had increased sensitivity to CCl4 administration compared to sufficient animals (Katz et al., 1998; Kovalovich et al., 2000). It has also been shown that defective tissue repair in the liver increases in a dose-dependent fashion after chemical injury, up to a point where tissue regeneration is inhibited and results in an unopposed progression of injury (Soni and Mehendale, 1998). This team for instance coexposed rats to a small non-toxic dose of chlordecone followed

by carbon tetrachloride (CCl4) that resulted in inhibition of hepatocellular proliferation which correlated with greater hepatotoxicity and mortality in mice (Mehendale, 1994).

We therefore hypothesized that the greater liver toxicity in APAP and O3-coexposed mice is related to the impaired regeneration seen in this group and that IL-6, an important inducer of liver regeneration, is involved in this process. To support our hypothesis, we exposed IL-6 sufficient and deficient mice to APAP and/or O3. If IL-6 were involved in liver impaired regeneration in APAP/O3-coexposed mice, this last group would not exhibit hepatocellular impaired regeneration and would have liver toxicity similar to the APAP alone deficient group. Because IL-6 deficient mice have been reported to be protected from O3 airway epithelial injury (Johnston et al., 2005; Yu et al., 2002), we further hypothesize that APAP/O3-coexposed IL-6 deficient mice will have airway epithelial injury similar to APAP alone-treated deficient animals.

III. MATERIAL AND METHODS

III – 1. Laboratory Animal

Pathogen-free male, IL-6 deficient (C57BL/6J-IL-6^{tm1Kopf}, referred to as IL-6 -/- or deficient animals) or IL-6 sufficient mice (C57BL/6J referred to as IL-6 wild type or sufficient animals) were purchased from the Jackson Laboratory at the age of 8-10 weeks. IL-6 gene disruption has been produced by placing a neomycin resistance cassette within the second exon of the IL-6 gene. Mice heterozygous for the mutation (IL-6+/-) were

interbred to produce homozygous mice deficient in both alleles of IL-6 (IL-6 -/-) (Kopf et al., 1994). Mice were housed in polycarbonate cages on heat-treated aspen hardwood bedding (Nepco-Northeastern Product Corp, Warrensburg, NY). Boxes were covered with filter bonnets and animals were provided free access to food (Harlan Tekad laboratory rodents 22/5 diet, Madison, WI) and water. Mice were maintained in Michigan State University (MSU) animal housing facilities accredited by the Association for Assessment and Acreditation of Laboratory Animal Care and according to National Institutes of Health guidelines as overseen by the MSU Institutional Animal Care and Use Committee. Rooms were maintained at temperatures of 21-24°C and relative humidities of 45-70%, with a 12-hour light/dark cycle starting at 7:30 AM.

III – 2. Experimental Protocol

Mice were randomly divided into 16 groups consisting of 6 animals each. IL-6 sufficient or deficient mice were administered intraperitoneally 0 (saline-vehicle) or 300 mg/kg body weight of APAP (Sigma Chemical Co., St. Louis, MO) in 20 ml/kg saline. Animals were fasted overnight prior to the administration of APAP. Two hours after APAP administration, mice were exposed to 0 (air) or 0.5 ppm O3 for 6 h. Mice were sacrificed 9 or 32 h after APAP (1 or 24 h after O3 exposure, respectively) (Figure 30). Mice were individually housed and exposed to O3 in stainless steel wire cage whole-body inhalation exposure chambers (HC-100, Lab Products, Maywood, NJ). O3 was generated with an OREC 03V1-O ozonizer (O3 Research and Equipment Corp., AZ) using compressed air as a source of oxygen. Total airflow through the exposure chambers

was 220 l/min (13 chamber air changes/h). The concentration of O3 within chambers was monitored during the exposure using Dasibi 1003 AH ambient air O3 monitors (Dasibi Environmental Corp., Glendale, CA). Two O3 sampling probes were placed in the middle of the ozone chambers, 10-15 cm above cage racks. Airborne concentrations during the inhalation exposures were 0.56+/-0.02 ppm (mean +/- standard error of the mean) for ozone chambers and 0.007+/- 0.002 ppm for filtered air chambers.

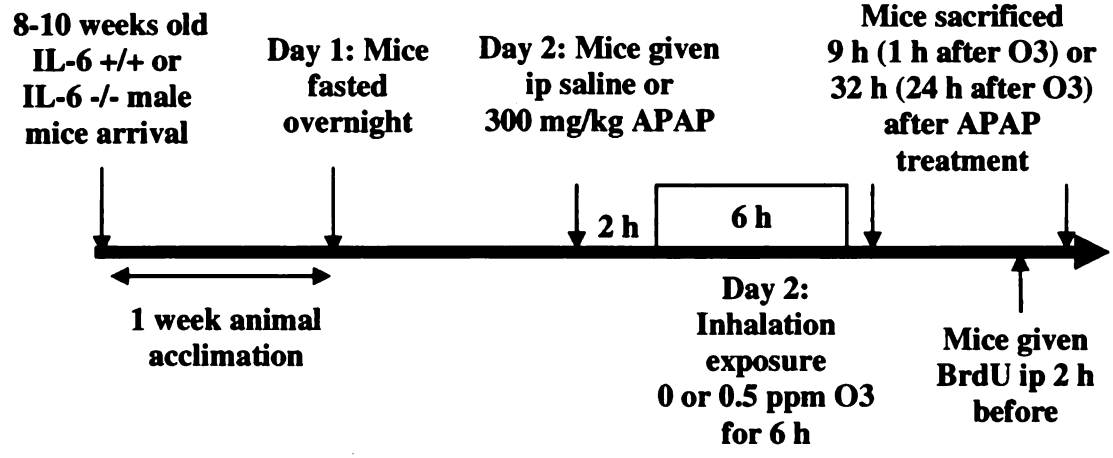

Figure 30. Experimental design of APAP and O3 studies in IL-6 sufficient and deficient mice. 8-10 weeks old C57BL/6 male mice were given 0 (saline) or 300 mg/kg APAP and then exposed to O3 (0 or 0.5 ppm) for 6 h. Mice were euthanized 9 or 32 h (1 or 24 h after O3 exposure, respectively) after APAP injection.

III – 3. Animal Necropsy, Bronchoalveolar Lavage, and Tissue Selection for Microscopic Evaluation

Two hours prior to scheduled sacrifice, mice euthanized at the 32 h time point were given 5-bromo-2-deoxyuridine (BrdU) intraperitoneally (50 mg/kg, Fisher Scientific, Fair Lawn, NJ) for nuclear incorporation and immunohistochemical detection of airway epithelial cells undergoing DNA synthesis (cycling cells in S phase). At the time of necropsy, mice were anesthetized with an intraperitoneal injection of sodium pentobarbital (50 mg/kg; Fatal Plus, Vortech Pharmaceuticals, Dearborn, MI), the abdominal cavity was opened and blood was collected from the abdominal vena cava in BD Microtainer tubes (Franklin Lakes, NJ). Animals were then killed by exsanguination.

Immediately after death, the liver was removed from the abdominal cavity. The left liver lobe was fixed in 10% neutral buffered formalin (Fisher Scientific, Fair Lawn, NJ) for light microscopic examination and morphometric analyses. The caudate liver lobe from each mouse was removed and placed in RNAlater (Qiagen, Valencia, CA) at 4 °C for 24 h and then stored at -20°C. The remaining liver lobes were frozen and stored at -80 °C. The thoracic cavity was then opened by puncturing the diaphragm to allow collapse of lung lobes. After the trachea was cannulated, the heart-lung block was excised and the lung was gently lavaged twice with 0.9 ml of sterile saline. Approximately 80% of the intratracheally instilled saline was recovered as BALF from the lavaged lung lobes and immediately placed on ice until further analysis. The right lung lobes were tied off at the bronchus level and severed from the left lobe. The left lobe attached to the heart bloc was gravity-perfusion inflated at a constant pressure of 25 cm of water for at least 1.5 hour using 10% neutral buffered formalin (NBF) (Fisher Scientific, Fair Lawn, NJ) and

then immersed in NBF for light microscopic and morphometric analyses. The right cranial lobe was immersed in RNAlater (Qiagen, Valencia, CA) at 4°C for 24 h and then transferred for storage to a -20°C freezer. The right middle and caudal lobes were frozen and stored at -80°C.

III – 4. Cellular Analysis of Bronchoalveolar Lavage Fluid

Total cell counts in the collected BALF from each mouse were determined using a hemocytometer. Cytological slides were prepared using a Shandon cytospin 3 (Shandon Scientific, Sewickley, PA), centrifuged at 600 rpm for 10 minutes and stained with Diff-Quick (Dade Behring, Newark, DE). Differential counts of neutrophils, eosinophils, macrophages and lymphocytes were assessed on a total of 200 cells. Remaining BALF were centrifuged at 1,500 rpm for 15 minutes to collect the supernatant fraction that was stored at -80°C for IL-6 evaluation by flow cytometry.

III – 5. Plasma Alanine Aminotransferase (ALT) Assay

Blood collected at the time of necropsy was used to evaluate plasma ALT activity by spectrophotometry using Infinity ALT reagents purchased form Thermo Electron Corp. (Louisville, CO).

III – 6. Flow Cytometric Analyses for Inflammatory Cytokines

BALF supernatants and plasma were assayed for IL-6. IL-6 was purchased as a Flex Set reagent (BD Biosciences, San Diego, CA). Analysis was performed using a FACSCalibur flow cytometer (BD Franklin Lakes, NJ). Briefly, 50 μl of BALF or plasma were added to the antibody-coated bead complex and incubation buffer. Samples were incubated with the beads. Phycoerythrin (PE)-conjugated secondary antibodies were then added to form sandwich complexes. Following acquisition of sample data using the flow cytometer, cytokine concentrations were calculated based on standard curve data using FCAP Array software (BD, Franklin Lakes, NJ).

III – 7. Lung and Liver Tissue Processing for Light Microscopy and Immunohistochemistry

The left lung lobe was collected as described previously and a section transverse to the axial airway was cut at the level of the fifth (fifth generation, G5) bifurcation from the axial airway. This section was embedded in paraffin and cut at a thickness of 5 μm. Transverse sections from the middle of the left liver lobe were embedded in paraffin and cut at a thickness of 5 μm. Lung and liver sections were stained with hematoxylin and eosin (H&E) for routine histopathological examination and morphometric analyses.

Routine immunohistochemical techniques were used for detection of hepatocellular or airway epithelium cell nuclear BrdU incorporation and airway epithelial cell Clara cell secretory protein (CCSP) detection. Neutrophils infiltration in the airway and liver parenchyma was also detected using immunohistochemistry. Briefly, tissue

sections were deparafinized in xylene and rehydrated through descending grades of ethanol and immersed in 3% hydrogen peroxide to block endogenous peroxides. Sections were incubated with normal sera to inhibit nonspecific proteins (normal horse, rabbit or goat sera for BrdU, neutrophils or CCSP immunostaining, respectively, Vector Laboratories Inc., Burlingame, CA) followed by specific dilutions of primary antibodies (1:40, monoclonal mouse anti-BrdU antibody, BD, Franklin Lakes, NJ; 1:2500, monoclonal rat anti-neutrophil antibody, AbD Serotec, Raleigh, NC; 1/1600, polyclonal rabbit anti-CCSP antibody, Seven Hills Bioreagents, Cincinnati, OH). Tissue sections were subsequently covered with secondary biotinylated antibodies and immunostaining was developed with the Vector RTU Elite ABC kit (BrdU and CCSP Vector Laboratories Inc) or the RTU Phosphatase-labeled Streptavidin kit (neutrophils, Kirkegaard Perry Labs, Gaithersburg, MD) and visualized with Vector Red (neutrophils and CCSP, Vector Laboratories Inc) or DAB (3,3'-diaminobenzidine) (BrdU, Sigma Chemicals, St. Louis, MO) chromogens. Slides were counterstained with Gill 2 hematoxylin (Thermo Fisher, Pittsburgh, PA).

III – 8. Lung and Liver Morphometric Analyses

Bromodeoxyuridine stained and unstained airway epithelial cell nuclei were counted in the axial airway and in all terminal bronchioles in the lung section. The BrdU labeling index was determined by dividing the number of BrdU positive cells counted in the axial airway (AA) or terminal bronchioles (TBs) by the number of total (stained and unstained) epithelial cells and multiplying by 100 (Cho et al., 1999). Similarly, the CCSP

lab eling index was determined by dividing the CCSP stained cells (cytoplasmic staining) by the total stained and unstained cells and multiplying by 100. Proximal or distal airway ac ute inflammatory infiltration was assessed by counting the numbers of immunohistochemically labeled neutrophils (cytoplasmic labeling) in the axial airway or terminal bronchioles surface epithelium, respectively, divided by the length of the underlying basal lamina (Cho et al., 1999). The length of the basal lamina underlying the surface epithelium was calculated from the contour length of the basal lamina, by using a National Institutes of Health (NIH) image analysis software (NIH Image; written by Wayne Rasband at the U.S. NIH). It is reported as the number of neutrophils per mm of basal lamina.

BrdU stained and unstained hepatocellular nuclei or neutrophils infiltration were counted in 10 medium power fields (X200) for each animal starting with a randomly selected field and evaluating every third field. The hepatocellular BrdU labeling index (LI) was determined by counting the number of BrdU labeled cells divided by the total number of hepatocytes (stained and unstained) and multiplying by 100.

To quantify APAP and/or O3-induced airway epithelial injury, morphometric analyses were conducted on H&E sections. The numeric epithelial cell density (i.e., number of epithelial cells per mm of basal lamina) was determined by counting the total number of surface epithelial cell nuclear profiles in transverse airway sections divided by the length of the underlying basal lamina (Cho et al., 1999). For the terminal bronchioles, the numeric cell density presented is the mean of numeric densities from all terminal bronchioles present on the section. The length of the basal lamina was measured using the NIH Image program (Wayne Rasband, U.S. National Institutes of Health).

The amount of hepatocellular degeneration/necrosis in sections from the left liver lobe were morphometrically determined using standard morphometric methods that are similar to those previously described in details in chapter 2 (Yee et al., 2000). Briefly, images at a magnification of X200 were evaluated employing a 168-point lattice grid overlaying fields of hepatic parenchyma. Sections from the liver of each mouse were systematically scanned using adjacent, non-overlapping microscopic fields. The first image field analyzed in each section was chosen randomly. Thereafter, every third field was evaluated (approximately 12 fields evaluated/section).

III – 9. Identification of IL-6 deficient gene by PCR and gel electrophoresis

IL-6 gene silencing in deficient mice was confirmed on liver tissue or BALF and plasma samples from wild type and deficient mice by PCR and gel electrophoresis or flow cytometry, respectively. Briefly, 2 PCR primers were used to identify the mutated and wild type alleles. The first primer (TTC CAT CCA GTT GCC TTC TTG G) hybridizes to the 5' upstream region of exon 2 in the wild type gene (the disrupted exon in the IL-6 gene) and the second primer (CCG GAG AAC CTG CGT GCA ATC C) is a downstream primer which hybridizes within the neomycin cassette used to disrupt exon 2. As shown in figure 31, the first primer was amplified as a 174 bp fragment while the mutated (second) primer was amplified as a 380 bp fragment (Hilbert et al., 1995). Furthermore, IL-6 protein was detected in the BALF or plasma of IL-6 sufficient (see below) but not deficient (data not shown) mice using flow cytometry as described above.

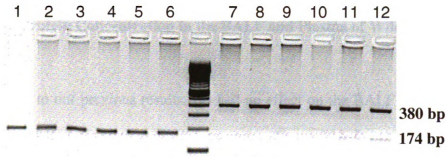

Figure 31. PCR and electrophoresis-based assessment of IL-6 gene disruption in the liver. Two primers, one to identify the wild type allele and the other one for the mutated allele, were used. The wild type allele was amplified as a 174 base pair (bp) fragment (from IL-6 sufficient mice Nos. 1 to 6) while the mutated primer was amplified as a 380 bp fragment (from IL-6 deficient mice Nos. 7 to 12).

III – 10. Statistical Analysis

Data were reported as mean +/- SE. Differences among groups were analysed by a one or two-way ANOVA followed by Student-Newman-keuls post hoc test. When normality or variance equality failed, a Kruskal-Wallis ranked test was conducted. All analyses were performed using a commercial statistical analysis software (SigmaStat; Jandel Scientific, San Rafael, CA). Significance was assigned to p values smaller or equal to 0.05.

IV. RESULTS

IV – 1. IL-6 Protein Concentration in the BALF and Plasma of Wild Type Mice

Similar to our previous results, O3 had no effect on the BALF or plasma protein concentration of IL-6 at any time in wild type mice (Figure 32A-D). However at 9 h, IL-6 protein concentration was elevated in the BALF and plasma of wild type APAP-treated mice but was greatest when APAP was coexposed with O3, although significance was not reached in the BALF (Figure 32A-D). No differences in IL-6 concentration were present between O3 alone, APAP alone or APAP/O3 groups at 32 h (Figure 32A-D). IL-6 deficient mice had no detectable IL-6 protein concentration in the BALF or plasma at any time or with any treatment (data not shown).

Figure 32. IL-6 protein concentration in the BALF (A and B) or plasma (C and D) of APAP and O3 exposed IL-6 sufficient mice. Animals were given 0 (saline) or 300 mg/kg APAP ip and 2 h later exposed to 0 (air) or 0.5 ppm O3 for 6 h. 9 or 32 h after APAP administration, animals were euthanized and BALF and plasma collected and IL-6 concentration evaluated as described in Material and Methods. Data are expressed as mean ± SE, (n = 6). a, significantly different from saline/air group, b, significantly different from saline/O3 group, c, significantly different from APAP/air group; ($p \leq 0.05$). ND, not detected.

Figure 32

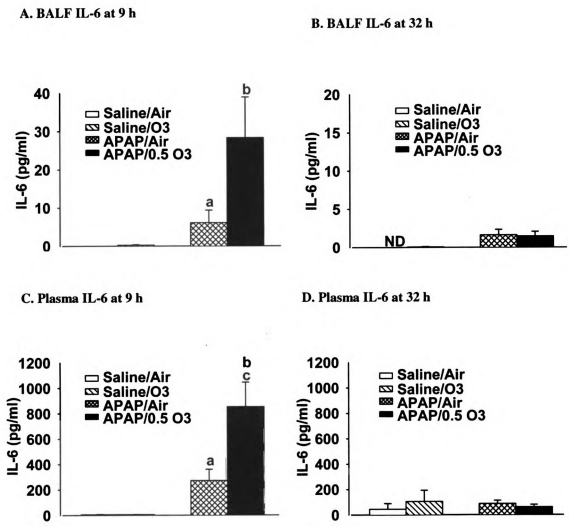
A. BALF IL-6 at 9 h
IL-6 (pg/ml)
40
30
20
10
0
Saline/Air
Saline/O3
APAP/Air
APAP/0.5 O3
a
b
B. BALF IL-6 at 32 h
IL-6 (pg/ml)
20
15
10
5
0
Saline/Air
Saline/O3
APAP/Air
APAP/0.5 O3
ND
C. Plasma IL-6 at 9 h
IL-6 (pg/ml)
1200
1000
800
600
400
200
0
Saline/Air
Saline/O3
APAP/Air
APAP/0.5 O3
a
b
c
D. Plasma IL-6 at 32 h
IL-6 (pg/ml)
1200
1000
800
600
400
200
0
Saline/Air
Saline/O3
APAP/Air
APAP/0.5 O3

IV – 2. Liver Histopathology and Morphometric Analyses

APAP overdose causes centrilobular hepatocellular necrosis in mice. This classic APAP lesion as well as O3 exacerbation of APAP damage has been described in chapter 2 of this dissertation. O3 exposure did not change ALT activity (a marker of hepatocellular injury) or cause hepatocellular damage in IL-6 sufficient or deficient mice compared to control animals (Figure 33A, B). APAP alone caused hepatocellular injury 9 or 32 h after administration in sufficient and deficient mice (Figure 33A-D). Some inter-individual variability was observed in ALT evaluation, however, morphometric analyses revealed that no differences were observed between APAP alone and APAP/O3-treated groups of the sufficient and deficient mice at 9 h (Figure 33A, C). At 32 h, a progression of injury was detected in APAP-treated groups compared to the 9 h time (Figure 33B, D). At this time, APAP and O3 coexposure resulted in greater necrosis and degeneration compared to APAP alone in either genotype (Figure 33A-D). IL-6 deletion delayed the onset of APAP-induced hepatocellular toxicity compared to wild type mice. Indeed, APAP alone and APAP/O3-coexposed groups had significantly less necrosis and degeneration in IL-6 deficient mice compared to their respective sufficient counterparts at 9 h (Figure 33A, C). At 32 h, no differences in ALT or hepatocellular damage were detected between APAP alone or APAP/O3 of the sufficient and deficient mice (Figure 33B, D).

Figure 33. Liver damage induced by APAP and O3 exposure in IL-6 sufficient or deficient mice. Alanine aminaotransferase (ALT) activity (A and B) in plasma and morphometric evaluation of hepatocellular damage (C and D). Animals were given 0 (saline) or 300 mg/kg APAP ip and 2 h later exposed to 0 (air) or 0.5 ppm O3 for 6 h. 9 or 32 h after APAP administration, animals were euthanized, blood and liver tissue were collected and ALT and liver tissue evaluated as described in Material and Methods. Data are expressed as mean ± SE, (n = 6). a, significantly different from respective saline/air group; b, significantly different from respective saline/O3 group; c, significantly different from APAP/air KO group; d, significantly different from APAP/O3 KO group; e, significantly different from APAP/air WT group; f significantly different from APAP/air KO group; ($p \leq 0.05$). ND, not detected.

Figure 33

A. Plasma ALT at 9 h

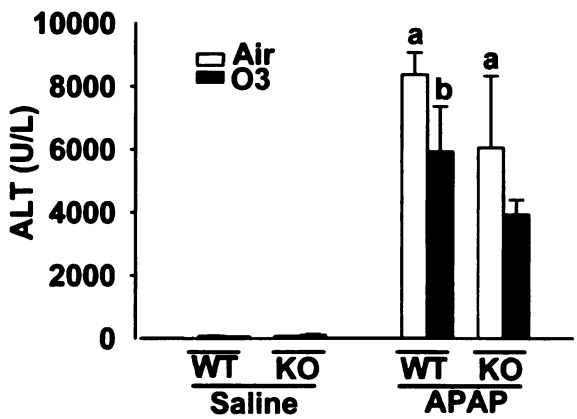

B. Plasma ALT at 32 h

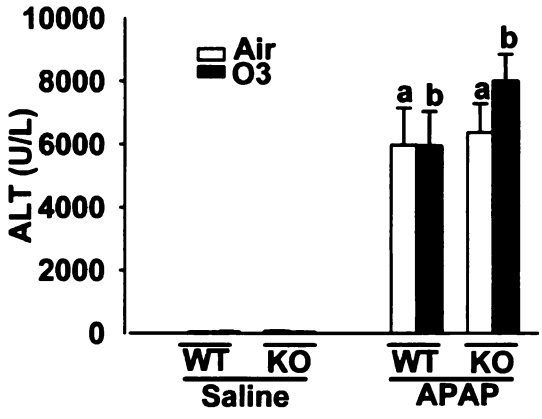

C. Liver injury at 9 h

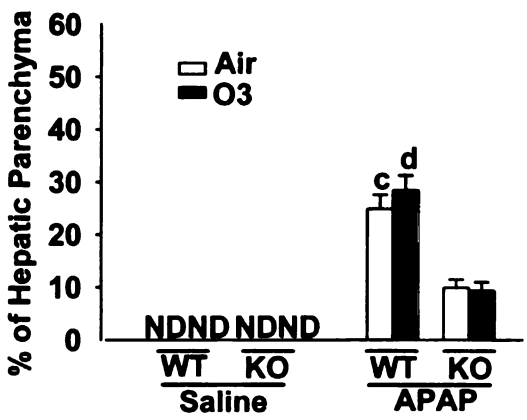

D. Liver injury at 32 h

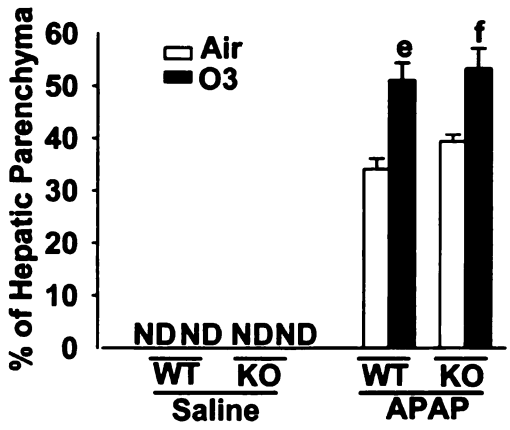

IV – 3. Liver Inflammation

O3 alone did not cause neutrophil accumulation in the liver of IL-6 sufficient or deficient mice at any time after APAP (Figure 34A, B). At 9 h, liver neutrophil accumulation was increased in damaged areas of APAP/air and APAP/O3 groups in IL-6 sufficient mice (Figure 34A). At the same time, IL-6 deficient mice given APAP or APAP and O3 had a nonsignificant increase in liver neutrophils consistent with the smaller hepatocellular injury measured at this time in these groups compared to the respective sufficient groups (Figure 34A). At 32 h, APAP alone and APAP/O3-coexposed mice had similar amounts of liver neutrophils in IL-6 sufficient or deficient mice (Figure 34B).

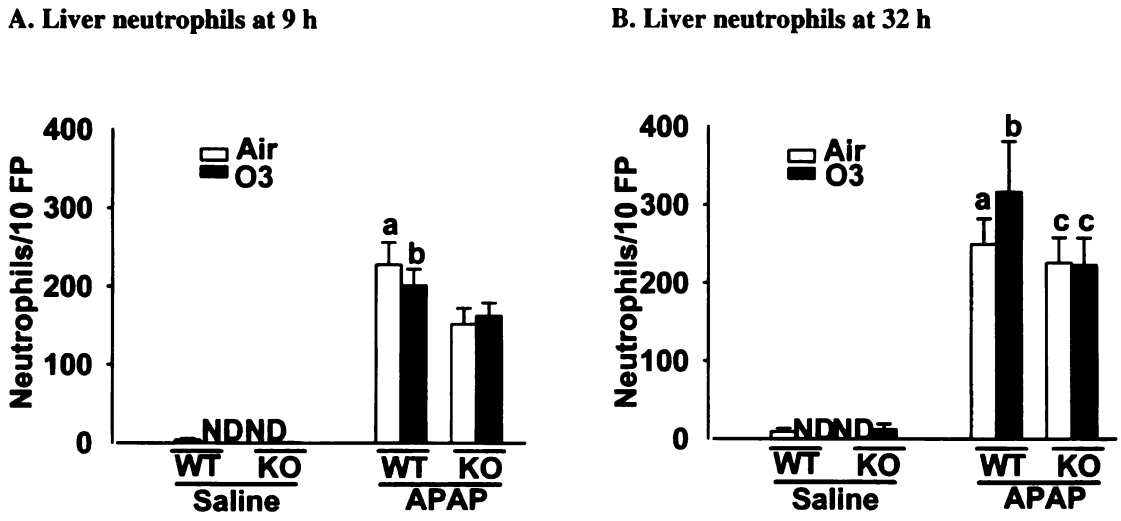

Figure 34. Liver neutrophil infiltration in APAP and O3 exposed IL-6 sufficient and deficient mice. Morphometric evaluation of neutrophil infiltration in hepatic parenchyma 9 or 32 h after APAP. Animals were given 0 (saline) or 300 mg/kg APAP ip and 2 h later exposed to 0 (air) or 0.5 ppm O3 for 6 h. Animals were euthanized and livers collected and evaluated as described in Material and Methods. Data are expressed as mean ± SE, (n = 6). a, significantly different from saline/air WT group; b, significantly different from saline/O3 WT group; c, significantly different from saline/air KO group; ($p \leq 0.05$). ND, not detected; FP, fields of parenchyma.

IV- 4. Liver Regeneration

O3 alone did not change the number of cycling hepatocytes in IL-6 sufficient or deficient mice 32 h after saline administration compared to control animals (Figure 35). In IL-6 sufficient mice, APAP alone caused a significant increase in the number of cycling hepatocytes 32 h after its administration (Figure 35). In these animals, O3 exposure following the APAP treatment resulted in a reduction in the number of proliferating hepatocytes down to control levels (Figure 35). In IL-6 deficient mice, APAP alone did not cause an elevation of cycling hepatocytes and APAP alone or APAP/O3-treated IL-6 deficient mice had a number of proliferating hepatocytes similar to control mice (Figure 35).

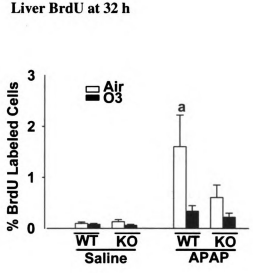

Figure 35. Hepatocellular proliferation in APAP and O3 exposed IL-6 sufficient and deficient mice. Morphometric evaluation of cycling hepatocytes in S phase 32 h after APAP. Animals were given 0 (saline) or 300 mg/kg APAP ip and 2 h later exposed to 0 (air) or 0.5 ppm O3 for 6 h. Animals were euthanized and livers collected and evaluated as described in Materials and Methods. Data are expressed as mean ± SE, (n = 6). a, significantly different from saline/air WT group; ($p \leq 0.05$).

IV – 5. Lung Histopathology and Morphometric Analyses

Histopathological examination indicated that O3 exposure did not cause airway epithelial damage or inflammation in IL-6 sufficient or deficient mice compared to controls. No differences in the nature of lesions (epithelial degeneration and necrosis and exfoliation of necrotic cells) in the airway epithelia have been observed between IL-6 sufficient and deficient mice given APAP alone or APAP and O3. We also found that in either genotype, APAP alone or APAP/O3 effects on airway epithelial cells were more pronounced in the axial airway compared to terminal bronchioles similar to previous results in wild type animals in chapter 3. These observations are confirmed after morphometric evaluation of airway epithelial injury or inflammation as reported below.

Morphometric evaluations revealed that in IL-6 sufficient mice, O3 alone had no effect on the airway epithelium at any time (Figure 36A-D). APAP alone or APAP and O3 coexposure resulted in a time-dependent increase in epithelial cell loss in the axial airway and terminal bronchioles between 9 and 32 h (Figure 36A-D). In these sufficient mice, APAP and O3-coexposed mice had greater damage in either location compared to APAP alone at the 9 h time (Figure 36A-D). In IL-6 deficient mice, O3 alone had no effect on airway epithelial cell densities (Figure 36A-D). In these deficient mice, APAP alone or APAP and O3 coexposure on the other hand caused epithelial cell loss in the axial airway and terminal bronchioles at 9 or 32 h (Figure 36A-D). In IL-6 deficient mice, APAP/O3-coexposed mice had more airway epithelial injury than APAP alone at 9 h but not at 32 h (Figure 36A-D). At the early time, IL-6 deficient mice had greater epithelial cell loss in the APAP/air or APAP/O3 groups when compared to sufficient

respective counterparts. At 32 h no differences in airway epithelial losses were detected between sufficient and deficient mice (Figure 36A-D).

Figure 36. Epithelial numeric cell density in the axial airway (A, B) and terminal bronchioles (C, D) of APAP and O3 exposed IL-6 sufficient and deficient mice. Animals were injected ip with 0 (saline) or 300 mg/kg APAP and 2 h later exposed to 0 (air) or 0.5 ppm O3 for 6 h. 9 or 32 h after APAP administration, animals were euthanized and left lung lobes collected, routinely stained and evaluated as described in Material and Methods. Data are expressed as mean ± SE, (n = 6). a, significantly different from respective saline/air group; b, significantly different from respective saline/O3 group; c, significantly different from respective APAP/air group; d significantly different from APAP/air WT group; e, significantly different from APAP/O3 WT group; ($p \leq 0.05$). BL, basal lamina.

Figure 36

A. Axial airway epithelial density at 9 h

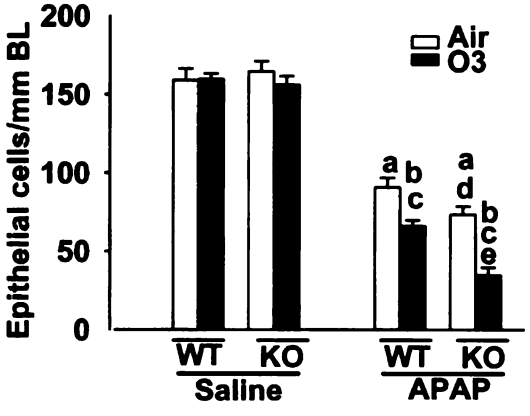

B. Axial airway epithelial density at 32 h

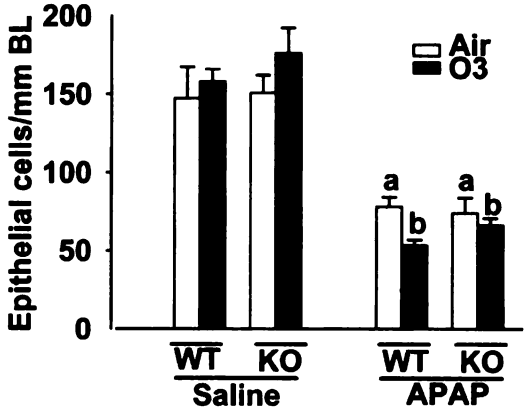

C. Terminal bronchioles epithelial density at 9 h

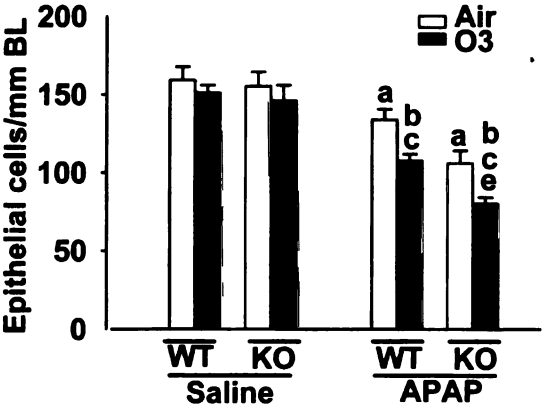

D. Terminal bronchioles epithelial density at 32 h

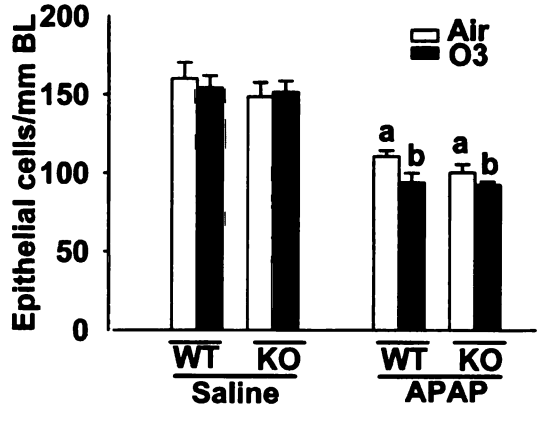

IV – 6. Lung Inflammation

Neutrophil accumulation was not detected in airways of IL-6 sufficient or deficient mice exposed to O3 at any time after APAP (Figure 37A-D). IL-6 sufficient mice given APAP alone or APAP and O3 had no significant neutrophil accumulation in their airways 9 h after injection (Figure 37A, C). At 32 h, APAP and O3 coexposed sufficient mice had greater axial airway neutrophil infiltration compared to control mice (Figure 37B, D). In deficient mice, the time course of inflammation was reversed and no neutrophil accumulation was present in the airways of the APAP/O3 group 32 h after APAP administration (Figure 37B, D) while significant neutrophil accumulation was detected in the axial airway and terminal bronchioles at 9 h (Figure 37A, C). At 9 or 32 h after APAP, APAP alone or APAP/O3-coexposed sufficient or deficient groups had an increased number of neutrophils in the alveolar septa. No differences in neutrophil accumulation between treatment (APAP and APAP/O3) or genotype (IL-6 deficient and sufficient mice) were observed in alveolar septa. Representative pictures of APAP-induced neutrophils accumulation in alveolar septa from control or APAP and O3-coexposed mice are presented in figure 38.

In the BALF, no significant total inflammatory cells, macrophages or neutrophils changes were detected with any treatment regimen or genotype 9 h after APAP (Figure 39A, C, E). At 32 h, APAP/air and APAP/O3 treatment regimen caused significant and comparable increase of total inflammatory cells and macrophages in IL-6 deficient and sufficient mice (Figure 39B, D). In the BALF of IL-6 sufficient mice, a statistical increase of neutrophils was detected in APAP alone and APAP/O3-coexposed group 32 h

after APAP (Figure 39F). No differences were however noticed between these 2 last groups. IL-6 deficient mice given APAP alone or APAP and O3 had no neutrophil accumulation in the BALF at any time (Figure 39F).

Figure 37. Neutrophil infiltration in the axial airway (A, B) and terminal bronchioles (C, D) of APAP and O3 exposed IL-6 sufficient and deficient mice. Animals were injected ip with 0 (saline) or 300 mg/kg APAP and 2 h later exposed to 0 (air) 0.5 ppm O3 for 6 h. Mice were euthanized 9 or 32 h after APAP. Data are expressed as mean ± SE, (n = 6). a, significantly different from saline/air KO; b, significantly different from saline/air WT; ($p \leq 0.05$). ND, not detected; BL, basal lamina.

Figure 37

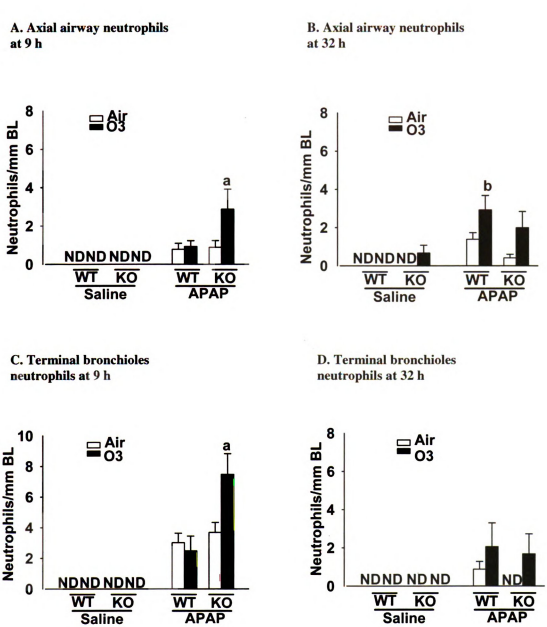
A. Axial airway neutrophils at 9 h
B. Axial airway neutrophils at 32 h
C. Terminal bronchioles neutrophils at 9 h
D. Terminal bronchioles neutrophils at 32 h
Neutrophils/mm BL
Air
O3
a
b
ND ND ND ND
WT KO WT KO
Saline
APAP

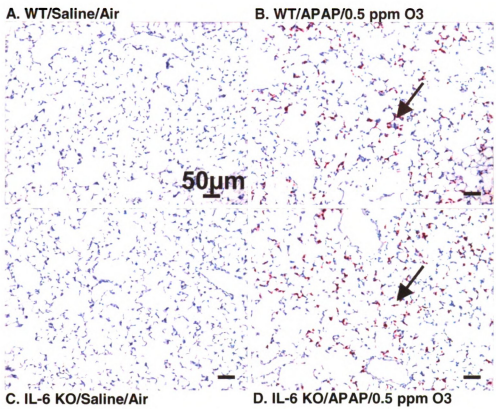

Figure 38. Neutrophil accumulation in alveolar septa of IL-6 sufficient and deficient mice 9 h after APAP. Light photomicrographs of lung sections from wild type (WT) mice treated with saline/air (A) or APAP/O3 (B) and from IL-6 knock-out (KO) mice given saline/air (C) or APAP/O3 (D). Black arrows indicate neutrophils in alveolar septa.

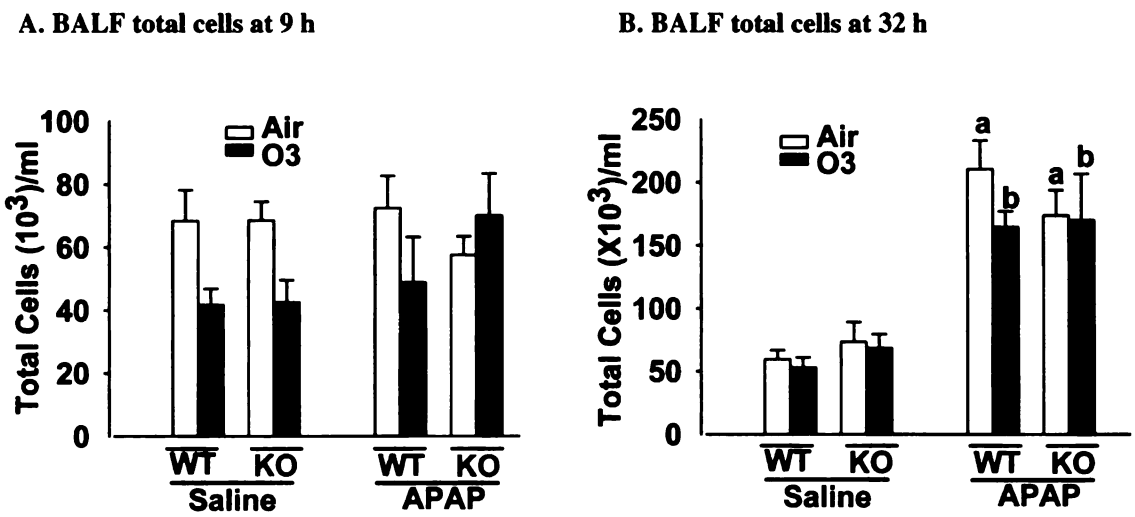

Figure 39. Inflammatory cell accumulation in the BALF of IL-6 sufficient and deficient mice. Total inflammatory cells (A, B), macrophages (C, D) and neutrophils (E, F) per ml of BALF. Animals were injected ip with 0 (saline) or 300 mg/kg APAP and 2 hours later exposed to 0 (air), 0.25 or 0.5 ppm O3 for 6 h. 9 or 32 h after APAP administration, animals were euthanized and BALF harvested and analyzed as described in Material and Methods. Data are expressed as mean ± SE, (n = 6). a, significantly different from respective saline/air group; b, significantly different from respective saline/O3 group; ($p \leq 0.05$). ND, not detected.

Figure 39 (cont'd)

C. BALF macrophages at 9 h

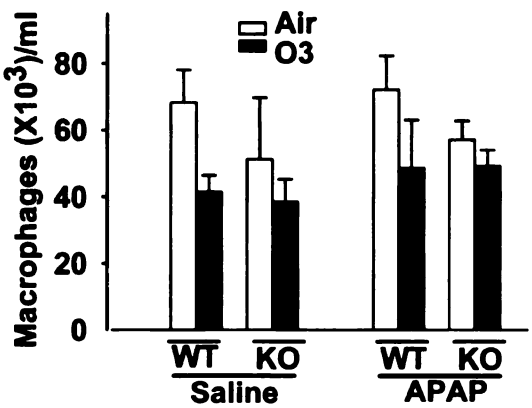

D. BALF macrophages at 32 h

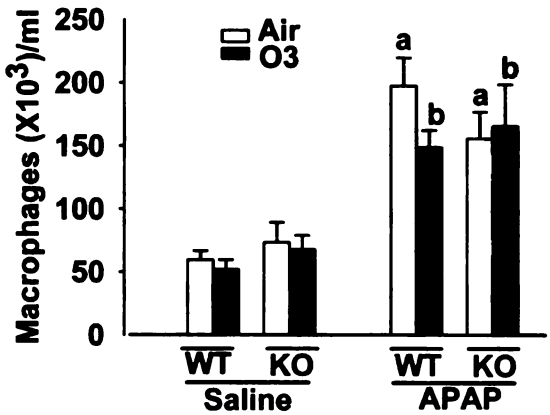

E. BALF neutrophils at 9 h

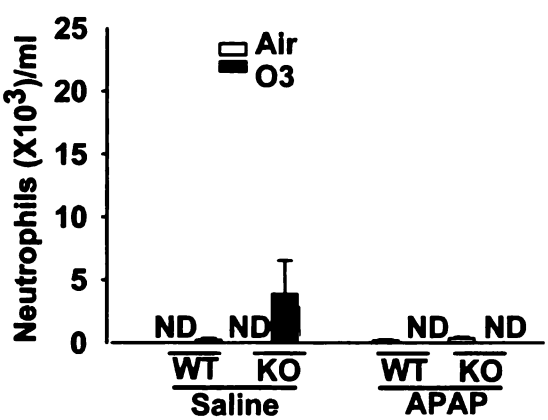

F. BALF neutrophils at 32 h

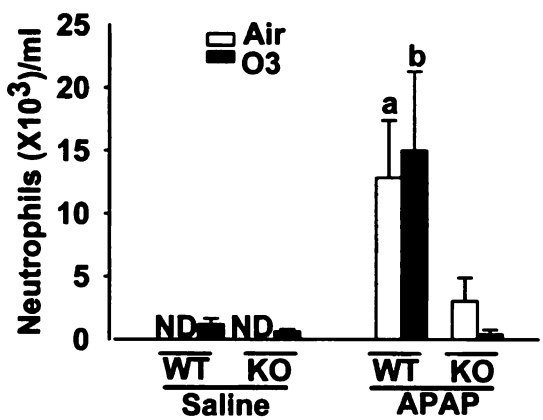

IV – 7. Lung Epithelial Regeneration

BrdU is incorporated in nuclei of cycling epithelial cells in S phase and used as an indicator of the proliferating epithelial cell pool. O3 alone did not cause significant change in the number of proliferating epithelial cell in the axial airway and terminal bronchioles in IL-6 sufficient or deficient mice (Figure 40A, B). APAP administration resulted in an increase of BrdU-labeled cells in the axial airway and terminal bronchioles of IL-6 sufficient mice 32 h after APAP (Figure 40A, B). In either location, O3 exposure resulted in reduction of APAP-induced cell proliferation in coexposed sufficient mice (Figure 40A, B). In IL-6 deficient mice, APAP administration did not result in an increase of BrdU-labeled cells in pulmonary airways and APAP/air and APAP/O3 groups had BrdU labeling indices similar to those of SAL/air control mice (Figure 40A, B). IL-6 deficient mice given APAP alone and APAP/O3 had less BrdU-labeled cells in the axial airway and terminal bronchioles compared to their respective IL-6 sufficient counterparts (Figure 40A, B).

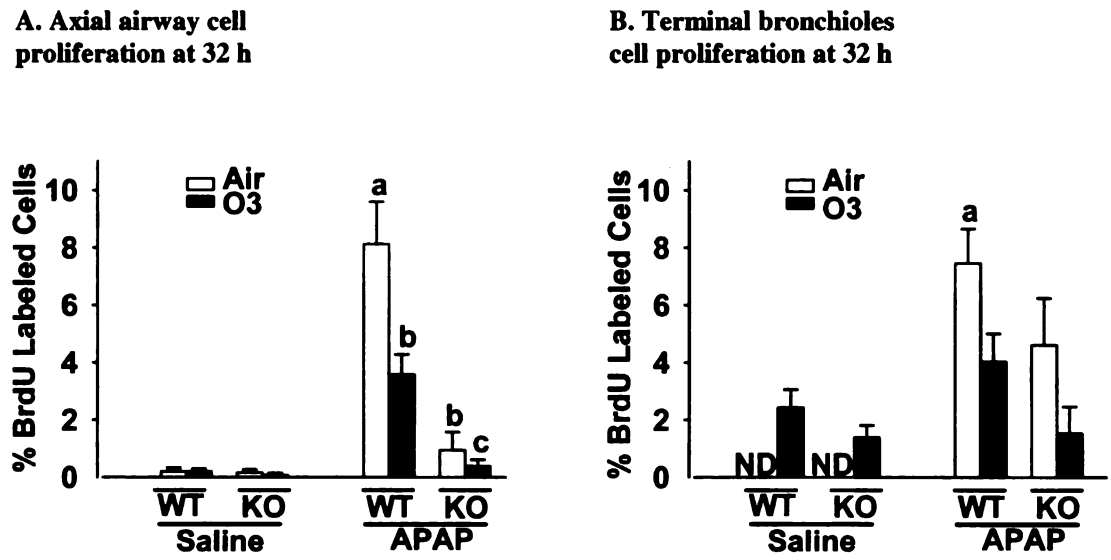

Figure 40. Airway epithelium cell proliferation in APAP and O3 exposed IL-6 sufficient and deficient mice 32 h after APAP. BrdU-labeled epithelial cells were evaluated in the axial airway (A) and in terminal bronchioles (B). Animals were injected ip with 0 (saline) or 300 mg/kg APAP and 2 h later exposed to 0 (air) or 0.5 ppm O3 for 6 h. Lung sections were immunohistochemically stained and evaluated as described in Material and Methods. Data are expressed as mean ± SE, (n = 6). a, significantly different from saline/air WT group; b, significantly different from APAP/air WT group; c, significantly different from APAP/O3 WT group; ($p \leq 0.05$). ND, not detected.

Clara cells are part of the cellular armamentarium responsible for airway epithelial regeneration (Bishop, 2004). O3 exposure did not change the number of Clara cells lining the axial airway and terminal bronchioles of IL-6 sufficient or deficient mice (Figure 41A-D). APAP alone caused significant loss of Clara cell in the axial airway and terminal bronchioles of sufficient or deficient mice 9 and 32 h after administration (Figure 41A-D). Similar to our finding after evaluation of total epithelial cell loss, the main difference between genotypes was observed at the early time where APAP alone or APAP/O3-cotreated deficient mice had less Clara cells in the axial airway compared to sufficient mice (Figure 41A-D). At 32 h, no differences in the number of Clara cells were detected in APAP alone or APAP/O3–coexposed sufficient mice compared to their deficient counterparts (Figure 41A-D).

Figure 41. Clara cell density in the axial airway (A, C) and terminal bronchioles (B, D) of IL-6 sufficient and deficient mice. Animals were injected ip with 0 (saline) or 300 mg/kg APAP and 2 h later exposed to 0 (air) or 0.5 ppm O3 for 6 h. 9 or 32 h after APAP administration, animals were euthanized, their left lung lobe were collected and processed as detailed in Material and Methods. Data are expressed as mean ± SE, (n = 6). a significantly different from respective saline/air group; b significantly different from respective saline/O3 WT group; c significantly different from APAP/air WT group; d significantly different from APAP/O3 WT group; e significantly different from APAP/air KO; ($p \leq 0.05$). BL, basal lamina.

Figure 41

A. Axial airway Clara cell density at 9 h

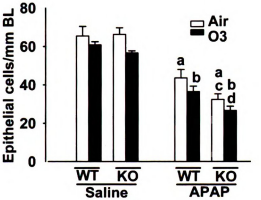

B. Axial airway Clara cell density at 32 h

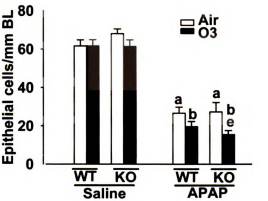

C. Terminal bronchioles Clara cell density at 9 h

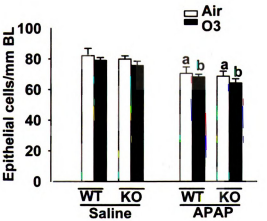

D. Terminal bronchioles Clara cell density at 32 h

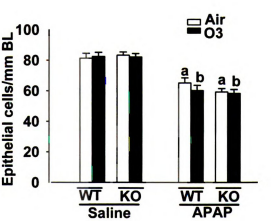

V. DISCUSSION

The main hypothesis behind this work was that O3-induced inhibition of IL-6 expression and protein concentration in APAP-treated mice impaired hepatocellular regeneration which in turn led to greater hepatocellular damage in the APAP and O3-coexposed group. We hypothesized that in mice deficient in IL-6, APAP and O3 coexposure will not cause impaired hepatocellular regeneration and will therefore exhibit injury similar to APAP alone-treated mice. We found that regardless of the genotype, mice given APAP alone or APAP and O3 had similar hepatocellular damage at 9 h. At 32 h, IL-6 sufficient or deficient mice given APAP and O3 had greater hepatocellular injury compared to APAP alone-treated mice of respective genotype. In addition, at the 9 h time, IL-6 deficient mice given APAP alone or APAP and O3 had less hepatocellular injury and neutrophil accumulation than their respective counterpart of the sufficient genotype. APAP administration caused a significant increase of BrdU-labeled hepatocytes in IL-6 sufficient mice 32 h after its administration. O3 exposure caused a reduction of this APAP-induced hepatocellular proliferation in the coexposed mice. In IL-6 deficient mice, APAP treatment did not cause hepatocellular proliferation at 32 h and APAP alone and APAP/O3–coexposed IL-6 deficient groups had BrdU labeling indices similar to control mice. In summary, contrary to our hypothesis, IL-6 deletion impaired regeneration in both APAP/air and APAP/O3 groups at 32 h. At the same time, O3 exacerbated APAP-induced livertoxicity in the deficient or sufficient coexposed group mice. In addition, impaired hepatocellular regeneration in APAP alone-treated

deficient mice did not increase liver toxicity compared to sufficient mice of similar treatment group.

Several teams previously reported the effects of APAP in IL-6 deficient mice (James et al., 2003a; Masubuchi et al., 2003). In one study, 300 mg/kg APAP in saline were injected ip in fasted male C57BL/6 mice (Masubuchi et al., 2003). APAP treatment in these animals caused IL-6 mRNA increase in the liver that reached a peak between 4 h and 8 h after APAP injection. At this dose of APAP, IL-6 deficient mice had more hepatocellular injury at 6, 12, 18 or 24 h post-APAP compared to IL-6 sufficient mice. In a second paper by James and collaborators (2003), 300 mg/kg APAP in saline ip using the same strain and mouse gender, caused no significant differences in liver toxicity between IL-6 deficient and sufficient mice 4 or 24 h after APAP. In this last study however, APAP toxicity was slightly smaller or greater at 4 or 24 h, respectively, in deficient compared to sufficient mice. At 48 h after APAP, deficient mice had more biochemical toxicity but less hepatocellular regeneration than sufficient mice (James et al., 2003a). This is more in line with our results where APAP alone or APAP and O3 liver toxicity was greater in sufficient animals at 9 h while no difference was detected at 32 h between sufficient and deficient mice. In the study by James and collaborators (2003), it is not clear whether the greater liver toxicity at 48 h was related to the impaired regeneration detected at the same time. In the same study, APAP-treated deficient mice still had defective hepatocellular regeneration at 72 h post-APAP while by this time toxicity resolved in either genotype. In our study, as described in the previous paragraph, APAP-treated deficient and sufficient mice had similar hepatocellular injury at 32 h while deficient animals had less BrdU labeled hepatocytes.

Our results indicated that in IL-6 deficient mice, the onset of APAP hepatotoxicity is delayed. The reasons for this protection from APAP toxicity at the early time remain unclear. IL-6 is apparently not essential for constitutive expression of cytochromes P450 isoforms including those involved in APAP metabolism such as Cyp1a2, 2a5, 2e1, and 3a11 (Kovalovich et al., 2000; Siewert et al., 2000; Warren et al., 2001). In addition, no differences in APAP protein adduct formation or nitrotyrosine immunostaining were detected between APAP-treated IL-6 sufficient and deficient mice (James et al., 2003a; Masubuchi et al., 2003). Other factors involved in APAP detoxication or in hepatic protection from xenobiotics have also been shown to be similarly produced in IL-6 sufficient or deficient mice. Thus, evaluation of hepatic total glutathione, glutathione reductase, glutathione peroxidase and glutathione-S-transferase levels showed no differences between saline-treated IL-6 sufficient and deficient mice (Warren et al., 2001). The course of hepatic glutathione depletion at 4 h (and resynthesis at 24 h) after APAP treatment was also similar between the 2 genotypes (James et al., 2003a). In a recent work, IL-6 was reported to have a role in glutathione metabolism (Bourdi et al., 2007). This team showed that interleukins 10 and 4 double-deficient mice were more susceptible to APAP liver effects and had lower hepatic concentrations of glutathione and high systemic level of IL-6. Administration of an anti-IL-6 antibody or disruption of IL-6 gene in these double-deficient mice protected from increased APAP liver damage and restored liver glutathione level. They speculated that IL-6 directly stimulates induction of nitric oxide synthase-2 (NOS-2) which then resulted in nitric oxide (NO) and peroxynitrite formation and decreased glutathione through peroxynitrite scavenging (Bourdi et al., 2007). Therefore, lack of NOS-2 induction and NO generation

might at least partially account for the hepatic protection offered by IL-6 deletion early in the course of APAP toxicity in our study. Other hepatoprotective factors such as interleukin-10 or cyclooxygenase-2 or proinflammatory cytokines such as TNF-α or interferon-gamma were not the basis for differences in toxicity observed between sufficient and deficient mice (Masubuchi et al., 2003).

O3-induced injury in the lung is dependent upon IL-6 and O3-exposed IL-6 deficient mice have less injury in the lung compared to sufficient animals (Johnston et al., 2005; Yu et al., 2002). We therefore hypothesized that the course of APAP alone and APAP/O3 airway toxicity will be similar in IL-6 deficient mice. Instead, we found that at 9 h post-APAP, IL-6 sufficient or deficient mice exposed sequentially to APAP and O3 had more airway epithelial injury than APAP alone-treated mice of respective genotype. At the later time, APAP alone and APAP/O3 groups had similar airway injury regardless of the animal genotype. Furthermore, IL-6 deficient mice given APAP alone or APAP/O3 had greater injury than their wild type respective counterpart at 9 h whereas at 32 h no genotype-related differences were detected. Airway neutrophil infiltration was significantly elevated at 9 h in APAP/O3 deficient mice while this was the case at 32 h in sufficient mice of the same group. Neutrophil exudation in the BALF was also detected in APAP alone or APAP/O3 sufficient groups at 32 h. In deficient mice, no neutrophil accumulation was observed in the BALF at any time nor with any treatment. APAP alone induced a significant increase of airway epithelial cell proliferation 32 h after administration in sufficient mice. In these animals, O3 exposure suppressed APAP-induced cell proliferation. In deficient mice, no differences in cell proliferation indices were detected between treated groups (O3 alone, APAP alone or APAP/O3) and control

(SAL/air) mice at 32 h. In conclusion, the onset of APAP alone or APAP/O3 toxicity and inflammation in the airway were accelerated in deficient animals as they had more epithelial injury and inflammation at the early time compared to sufficient animals. At this time, APAP/O3-coexposed deficient or sufficient mice had more airway injury than APAP alone-treated animals of respective genotype. This is not in accordance with our hypothesis that IL-6 deficient mice would be protected from O3 effects resulting in comparable airway injury between the coexposure group and animals given APAP alone.

Factors responsible for the accelerated toxicity in the airway of APAP alone or APAP/O3-treated deficient mice is not known at this time. O3 injury as previously decribed is dependent upon the presence of IL-6 and deficient animals seem to be protected from O3 airway damage (Johnston et al., 2005; Yu et al., 2002). To our knowledge, there is no publication on the airway effects of APAP in IL-6 deficient mice. In a study of factors involved in lung-liver communication during APAP toxicity, Neff and collaborators (2003) showed that in C57BL/6 fasted mice, 300 mg/kg APAP resulted in lung and liver injury while this was not the case in non-fasted, fed mice. In these non-fasted, fed mice, liver was protected from 300 mg/kg APAP toxicity at 8 or 24 h while bronchiolar epithelial cells exhibited necrosis and neutrophils accumulation were evident by 24 h post-APAP (Neff et al., 2003). This team reported that eotaxin is a risk factor for the lung injury in non-fasted, fed mice as this chemokine was increased in the lung of these animals but not in fasted mice. Furthermore, immunoneutralization of eotaxin before APAP injection protected non-fasted, fed mice from APAP lung injury and BALF neutrophil extravasation (Neff et al., 2003). Although eotaxin has not been evaluated in

IL-6 deficient animals in our study, this chemokines might have had a role in the heightened lung toxicity detected early in IL-6 deficient animals.

Several studies suggest that IL-6 in the lung has protective effects and that its deletion or suppression constitute results in greater damage as observed with APAP or APAP and O3 coexposure at the early time point in our study. For instance, intraperitoneal administration of LPS in IL-6 deficient mice resulted in greater pulmonary oxidative stress as evidenced by increased lung mRNA expression and protein concentration of inducible nitric oxide and heme oxygenase-1 as well as greater lipid peroxidation and 8-hydroxy-2'-deoxyguanosine immunostaining relative to wild type levels (Inoue et al., 2008). Similarly, Kida and collaborators (2005) using in vitro systems showed that lung epithelial cells from wild type mice were more resistant compared to cells isolated from IL-6 deficient mice. Wild type-derived lung epithelial cell resistance was abrogated by treatment with an anti-IL-6 antibody (Kida et al., 2005).

APAP alone or APAP and O3 coexposure in the wild type animals resulted in significant extravasation and accumulation of neutrophils into the BALF 32 h after administration. The absence of significant neutrophil accumulation in the BALF of APAP alone or APAP/O3-coexposed deficient mice at 9 or 32 h was not expected. Airway neutrophil accumulation was detected in wild type or deficient mice and correlated with the extent and timing of the damage. The effects of IL-6 on neutrophil emigration is unclear as endotoxin exposure resulted in exacerbation of neutrophil lung accumulation in IL-6 deficient mice (Inoue et al., 2004; Qiu et al., 2004; Xing et al., 1998) whereas the reverse was observed with O3 or bleomycin treatment (Johnston et al., 2005; Saito et al., 2008; Yu et al., 2002). Additionally, administration of IL-6 in rabbits resulted in a

biphasic neutrophilia due first to systemic release of the marginated pool and subsequently to accelerated release of neutrophils from the bone marrow (Suwa et al., 2000). The same team showed that IL-6 administration resulted in preferential sequestration of neutrophils into alveolar capillaries (Suwa et al., 2001). This effect of IL-6 mainly targeted immature neutrophils and was ascribed to the lesser deformability of these cells due to their high content in F-actin (Suwa et al., 2001). Although these results seem to be in contradiction with our data, Suwa and collaborators did not report the effects of IL-6 on extravasation of neutrophils into alveolar spaces or BALF. Species-related differences could also be an important factor as this team used rabbits while our studies focused on mice. The alveolar capillaries are the main site of neutrophils extravasation into alveolar spaces (Wagner and Roth, 2000). However, the mechanism of neutrophil extravasation from the alveolar capillary bed compared to the systemic or bronchial extravasation presents few differences. Those differences include the site of extravasation (alveolar capillaries into alveolar space or post-capillary venules in systemic or bronchial circulation), the size of alveolar capillaries (smaller than the diameter of neutrophils) and molecules involved in the extravasation process (CD18-dependence or independence) (Wagner and Roth, 2000). These differences could partially explain the discordant neutrophilia in airways or rather lack thereof in the BALF of deficient mice.

APAP administration induced airway epithelial cell proliferation in sufficient mice at 32 h. In those IL-6 sufficient mice, O3 exposure resulted in reduction of APAP-induced airway epithelial cell proliferation. Airway epithelial cell proliferation was not detected in APAP or APAP/O3-coexposed deficient mice. Several studies reported

defective regeneration in mice lacking IL-6 in various organs. IL-6 is important in successful liver regeneration after partial hepatectomy or chemical injury (Kovalovich et al., 2000). Furthermore, IL-6 deletion impaired wound repair in the skin while IL-6 promoted post-traumatic repair in the central nervous system (Gallucci et al., 2000; Gallucci et al., 2001; Sugawara et al., 2001; Swartz et al., 2001). In the lung, IL-6 deficient mice exhibited lower regenerative capacities in animals exposed to O3 or cigarette smoke and O3 together (Yu et al., 2002). In addition, IL-6 enhanced pulmonary epithelial cell survival (Kida et al., 2005; Ward et al., 2000). The mechanism behind IL-6 promotion of airway epithelial regeneration is unclear. In one study, administration of naphthalene in mice lacking STAT3 (a cytoplasmic factor responsible for numerous transcriptional responses of IL-6) or GP130 (the membrane co-receptor for IL-6 and activator of STAT3) resulted in defective bronchiolar epithelial cell shape and number recovery (Kida et al., 2008). Importantly, IL-6 is one of the ligand for the co-receptor GP130, and STAT3 is an important downstream effector of IL-6 for liver and probably lung regeneration (Dierssen et al., 2008; Moran et al., 2008; Wuestefeld et al., 2003).

In this study, we found that IL-6 is involved in hepatocellular regeneration after APAP injury as no regeneration was detected 32 h after administration in deficient mice. However, no hepatocellular proliferation was detected in APAP alone or APAP/O3-coexposed deficient mice suggesting that IL-6 is not the mediator of the impaired regeneration observed in APAP/O3-coexposed sufficient mice. Furthermore, APAP alone and APAP/O3 groups in deficient mice both had defective proliferation but the second group had greater hepatocellular toxicity compared to the former one. Taken together, these observations suggest that IL-6 is not involved in the delayed proliferation observed

in sufficient APAP/O3-coexposed mice or O3 exacerbation of APAP toxicity. In the lung, regardless of the genotype, APAP/O3-coexposed mice had more airway epithelial injury than APAP alone at 9 h while at 32 h no significant differences were detected. In addition, APAP alone or APAP/O3–coexposed deficient mice had more airway injury than their respective wild type counterpart at the early time point. No airway epithelial proliferation was observed in APAP alone or APAP/O3-coexposed deficient mice while APAP alone caused significant epithelial cell proliferation at 32 h. This seems to indicate that IL-6 protected the lung from early APAP toxicity and that IL-6 plays a role in airway epithelial proliferation after chemical injury. Finally, IL-6 had a role in neutrophils extravasation from alveolar capillaries as no neutrophils were detected in the BALF of APAP alone or APAP/O3-treated deficient mice while BALF neutrophilia was observed in sufficient mice.

VI. REFERENCES

Bishop, A.E., 2004. Pulmonary epithelial stem cells. Cell Prolif 37, 89-96.

Bourdi, M., Eiras, D.P., Holt, M.P., Webster, M.R., Reilly, T.P., Welch, K.D., Pohl, L.R., 2007. Role of IL-6 in an IL-10 and IL-4 double knockout mouse model uniquely susceptible to acetaminophen-induced liver injury. Chem Res Toxicol 20, 208-216.

Bourdi, M., Masubuchi, Y., Reilly, T.P., Amouzadeh, H.R., Martin, J.L., George, J.W., Shah, A.G., Pohl, L.R., 2002. Protection against acetaminophen-induced liver injury and lethality by interleukin 10: role of inducible nitric oxide synthase. Hepatology 35, 289-298.

Camargo, C.A., Jr., Madden, J.F., Gao, W., Selvan, R.S., Clavien, P.A., 1997. Interleukin-6 protects liver against warm ischemia/reperfusion injury and promotes hepatocyte proliferation in the rodent. Hepatology 26, 1513-1520.

Cho, H.Y., Hotchkiss, J.A., Harkema, J.R., 1999. Inflammatory and epithelial responses during the development of ozone-induced mucous cell metaplasia in the nasal epithelium of rats. Toxicol Sci 51, 135-145.

Cressman, D.E., Greenbaum, L.E., DeAngelis, R.A., Ciliberto, G., Furth, E.E., Poli, V., Taub, R., 1996. Liver failure and defective hepatocyte regeneration in interleukin-6-deficient mice. Science 274, 1379-1383.

Dierssen, U., Beraza, N., Lutz, H.H., Liedtke, C., Ernst, M., Wasmuth, H.E., Trautwein, C., 2008. Molecular dissection of gp130-dependent pathways in hepatocytes during liver regeneration. J Biol Chem 283, 9886-9895.

Fausto, N., Campbell, J.S., Riehle, K.J., 2006. Liver regeneration. Hepatology 43, S45-53.

Gallucci, R.M., Simeonova, P.P., Matheson, J.M., Kommineni, C., Guriel, J.L., Sugawara, T., Luster, M.I., 2000. Impaired cutaneous wound healing in interleukin-6-deficient and immunosuppressed mice. FASEB J 14, 2525-2531.

Gallucci, R.M., Sugawara, T., Yucesoy, B., Berryann, K., Simeonova, P.P., Matheson, J.M., Luster, M.I., 2001. Interleukin-6 treatment augments cutaneous wound healing in immunosuppressed mice. J Interferon Cytokine Res 21, 603-609.

Hilbert, D.M., Kopf, M., Mock, B.A., Kohler, G., Rudikoff, S., 1995. Interleukin 6 is essential for in vivo development of B lineage neoplasms. J Exp Med 182, 243-248.

Inoue, K., Takano, H., Yanagisawa, R., Sakurai, M., Shimada, A., Morita, T., Sato, M., Yoshino, S., Yoshikawa, T., Tohyama, C., 2004. Protective role of interleukin-6 in coagulatory and hemostatic disturbance induced by lipopolysaccharide in mice. Thromb Haemost 91, 1194-1201.

Inoue, K., Takano, H., Yanagisawa, R., Sakurai, M., Shimada, A., Satoh, M., Yoshino, S., Yamaki, K., Yoshikawa, T., 2008. Antioxidative role of interleukin-6 in septic lung injury in mice. Int J Immunopathol Pharmacol 21, 501-507.

James, L.P., Lamps, L.W., McCullough, S., Hinson, J.A., 2003a. Interleukin 6 and hepatocyte regeneration in acetaminophen toxicity in the mouse. Biochem Biophys Res Commun 309, 857-863.

James, L.P., McCullough, S.S., Lamps, L.W., Hinson, J.A., 2003b. Effect of N-acetylcysteine on acetaminophen toxicity in mice: relationship to reactive nitrogen and cytokine formation. Toxicol Sci 75, 458-467.

Johnston, R.A., Schwartzman, I.N., Flynt, L., Shore, S.A., 2005. Role of interleukin-6 in murine airway responses to ozone. Am J Physiol Lung Cell Mol Physiol 288, L390-397.

Katz, A., Chebath, J., Friedman, J., Revel, M., 1998. Increased sensitivity of IL-6-deficient mice to carbon tetrachloride hepatotoxicity and protection with an IL-6 receptor-IL-6 chimera. Cytokines Cell Mol Ther 4, 221-227.

Kida, H., Mucenski, M.L., Thitoff, A.R., Le Cras, T.D., Park, K.S., Ikegami, M., Muller, W., Whitsett, J.A., 2008. GP130-STAT3 regulates epithelial cell migration and is required for repair of the bronchiolar epithelium. Am J Pathol 172, 1542-1554.

Kida, H., Yoshida, M., Hoshino, S., Inoue, K., Yano, Y., Yanagita, M., Kumagai, T., Osaki, T., Tachibana, I., Saeki, Y., Kawase, I., 2005. Protective effect of IL-6 on alveolar epithelial cell death induced by hydrogen peroxide. Am J Physiol Lung Cell Mol Physiol 288, L342-349.

Kishimoto, T., 1989. The biology of interleukin-6. Blood 74, 1-10.

Klein, C., Wustefeld, T., Assmus, U., Roskams, T., Rose-John, S., Muller, M., Manns, M.P., Ernst, M., Trautwein, C., 2005. The IL-6-gp130-STAT3 pathway in hepatocytes triggers liver protection in T cell-mediated liver injury. J Clin Invest 115, 860-869.

Kopf, M., Baumann, H., Freer, G., Freudenberg, M., Lamers, M., Kishimoto, T., Zinkernagel, R., Bluethmann, H., Kohler, G., 1994. Impaired immune and acute-phase responses in interleukin-6-deficient mice. Nature 368, 339-342.

Kovalovich, K., DeAngelis, R.A., Li, W., Furth, E.E., Ciliberto, G., Taub, R., 2000. Increased toxin-induced liver injury and fibrosis in interleukin-6-deficient mice. Hepatology 31, 149-159.

Masubuchi, Y., Bourdi, M., Reilly, T.P., Graf, M.L., George, J.W., Pohl, L.R., 2003. Role of interleukin-6 in hepatic heat shock protein expression and protection against acetaminophen-induced liver disease. Biochem Biophys Res Commun 304, 207-212.

Mehendale, H.M., 1994. Amplified interactive toxicity of chemicals at nontoxic levels: mechanistic considerations and implications to public health. Environ Health Perspect 102 Suppl 9, 139-149.

Moran, D.M., Mattocks, M.A., Cahill, P.A., Koniaris, L.G., McKillop, I.H., 2008. Interleukin-6 mediates G(0)/G(1) growth arrest in hepatocellular carcinoma through a STAT 3-dependent pathway. J Surg Res 147, 23-33.

Naka, T., Nishimoto, N., Kishimoto, T., 2002. The paradigm of IL-6: from basic science to medicine. Arthritis Res 4 Suppl 3, S233-242.

Neff, S.B., Neff, T.A., Kunkel, S.L., Hogaboam, C.M., 2003. Alterations in cytokine/chemokine expression during organ-to-organ communication established via acetaminophen-induced toxicity. Exp Mol Pathol 75, 187-193.

Qiu, Z., Fujimura, M., Kurashima, K., Nakao, S., Mukaida, N., 2004. Enhanced airway inflammation and decreased subepithelial fibrosis in interleukin 6-deficient mice following chronic exposure to aerosolized antigen. Clin Exp Allergy 34, 1321-1328.

Saito, F., Tasaka, S., Inoue, K., Miyamoto, K., Nakano, Y., Ogawa, Y., Yamada, W., Shiraishi, Y., Hasegawa, N., Fujishima, S., Takano, H., Ishizaka, A., 2008. Role of interleukin-6 in bleomycin-induced lung inflammatory changes in mice. Am J Respir Cell Mol Biol 38, 566-571.

Sakamoto, T., Liu, Z., Murase, N., Ezure, T., Yokomuro, S., Poli, V., Demetris, A.J., 1999. Mitosis and apoptosis in the liver of interleukin-6-deficient mice after partial hepatectomy. Hepatology 29, 403-411.

Siewert, E., Bort, R., Kluge, R., Heinrich, P.C., Castell, J., Jover, R., 2000. Hepatic cytochrome P450 down-regulation during aseptic inflammation in the mouse is interleukin 6 dependent. Hepatology 32, 49-55.

Soni, M.G., Mehendale, H.M., 1998. Role of tissue repair in toxicologic interactions among hepatotoxic organics. Environ Health Perspect 106 Suppl 6, 1307-1317.

Sugawara, T., Gallucci, R.M., Simeonova, P.P., Luster, M.I., 2001. Regulation and role of interleukin 6 in wounded human epithelial keratinocytes. Cytokine 15, 328-336.

Suwa, T., Hogg, J.C., English, D., Van Eeden, S.F., 2000. Interleukin-6 induces demargination of intravascular neutrophils and shortens their transit in marrow. Am J Physiol Heart Circ Physiol 279, H2954-2960.

Suwa, T., Hogg, J.C., Klut, M.E., Hards, J., van Eeden, S.F., 2001. Interleukin-6 changes deformability of neutrophils and induces their sequestration in the lung. Am J Respir Crit Care Med 163, 970-976.

Swartz, K.R., Liu, F., Sewell, D., Schochet, T., Campbell, I., Sandor, M., Fabry, Z., 2001. Interleukin-6 promotes post-traumatic healing in the central nervous system. Brain Res 896, 86-95.

Taub, R., 2004. Liver regeneration: from myth to mechanism. Nat Rev Mol Cell Biol 5, 836-847.

Wagner, J.G., Roth, R.A., 2000. Neutrophil migration mechanisms, with an emphasis on the pulmonary vasculature. Pharmacol Rev 52, 349-374.

Ward, N.S., Waxman, A.B., Homer, R.J., Mantell, L.L., Einarsson, O., Du, Y., Elias, J.A., 2000. Interleukin-6-induced protection in hyperoxic acute lung injury. Am J Respir Cell Mol Biol 22, 535-542.

Warren, G.W., van Ess, P.J., Watson, A.M., Mattson, M.P., Blouin, R.A., 2001. Cytochrome P450 and antioxidant activity in interleukin-6 knockout mice after induction of the acute-phase response. J Interferon Cytokine Res 21, 821-826.

Wuestefeld, T., Klein, C., Streetz, K.L., Betz, U., Lauber, J., Buer, J., Manns, M.P., Muller, W., Trautwein, C., 2003. Interleukin-6/glycoprotein 130-dependent pathways are protective during liver regeneration. J Biol Chem 278, 11281-11288.

Xing, Z., Gauldie, J., Cox, G., Baumann, H., Jordana, M., Lei, X.F., Achong, M.K., 1998. IL-6 is an antiinflammatory cytokine required for controlling local or systemic acute inflammatory responses. J Clin Invest 101, 311-320.

Yee, S.B., Kinser, S., Hill, D.A., Barton, C.C., Hotchkiss, J.A., Harkema, J.R., Ganey, P.E., Roth, R.A., 2000. Synergistic hepatotoxicity from coexposure to bacterial endotoxin and the pyrrolizidine alkaloid monocrotaline. Toxicol Appl Pharmacol 166, 173-185.

Yu, M., Zheng, X., Witschi, H., Pinkerton, K.E., 2002. The role of interleukin-6 in pulmonary inflammation and injury induced by exposure to environmental air pollutants. Toxicol Sci 68, 488-497.

Zimmermann, A., 2004. Regulation of liver regeneration. Nephrol Dial Transplant 19 Suppl 4, iv6-10.

CHAPTER 5

SUMMARY AND CONCLUSIONS

APAP at high doses targets the liver and causes centrilobular hepatocellular degeneration and necrosis in laboratory animals and people (Bessems and Vermeulen, 2001; Clark et al., 1973; Davis et al., 1974; Dixon et al., 1975; Dixon et al., 1971; Placke et al., 1987; Portmann et al., 1975). APAP also causes airway epithelial toxicity in mammalian species (Amatya et al., 2002; Baudouin et al., 1995; Khanlou et al., 1999; Neff et al., 2003). O3 exposure on the other hand causes pulmonary airway epithelial damage and inflammation in rodents and people (Calderon-Garciduenas et al., 2000; Jorres et al., 2000; Koren et al., 1989; Pino et al., 1992). More recently, O3 exposure in rat or mouse has been shown to result in nitric oxide and protein synthesis induction in the liver and a cachexia-like syndrome with modulation of lipid and carbohydrates metabolisms (Laskin et al., 1994; Last et al., 2005). In the study by Last and collaborators (2005), O3 inhalation downregulated several cytochromes P450 isoforms and interferon-gamma-dependent genes in the liver. To our knowledge, there are no published studies on the effects of APAP and O3 coexposure in the liver and lung. We therefore undertook this work to address the hypothesis that combined APAP and O3 exposure will result in greater toxic effects in both organs compared to individual substances.

In the liver, we found that O3 exposure expanded APAP-induced centrilobular hepatocellular injury from centrilobular toward midzonal areas and increased acute inflammatory changes. Morphometric evaluation of hepatocellular degeneration and

necrosis and evaluation of plasma alanine aminotransferase activity showed that APAP and O3 coexposure had significantly more liver injury than APAP alone-treated mice. Although not significant, neutrophil infiltration was also greater in the coexposed group compared to APAP alone. O3 alone did not cause hepatocellular injury or inflammation. APAP alone resulted in increased number of cycling hepatocytes (evaluated by BrdU immunostaining) compared to control saline/air mice. Surprisingly, APAP and O3-coexposed mice had smaller levels of hepatocellular proliferation compared to the APAP alone group. In addition, APAP and O3-coexposed mice had slight increase in gene expression or protein concentration of IL-6, an important initiator of hepatocellular proliferation, while APAP alone-treated animals had upregulation of IL-6 at the gene and protein levels.

In the lung APAP caused airway epithelial injury and acute inflammation in our studies. Injury had an apparent proximal to distal gradient as axial airway at the level of the fifth bifurcation had more injury than the terminal bronchioles at the level of the eleventh bifurcation. O3 exposure usually causes airway injury and inflammation, particularly in distal parts of the airway tree (terminal bronchioles and junction with alveolar ducts) (Pino et al., 1992). O3 exposure at the dose of 0.5 ppm utilized in our studies did not cause airway epithelial or inflammatory changes. APAP and O3 coexposure however resulted in airway epithelial injury and acute inflammation greater than APAP alone-induced airway changes. In the axial airway or terminal bronchioles, APAP and O3-coexposed mice had epithelial numeric cell densities than APAP alone-treated animals. In the axial airway, coexposed mice had greater neutrophil infiltration than APAP alone and a nonsimmmmgnificant trend was observed in terminal

bronchioles. Similar to the hepatic proliferation indices, APAP and O3-coexposed mice had less airway proliferating epithelial cells compared to the APAP alone group. In reverse of the liver, IL-6 expression was greatest in the lung and systemic circulation of APAP and O3-coexposed animals compared to APAP or O3-exposed mice.

Mehendale showed that pretreatment of laboratory rodents with a nontoxic dose of chlordecone potentiated the hepatotoxicity and lethality of carbon tetrachloride, chloroform or bromotrichloromethane (Soni and Mehendale, 1998). This team showed that the exacerbation of hepatotoxicity by chlordecone was related to inhibition of the initial phase of hepatocellular regeneration that resulted in unopposed progression of cell injury. Moreover, mice deficient in IL-6 exhibited impaired liver regeneration and greater hepatocellular injury after partial hepatectomy or chemical administration (Cressman et al., 1996; Kovalovich et al., 2000). We therefore investigated the role of IL-6 in impaired regeneration of the APAP and O3 co-treated group and the contribution of this cytokine in the heightened liver toxicity.

We exposed IL-6 sufficient or deficient mice to APAP and/or O3 and found that both APAP alone and APAP and O3-coexposed groups had impaired hepatocellular regeneration in deficient animals. At the same time, coexposure of APAP and O3 resulted in greater hepatocellular toxicity compared to APAP alone in deficient mice. This suggests that IL-6 is involved in hepatocellular regeneration after APAP treatment but not in impaired regeneration in the APAP/O3 group or in O3 exacerbation of APAP toxicity. We compared APAP and O3 toxicity in airways of IL-6 deficient and sufficient mice. Airway epithelial regeneration was also inhibited in APAP alone or APAP/O3-treated deficient mice suggesting that IL-6 is involved in pulmonary airway regeneration.

IL-6 deficiency had no effect on O3 exacerbation of APAP airway toxicity and greater airway epithelial damage was observed in APAP and O3-coexposed deficient mice compared to APAP alone-treated animals. IL-6 deficient mice given APAP or APAP and O3 had more airway injury early in time compared to the sufficient respective groups. Other results presented in this dissertation are summarized in figure 42.

In addition to the impaired regeneration detected in the liver, additional proteins such as MCP-1 and PAI-1 or P21 have been down- or upregulated in the group given APAP and O3, respectively, and could be responsible for the impaired regeneration detected in this group. MCP-1 has been shown to be important in cell regeneration in different organs and its absence correlated with delayed or impaired regeneration as discussed in chapter 2. PAI-1 absence in a mice model of APAP liver injury resulted in greater injury and delayed hepatocellular regeneration as also discussed in chapter 2. In our studies, MCP-1 and PAI-1 exhibited significantly lower levels of expression in the APAP and O3-coexposed animals and might have been important in the impaired regeneration observed in this last group. P21, a cyclin-dependent kinase inhibitor, acts as an important sensor of DNA damage and halts the cell cycle to allow epithelial cell DNA repair as described in chapter 2. P21 had significantly greater expression in the APAP and O3-coexposed mice compared to either substance alone-exposed group. As also discussed in chapter 2, APAP or O3 cause oxidative DNA damage and their combined exposure might have resulted in greater oxidative DNA damage responsible for the greater expression of P21 and impaired hepatocellular regeneration in this group.

Clara cells are progenitor cells in the airways and are able to regenerate themselves but also ciliated cells after injury (Stripp and Reynolds, 2008; Stripp et al.,

2000). Mice given APAP and O3 had greater loss of Clara cell and the impaired airway epithelial regeneration observed in these animals might have been the result of a depletion of progenitor or a temporal change in the function of remnant Clara cells toward a more protective phenotype to the expense of their progenitor role. The impaired airway epithelial regeneration could also be related to a greater DNA oxidative damage as P21 is also greatest in the coexposure group compared to animals given APAP or O3 alone.

Evidence of increased markers of oxidative stress is detected in the liver of APAP and O3-coexposed or O3 alone-exposed mice and could be related to the effects on liver cells of O3 secondary mediators (generated upon the interaction of O3 with lung epithelial lining fluid or lung epithelial cell membrane). These secondary mediators comprise but are not limited to hydrogen peroxide, polyunsaturated fatty acids such as lipid hydroperoxides, endoperoxides and ozonides or end products such as aldehydes (malonaldehyde, etc).

Similarly, greater induction of oxidative stress markers was observed in the lung and might have been related to the direct toxic effects of APAP and O3 on airway epithelial cells as these substances have been reported to each cause oxidant damage (chapter 3). In the lung, APAP and O3 coexposure produced greater damage to the Clara cell population and reduced intracellular CCSP staining. CCSP has been shown to protect the airway epithelium due to its antioxidant and anti-inflammatory properties as discussed in chapter 3 and the lesser staining detected in the combined exposure is probably another indicator of greater oxidative damage.

The role of neutrophils in the progression of epithelial cell death including in APAP-induced hepatocellular injury has previously been reported (Ho et al., 1996; Roth et al., 1997). The enhanced neutrophilic inflammation in the APAP and O3-coexposed group in the liver and lung might have contributed to the oxidative stress described in the two previous paragraphs. Neutrophils also secrete an array of proteases known to induce epithelial cell damage which constitute an additional mechanism of toxicity

The hepatocytes at the periphery of necrotic areas in the APAP alone-treated mice are in a hypoxic state. Hypoxia could have been the functional result, in the poorly oxygenated centrilobular area, of the greater pulmonary airway injury seen in the APAP and O3-coexposed mice. Hypoxia could also be related to the known systemic effects of O3 secondary mediators on red blood cell and their capacity to deliver adequate levels of oxygen to cells (EPA, 2008).

Future studies should be designed to study the role of MCP-1 and PAI-1 or P21 in the impaired liver and/or lung epithelial regeneration due to APAP and O3 coexposure. The role of Clara cells in airway epithelial regeneration should also be further investigated in this model.

Lastly, oxidative stress seemed a central mechanism in the O3 potentiation of APAP toxicity as any of the other mechanisms can be linked to oxidative cell damage. Thus, oxidative damage for instance is one of the main mechanisms of neutrophil-induced cell injury as discussed in chapter 3. Impaired regeneration could potentially be a consequence of increased oxidative DNA damage and cell cycle arrest as suggested by increased P21 in both the lung and liver of APAP/O3-treated animals. APAP-induced HIF-1α accumulation has also been detected in vitro under high oxygen atmosphere and

other scientists suggested that this effect was rather a marker of oxidative stress (James et al., 2006). Therefore, oxidative stress is more likely to be the main player in the interaction of APAP and O3 and should be further investigated. The definition of oxidative stress includes 2 components. The first level of this definition comprises changes in concentrations of antioxidants. Associated to this is an increased generation of reactive oxygen species. Our results showed some evidence of changes in antioxidant concentrations during APAP and O3 coexposure. This could be further investigated by measuring other antioxidant molecules concentrations (superoxide dismutase, catalase, peroxiredoxins etc). In addition, investigation of reactive oxygen species in the lung, liver and blood (electron spin resonance spectroscopy, chemiluminescence etc) would further support an implication of oxidative stress in the greater toxicity seen in APAP and O3-coexposed animals. The contribution of the enhanced acute inflammation to this oxidative stress should also be investigated in the APAP and O3-coexposed group.

Figure 42. Summary of Results. APAP and O3 coexposure resulted in greater epithelial injury in the liver and pulmonary airway epithelia in mice. In the APAP and O3-coexposed mice, impaired epithelial regeneration was detected in both organs. The role of IL-6 was investigated using IL-6 deficient mice and this molecule was found not to be involved in this impaired epithelial regeneration or enhanced toxicity seen in the APAP and O3 coexposure group. Other candidates for the impaired regeneration in the liver could be MCP-1 and PAI-1 both shown to be important for hepatocellular regeneration and significantly downregulated in the APAP and O3-coexposed animals. In the lung, Clara cells are progenitor cells in the airway epithelium and the greatest loss of these cells have been detected in the coexposure group. P21, a cyclin-dependent kinase inhibitor known to stop the cell cycle to allow repair during DNA damage could also be responsible for the impaired regeneration in both organs. Greater induction of oxidative stress markers (CCSP, MT-1, GCLC, GSSG, TBARS) was detected in the APAP/O3 group or with O3 alone and could account for the enhanced toxicity seen in APAP and O3-coexposed animals. The combined exposure resulted in greater neutrophilic inflammation that could have played a role in this enhanced toxicity. Hepatocytes surrounding affected areas in APAP-treated animals are in hypoxic (based on glycogen depletion and intracellular HIF-1α accumulation) conditions and died when animals where coexposed to APAP and O3 also suggesting a role for hypoxia in this model.

Figure 42

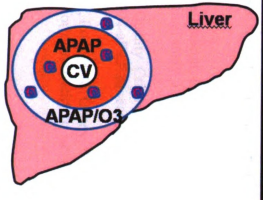

Liver	Lung
Impaired Regeneration	
IL-6; MCP-1; PAI-1; P21	Clara cells, P21
Oxidative Stress	
GSSG; MT-1; TBARS	GSSG, CCSP; MT-1; GCLC
Acute inflammation	
Neutrophil infiltration	Neutrophil infiltration
Hypoxia	
Glycogen, HIF-1α	None

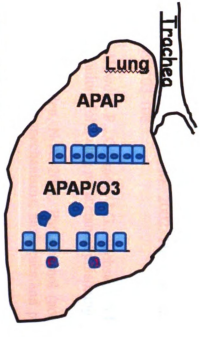

CV Central Vein
- Neutrophil
- APAP-induced liver necrosis
- APAP/O3-induced liver necrosis
- Airway epithelial cell
- Necrotic airway epithelial cell

REFERENCES

Amatya, B.M., Kimula, Y., Koike, M., 2002. The Clara cells activated by acetaminophen. J Med Dent Sci 49, 103-108.

Baudouin, S.V., Howdle, P., O'Grady, J.G., Webster, N.R., 1995. Acute lung injury in fulminant hepatic failure following paracetamol poisoning. Thorax 50, 399-402.

Bessems, J.G., Vermeulen, N.P., 2001. Paracetamol (acetaminophen)-induced toxicity: molecular and biochemical mechanisms, analogues and protective approaches. Crit Rev Toxicol 31, 55-138.

Calderon-Garciduenas, L., Devlin, R.B., Miller, F.J., 2000. Respiratory tract pathology and cytokine imbalance in clinically healthy children chronically and sequentially exposed to air pollutants. Med Hypotheses 55, 373-378.

Clark, R., Borirakchanyavat, V., Davidson, A.R., Thompson, R.P., Widdop, B., Goulding, R., Williams, R., 1973. Hepatic damage and death from overdose of paracetamol. Lancet 1, 66-70.

Cressman, D.E., Greenbaum, L.E., DeAngelis, R.A., Ciliberto, G., Furth, E.E., Poli, V., Taub, R., 1996. Liver failure and defective hepatocyte regeneration in interleukin-6-deficient mice. Science 274, 1379-1383.

Davis, D.C., Potter, W.Z., Jollow, D.J., Mitchell, J.R., 1974. Species differences in hepatic glutathione depletion, covalent binding and hepatic necrosis after acetaminophen. Life Sci 14, 2099-2109.

Dixon, M.F., Dixon, B., Aparicio, S.R., Loney, D.P., 1975. Experimental paracetamol-induced hepatic necrosis: a light- and electron-microscope, and histochemical study. J Pathol 116, 17-29.

Dixon, M.F., Nimmo, J., Prescott, L.F., 1971. Experimental paracetamol-induced hepatic necrosis: a histopathological study. J Pathol 103, 225-229.

EPA, U.S., 2008. Air Quality Criteria for O3 and Related Photochemical Oxidants (Final). EPA 600/R-05/004-aF-cF Research Triangle Park.

Ho, J.S., Buchweitz, J.P., Roth, R.A., Ganey, P.E., 1996. Identification of factors from rat neutrophils responsible for cytotoxicity to isolated hepatocytes. J Leukoc Biol 59, 716-724.

James, L.P., Donahower, B., Burke, A.S., McCullough, S., Hinson, J.A., 2006. Induction of the nuclear factor HIF-1alpha in acetaminophen toxicity: evidence for oxidative stress. Biochem Biophys Res Commun 343, 171-176.

Jorres, R.A., Holz, O., Zachgo, W., Timm, P., Koschyk, S., Muller, B., Grimminger, F., Seeger, W., Kelly, F.J., Dunster, C., Frischer, T., Lubec, G., Waschewski, M., Niendorf, A., Magnussen, H., 2000. The effect of repeated ozone exposures on inflammatory markers in bronchoalveolar lavage fluid and mucosal biopsies. Am J Respir Crit Care Med 161, 1855-1861.

Khanlou, H., Souto, H., Lippmann, M., Munoz, S., Rothstein, K., Ozden, Z., 1999. Resolution of adult respiratory distress syndrome after recovery from fulminant hepatic failure. Am J Med Sci 317, 134-136.

Koren, H.S., Devlin, R.B., Graham, D.E., Mann, R., McGee, M.P., Horstman, D.H., Kozumbo, W.J., Becker, S., House, D.E., McDonnell, W.F., et al., 1989. Ozone-induced inflammation in the lower airways of human subjects. Am Rev Respir Dis 139, 407-415.
Kovalovich, K., DeAngelis, R.A., Li, W., Furth, E.E., Ciliberto, G., Taub, R., 2000. Increased toxin-induced liver injury and fibrosis in interleukin-6-deficient mice. Hepatology 31, 149-159.

Laskin, D.L., Pendino, K.J., Punjabi, C.J., Rodriguez del Valle, M., Laskin, J.D., 1994. Pulmonary and hepatic effects of inhaled ozone in rats. Environ Health Perspect 102 Suppl 10, 61-64.

Last, J.A., Gohil, K., Mathrani, V.C., Kenyon, N.J., 2005. Systemic responses to inhaled ozone in mice: cachexia and down-regulation of liver xenobiotic metabolizing genes. Toxicol Appl Pharmacol 208, 117-126.

Neff, S.B., Neff, T.A., Kunkel, S.L., Hogaboam, C.M., 2003. Alterations in cytokine/chemokine expression during organ-to-organ communication established via acetaminophen-induced toxicity. Exp Mol Pathol 75, 187-193.

Pino, M.V., Levin, J.R., Stovall, M.Y., Hyde, D.M., 1992. Pulmonary inflammation and epithelial injury in response to acute ozone exposure in the rat. Toxicol Appl Pharmacol 112, 64-72.

Placke, M.E., Wyand, D.S., Cohen, S.D., 1987. Extrahepatic lesions induced by acetaminophen in the mouse. Toxicol Pathol 15, 381-387.

Portmann, B., Talbot, I.C., Day, D.W., Davidson, A.R., Murray-Lyon, I.M., Williams, R., 1975. Histopathological changes in the liver following a paracetamol overdose: correlation with clinical and biochemical parameters. J Pathol 117, 169-181.

Roth, R.A., Harkema, J.R., Pestka, J.P., Ganey, P.E., 1997. Is exposure to bacterial endotoxin a determinant of susceptibility to intoxication from xenobiotic agents? Toxicol Appl Pharmacol 147, 300-311.

Soni, M.G., Mehendale, H.M., 1998. Role of tissue repair in toxicologic interactions among hepatotoxic organics. Environ Health Perspect 106 Suppl 6, 1307-1317.
Stripp, B.R., Reynolds, S.D., 2008. Maintenance and repair of the bronchiolar epithelium. Proc Am Thorac Soc 5, 328-333.

Stripp, B.R., Reynolds, S.D., Plopper, C.G., Boe, I.M., Lund, J., 2000. Pulmonary phenotype of CCSP/UG deficient mice: a consequence of CCSP deficiency or altered Clara cell function? Ann N Y Acad Sci 923, 202-209.